



DEVELOPMENT AND OPTIMIZATION OF FINASTERIDE-LOADED
MICROEMULSIONS FOR TRANSDERMAL DELIVERY



A Thesis Submitted in Partial Fulfillment of the Requirements
for Doctor of Philosophy (PHARMACEUTICAL TECHNOLOGY)
Department of PHARMACEUTICAL TECHNOLOGY
Graduate School, Silpakorn University
Academic Year 2018
Copyright of Graduate School, Silpakorn University

การพัฒนาและการหาสูตรตำรับที่เหมาะสมของไมโครอิมัลชันที่กักเก็บยาฟิแนสเทอร์
ไรด์สำหรับการนำส่งทางผิวหนัง



โดย
นางนภัช รัตนะจิตร์วัช

วิทยานิพนธ์นี้เป็นส่วนหนึ่งของการศึกษาตามหลักสูตรปรัชญาดุษฎีบัณฑิต
สาขาวิชาเทคโนโลยีเภสัชกรรม แบบ 1.1 ปรัชญาดุษฎีบัณฑิต
ภาควิชาเทคโนโลยีเภสัชกรรม
บัณฑิตวิทยาลัย มหาวิทยาลัยศิลปากร
ปีการศึกษา 2561
ลิขสิทธิ์ของบัณฑิตวิทยาลัย มหาวิทยาลัยศิลปากร

DEVELOPMENT AND OPTIMIZATION OF FINASTERIDE-
LOADED MICROEMULSIONS FOR TRANSDERMAL DELIVERY



A Thesis Submitted in Partial Fulfillment of the Requirements
for Doctor of Philosophy (PHARMACEUTICAL TECHNOLOGY)
Department of PHARMACEUTICAL TECHNOLOGY
Graduate School, Silpakorn University
Academic Year 2018
Copyright of Graduate School, Silpakorn University

Title	Development and optimization of finasteride-loaded microemulsions for transdermal delivery
By	Napapat RATTANACHITTHAWAT
Field of Study	(PHARMACEUTICAL TECHNOLOGY)
Advisor	TANASAIT NGAWHIRUNPAT

Graduate School Silpakorn University in Partial Fulfillment of the Requirements for the Doctor of Philosophy

..... Dean of graduate school
(Associate Professor Jurairat Nunthanid, Ph.D.)

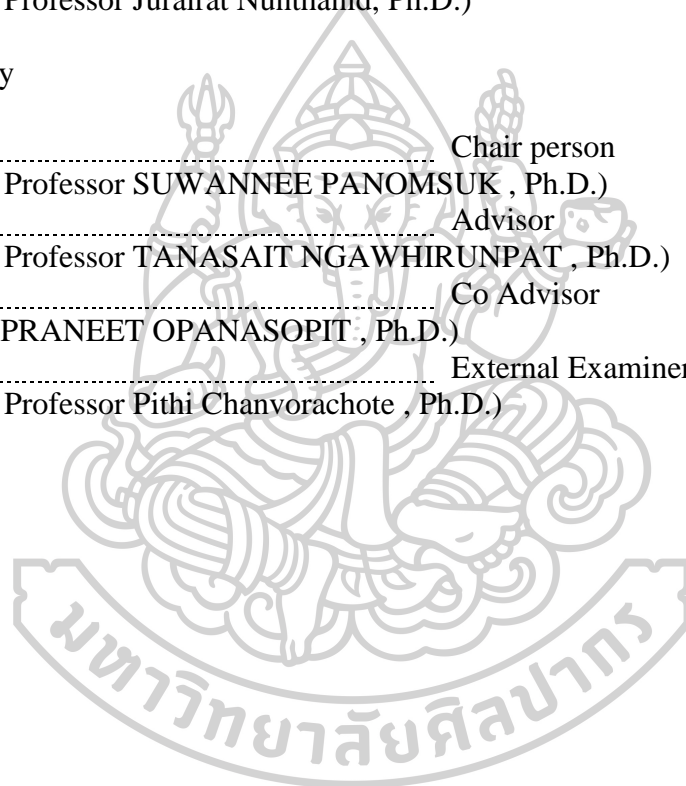
Approved by

..... Chair person
(Associate Professor SUWANNEE PANOMSUK , Ph.D.)

..... Advisor
(Associate Professor TANASAIT NGAWHIRUNPAT , Ph.D.)

..... Co Advisor
(Professor PRANEET OPANASOPIT , Ph.D.)

..... External Examiner
(Associate Professor Pithi Chanvorachote , Ph.D.)



57353802 : Major (PHARMACEUTICAL TECHNOLOGY)

Keyword : Finasteride, Dermal papilla cells, Microemulsions, Transdermal drug delivery

MRS. NAPAPAT RATTANACHITTHAWAT : DEVELOPMENT AND OPTIMIZATION OF FINASTERIDE-LOADED MICROEMULSIONS FOR TRANSDERMAL DELIVERY THESIS ADVISOR : ASSOCIATE PROFESSOR TANASAIT NGAWHIRUNPAT, Ph.D.

This study aimed to examine the effect of finasteride (FN) to dermal papilla cells (DPCs) and human primary dermal papilla cells (HDPCs) then FN-loaded microemulsions (MEs) for transdermal delivery were developed and evaluated for the physicochemical characteristics (droplet size, size distribution, electrical conductivity, pH and entrapment efficiency) and *in vitro* skin permeation. DPCs have been recognized as functioning cells to secrete the signals that control hair follicles and these cells are hypothesized as the key targets of androgen in androgenetic alopecia (AGA) pathophysiology. FN exhibited a possible effect on stemness which increased stem cell related-transcription factors through the Wnt/ β -catenin signaling pathway in DPCs and HDPCs. Treatment of the DPCs with FN at non-toxic concentrations was able to significantly increase the aggregation behavior with significant increase of stem cell transcription factors Sox-2 and Nanog, when compared with the non-treated control cells. For mechanisms, FN was found to up-regulate the stem cell regulatory proteins through the activation of protein kinase B (AKT), β -catenin, and integrin- β 1. FN-loaded MEs were developed and composed of cinnamon oil as oil phase, Tween20 as surfactant, propylene glycol (PG) as co-surfactant and water. The surfactant mixture (S_{mix}) (Tween20 and PG) at 3:1 weight ratio showed the largest area of MEs, therefore it was selected to develop FN-loaded MEs. The results revealed that the component ratio and amount of FN affected the physicochemical characteristic of MEs. 0.3% w/w of FN-loaded ME1 (15% of oil phase, 55% of S_{mix} and 30% of water phase) and ME6 (25% of oil phase, 55% of S_{mix} and 10% of water phase) had small droplet size, 179.33 ± 31.57 nm and 176.91 ± 34.70 nm, respectively. Moreover, 0.3% w/w of FN-loaded ME1 which had high ratio of water (30%) presented the highest skin permeation flux (2.32 ± 0.19 $\mu\text{g}/\text{cm}^2/\text{h}$). Design Expert[®] Software was used to optimize the MEs, the optimal ME formulation was 11.85% of oil phase, 58.42% of S_{mix} and 30% of water phase. This study indicated that FN maintained stemness of DPCs and could be beneficial for the development of hair regeneration approaches.

ACKNOWLEDGEMENTS

First of all, I would like to express my sincere gratitude and appreciation to my thesis advisor, Assoc. Prof. Tanasait Ngawhirunpat, for the kind of supervision, suggestion, guidance and encouragement throughout my study. He gave me the opportunity to study in my proposition interests. Prof. Dr. Praneet Opanasopit, my co-advisor, for her supported. She have intensively helped, led and advised me to solve problems and to complete this thesis.

I would like to acknowledge to Assoc. Prof. Pithi Chanvorachote for gave me the great opportunities to work at his laboratory, Cell-Based Drug and Health Product Development Research Unit, Department of Pharmacology and Physiology Faculty of Pharmaceutical Science, Chulalongkorn University. He gave me the new experience in my education. My acknowledgement also include all student in this lab for help me in everything that I cannot do.

Moreover, I would like to appreciate to Assoc. Prof. Sinchai Kaewkitichai who gave me the opportunity to work in Faculty of Pharmaceutical Science, Burapha University and gave me the grant for study the PhD. Program.

In addition, I would like to thanks to Asst. Prof. Sureewan Duangjit for advised me about Design Expert® software and support me in everything of my research.

I also thank to all my friend, brothers, sisters and all member of the Pharmaceutical Development of Green Innovation Group (PDGIG) who gave me the great time at Silpakorn University.

Finally, I sincerely appreciate my parents, all my teachers, colleagues and friends for their love, advice, and encouragement throughout this study. Without all these persons mentioned above, this thesis would not have been developed and completed.

Napapat RATTANACHITTHAWAT

TABLE OF CONTENTS

	Page
ABSTRACT.....	D
ACKNOWLEDGEMENTS.....	E
TABLE OF CONTENTS.....	F
LIST OF TABLES.....	H
LIST OF FIGURES.....	I
CHAPTER 1 INTRODUCTION.....	1
1.1 Statement and significance of the problem.....	1
1.2 Objectives of this research.....	7
1.3 The research hypothesis.....	7
CHAPTER 2 LITERATURE REVIEWS.....	8
2.1 Hair.....	9
2.2 Androgenetic alopecia (AGA).....	17
2.3 Transdermal drug delivery technology.....	21
2.4 Microemulsions.....	22
CHAPTER 3 MATERIAL AND METHODS.....	29
3.1 Materials.....	31
3.2 Equipments.....	33
3.3 Methods.....	35
CHAPTER 4 RESULTS AND DISCUSSIONS.....	43
4.1 Effect of FN on DPCs.....	44
4.2 Formulations of FN-loaded MEs.....	57
4.3 Characterization of FN-loaded MEs.....	63
4.4 <i>In vitro</i> skin permeation study.....	68

4.5 Optimization of FN-loaded ME formulations by computer design	70
CHAPTER 5 CONCLUSIONS	76
REFERENCES	78
APPENDIX.....	84
VITA.....	94



LIST OF TABLES

	Page
Table 1 The differences between macroemulsions and microemulsions	23
Table 2 Solubility of FN in various oils and co-surfactants (n=3).....	58
Table 3 The amount of each component of seven ME formulations (%w/w) with S _{mix} at 3:1 ratio	63
Table 4 The prediction value of the physicochemical characteristic from the optimal FN-loaded MEs.....	75
Table 5 Cytotoxicity of FN on DPCs and 2 different sources of HDPCs	86
Table 6 Aggregation size and aggregation number of DPCs	86
Table 7 Physicochemical characteristics of blank MEs and FN-loaded MEs (droplet size)	91
Table 8 Physicochemical characteristics of blank MEs and FN-loaded MEs (size distribution (PDI)).....	91
Table 9 Physicochemical characteristics of blank MEs and FN-loaded MEs (conductivity).....	92
Table 10 Physicochemical characteristics of blank MEs and FN-loaded MEs (pH) 92	92
Table 11 Drug content of FN-loaded MEs presented by % entrapment efficiency	93
Table 12 Skin permeation flux of FN-loaded MEs	93

LIST OF FIGURES

	Page
Figure 1 Morphology of human hair.....	9
Figure 2 The cross section of hair shaft showing the cuticle layer, the cortex layer and the medulla layer.....	10
Figure 3 The compartment of hair follicle: infundibulum, isthmus, suprabalbar and bulb. 11	11
Figure 4 Hair growth cycle: anagen phase, catagen phase and telogen phase.....	12
Figure 5 Schematic view of Wnt/ β -catenin signaling.....	14
Figure 6 Different mechanism of action of herb and their active constituents.....	16
Figure 7 The conversion of testosterone to dihydrotestosterone by 5 α -reductase enzyme 17	17
Figure 8 Structure of FN and mechanism of 5 α -reductase enzyme inhibitor.....	19
Figure 9 Transdermal delivery pathway of the substances.....	22
Figure 10 Molecular structure of a) Ethanol, b) Isopropanol and c) PG.....	26
Figure 11 Cytotoxicity of FN (0.01-100 μ M) on DPCs. (a) DPCs was treated for 24 h and determined by MTT assay. The data represent the means of three independent samples \pm SD. (b) Hoechst 33342/PI apoptosis assay for investigation mode of cell death after treatment for 24 h. (c) Morphology of DPCs.....	45
Figure 12 Cytotoxicity of FN on 2 different sources of HDPCs. Cells were treated with FN (0.01-100 μ M) for 24 h and determined the cytotoxicity by MTT assay....	46
Figure 13 Aggregation behavior of DPCs. (a) Aggregation behavior of DPCs after indicated treatment with FN (10-100 μ M) for five days. (b) The SEM image for aggregation behavior of DPCs after indicated treatment with FN (100 μ M) for five days. 47	47
Figure 14 Effect of FN on aggregation behavior of DPCs (a) Aggregation size and (b) Aggregation number were determined by image analyzer. The data represent the mean of three independent samples \pm SD. *P < 0.05 versus non-treated control.	48

Figure 15 Effect of FN on Wnt/ β -catenin signaling in DPCs. Cells were culture in the various concentration of FN (10-100 μ M) for 24 h. (a) After treatment, the levels of Wnt/ β -catenin signaling (p-Akt (Ser473) and β -catenin) were analyzed by western blot. β -actin was served as the loading control. The immunoblot signals were quantified by densitometry and the mean data from independent experiments were normalized to the results. The data represent the means of three independent samples \pm SD. *P < 0.05 versus non-treated control. (b) Expression of β -catenin was analyzed by immunofluorescence staining.....49

Figure 16 Effect of FN on stem cell-like phenotype and self-renewal transcription factors in DPCs. Cells were culture in the various concentration of FN (10-100 μ M) for 24 h. (a and b) After treatment, the levels of integrin β -1, CD44, Nanog, Sox-2 were analyzed by western blot. β -actin was served as the loading control. The immunoblot signals were quantified by densitometry and the mean data from independent experiments were normalized to the results. The data represent the means of three independent samples \pm SD. *P < 0.05 versus non-treated control. (c and d) Expression of Nanog and Sox-2 was analyzed by immunofluorescence staining. 51

Figure 17 Effect of FN on Wnt/ β -catenin signaling and self-renewal transcription factors in HDPCs were investigated. Expression of β -catenin, Nanog and Sox-2 was analyzed by immunofluorescence staining.55

Figure 18 Chemical structure of the main constituents of cinnamon oil59

Figure 19 Pseudoternary phase diagram of cinnamon oil MEs with different surfactants mixed with PG at 1:1 ratio by weight.; (a) Emulgin[®] O5, (b) SG-CG[®]700, and (c) Tween 20.....60

Figure 20 Pseudoternary phase diagram of cinnamon oil MEs with different ratio of S_{mix} (Tween 20:PG); (a) 1:1 ratio, (b) 2:1 ratio, and (c) 3:1 ratio.61

Figure 21 The seven different ME formulations were selected from ME region of pseudoternary phase diagram with S_{mix} at 3:1 ratio.62

Figure 22 Droplet size of seven formulations of FN-loaded MEs at three concentrations of FN (Blank, 0.1% and 0.3⁰ow/w).64

Figure 23	Size distribution of seven formulations of FN-loaded MEs at three concentrations of FN (Blank, 0.1% and 0.3% ⁰ w/w).....	65
Figure 24	Conductivity of seven formulations of FN-loaded MEs at three concentrations of FN (Blank, 0.1% and 0.3% ⁰ w/w).....	66
Figure 25	pH of seven formulations of FN-loaded MEs at three concentrations of FN (Blank, 0.1% and 0.3% ⁰ w/w).....	67
Figure 26	% Entrapment efficiency of FN-loaded MEs.....	67
Figure 27	The skin permeation profile of seven formulations of 0.3% ⁰ w/w FN-loaded MEs.	69
Figure 28	The skin permeation flux of 0.3% ⁰ w/w FN-loaded ME formulations...	69
Figure 29	The response surface of a) droplet size, b) PDI, c) conductivity and d) pH for blank ME (left column) and 0.3% w/w FN-loaded MEs (right column).	72
Figure 30	The response surface of a) % Entrapment efficiency (EE) and b) Skin permeation flux of 0.3% w/w FN-loaded MEs.....	73
Figure 31	The response surface of the optimal FN-loaded ME formulation.....	74
Figure 32	Standard curve for in vitro skin permeation study	88
Figure 33	HPLC chromatogram of standard FN solution.....	89
Figure 34	HPLC chromatogram of FN in sample.....	89

CHAPTER 1

INTRODUCTION

1.1 Statement and significance of the problem

Androgenetic alopecia (AGA), also known as male pattern hair loss in men and female pattern hair loss in women (Ellis & Sinclair, 2008), is hereditary thinning of hair from the scalp induced by androgens in genetically susceptible men and women. AGA affects at least 50% of men by the age of 50 years, and up to 70% of all males in later life (Norwood, 1975). AGA is caused by vellus transformation of scalp hair (Inui, Nakajima, & Itami, 2009), which corresponds miniaturization of hair follicles by repeated hair cycles with shortened anagen phase (Uno H, Allegra F, Adachi K, & W., 1967), leading to gradual replacement of large, pigmented hairs (terminal hairs) by barely visible, depigmented hairs (vellus hairs) (Paus & Cotsarelis, 1999). Male pattern AGA is characterized by its typical bitemporal recession of hair and balding vertex, whereas female pattern AGA is set apart by its diffuse thinning of the crown and intact frontal hair line (Trueb, 2002).

It has long been known that the presence of testosterone in hair follicle is a prerequisite for AGA. No baldness is seen in pseudohermaphrodites who lack a functional 5α -reductase type II enzyme (Imperato-McGinley, Guerrero, Gautier, German, & Peterson, 1975). This enzyme, along with its isozyme, 5α -reductase type I and III, is responsible for the conversion of testosterone (T) to dihydrotestosterone (DHT) (Azzouni, Godoy, Li, & Mohler, 2012) in the cell cytoplasm. Both T and DHT appear to bind to the same androgen receptor in the cell nucleus (Brown et al., 1989), exposing

DNA binding sites, and thereby regulating transcription of androgen dependent genes (Randall, Thornton, Hamada, & Messenger, 1994) and finally its translation into proteins, which exert biological activity. This multi-step molecular pathway can be involved in the pathogenesis of AGA. Currently there are two medications approved by the US Food and Drug Administration (FDA) for hair regrowth and reversal of miniaturization of androgenetic alopecia, topical minoxidil and oral finasteride (Ellis & Sinclair, 2008).

Minoxidil, a vasodilator was initially approved as a drug to control hypertension (Haber, 2004), but observing hypertensive patients taking minoxidil showed increase in hair growth. The 2% and 5% topical solutions of minoxidil were approved by the US FDA for use as a treatment for AGA (Ellis & Sinclair, 2008). However, the biological basis for this effect of minoxidil remains unknown. Some studies mention that the vasodilatory properties of this compound that served to increase blood supply to the scalp providing the mechanism through which minoxidil may exert its effects (Haber, 2004). Other proposed mechanisms of action of minoxidil include stimulation of cell proliferation, and of prostaglandin (PG) synthesis (Messenger & Rundegren, 2004). However, minoxidil does not permanently inhibit hair loss process; cessation of minoxidil treatment is quickly followed by rapid shedding of hairs returning the scalp to an untreated state (Olsen & Weiner, 1987). In recent year, minoxidil was developed into 5% minoxidil foam. The minoxidil topical solution consists of a liquid solution and takes time to dry. The newly hydroalcoholic foam has been shown to be more easily applied to target area, and the clinical trials of this product demonstrated that minoxidil foam is effective, safe and well accepted cosmetically by patients (Olsen et al., 2007).

Finasteride (FN) is widely used for the treatment of benign prostatic hyperplasia (BPH)(Schmidt & Tindall, 2011), prostate cancer (Cha & Shariat, 2011) and androgenetic alopecia (Tabbakhian, Tavakoli, Jaafari, & Daneshamouz, 2006). FN has a molecular formula of $C_{23}H_{36}N_2O_2$, a molecular weight of 372.6, log Po/w of 3.03 (lipophilic drug). FN is N-(1,1-dimethylethyl)-3-oxo-4-aza-5 α -androst-1-inhibitor of steroid type-II 5 α -reductase but it has no affinity for androgen receptor. Inhibition of this enzyme blocks the peripheral conversion of testosterone, resulting in significant decreases in serum and tissue DHT concentration (Tabbakhian et al., 2006). It has been reported that oral administration of daily dose of 1 mg reduces concentration of scalp DHT and serum DHT by 64% and 68%, respectively (Drake et al., 1999), and inhibits or reverses miniaturization of hair follicle. However, several adverse effects had been observed in the majority of patients such as impaired reproductive function, impotence, erectile dysfunction, and gynecomastia (Hajheydari, Akbari, Saeedi, & Shokoohi, 2009; Kumar, Singh, Bakshi, & Katare, 2007), so topical formulations should be preferable to oral. In many recent years, there are many studies about development of finasteride topical formulations. In 2006, Tabbakhian et al., investigated the topical application of finasteride-containing vesicles (liposomes and niosomes) compared with finasteride hydroalcoholic (HA) solution in enhancing drug concentration at pilosebaceous unit (PSU) which is the target site for the treatment of AGA. The results indicated that finasteride in liquid-state vesicles made from dimyristoyl phosphatidylcholine (DMPC) or Brij97:Brij76 (1:1) were able to deposit in PSU higher than finasteride in gel-state vesicle or HA solution. Both in vitro permeation and in vivo deposition studies demonstrated the potential of liquid-state liposomes and niosomes for successful delivery of finasteride to the PSU.

In 2014, Caon et al., developed the negative charge polymersomes based on polystyrene (PS) and poly (acrylic acid) (PAA) block copolymers decorated with chitosan containing finasteride to provide high finasteride retention in the dermis and epidermis while allowing some control of drug release. Two groups of finasteride-loaded polymersome showed higher permeation coefficient values than the hydroethanolic finasteride solution (control), and it was observed that the addition of chitosan contributed to increase of the accumulation of finasteride in the epidermis (Caon et al., 2014).

Moreover, topical and transdermal delivery formulations of finasteride had been developed into ethosomes (Y. Rao et al., 2015; Sujatha S, Sowmya G, & Chaitanya M, 2016), lipid nanoparticles (Gomes, Martins, Ferreira, Segundo, & Reis, 2014), liquid crystalline nanoparticles (Madheswaran et al., 2013) etc., to enhance skin permeation and skin retention of the drug. Although, these delivery systems exhibited the increasing of skin penetration and skin retention of finasteride but some formulation had expensive raw material or difficult to produce in the commercial industry. However, there is an attractive delivery system that can enhance the penetration of the drug through the skin, easily to prepare and has the thermodynamically stable system, it is microemulsions.

Microemulsions are ideal liquid vehicles for drug delivery since they provide all the possible requirement of a liquid system including thermodynamic stability (long shelf-life), easy formation (zero interfacial tension and almost spontaneous formation), low viscosity with Newtonian behavior, high surface area (high solubilization capacity), and very small droplet size. Both water-insoluble and lipid-insoluble

components can be solubilized in microemulsions to synergist the effect for a specific therapeutic goal. Microemulsions can be used by orally, topically, or nasally as an aerosol for direct entry into the lungs (Kogan & Garti, 2006). Microemulsions consist of oil, water, surfactant and co-surfactant and have small droplet size which typically less than 150 nm (Jaipakdee, Limpongsa, & Pongjanyakul, 2016). However, microemulsions contain high surfactant concentration and in most cases they are composed of high alcohol, solvent and co-surfactant content that are always a hazard to the human body.

The application of microemulsion vehicles for transdermal drug delivery becomes increasingly interesting due to their high solubilization capability for both lipophilic and hydrophilic substances. Many studies demonstrated that the permeation rates of the drug from microemulsions were significantly higher than the conventional emulsions (creams, lotions, etc.). In addition, the conventional emulsions are not stable formulations and coalescence of the formulation was detected. In 2007, Biruss et al., developed microemulsion systems containing eucalyptus oil for transdermal delivery of selected steroid drugs, 17- β -estradiol, progesterone, cyproterone acetate, and finasteride. Microemulsions consisting of ethanol, Brij-30, eucalyptus oil and demineralised water were prepared with incorporation of the steroid drugs. In all cases, clear optical transparent and volatile microemulsions resulted with odor of eucalyptus oil and semisolid formulations emerged by adding polycarbophil, polymeric emulsifier and silicon dioxide, respectively. The addition of polymeric agents leads to an improvement of permeation of steroid hormones incorporated in microemulsions as a

consequence of a synergistic effect between eucalyptus oil and polymers (Biruss, Kahlig, & Valenta, 2007).

It is important to optimize the microemulsions formulation in the development of suitable microemulsions for transdermal delivery system. The ideal microemulsions are high skin permeability without inducing skin irritation. The compositions of microemulsions can affect the physicochemical properties and skin permeability of microemulsions. In 2015, capsaicin-loaded microemulsion systems were developed by Duangjit et al. based on computer design to be transdermal drug delivery system. The capsaicin-loaded microemulsions consisted of isopropyl myristate (IPM) as oil phase, cocamide diethanolamine (cocamide DEA) as the surfactant, ethanol as the co-surfactant and reverse osmosis water (RO water) as aqueous phase, and 0.15% w/w of capsaicin extract. The physicochemical characteristics of microemulsions (e.g. droplet size, size distribution, zeta potential, electrical conductivity and pH) and the skin permeability were determined. The response surface and the optimal microemulsion formulations were estimated using the Design Expert[®] Software. The results indicated that the optimal microemulsions and all candidate microemulsion formulations had significantly greater skin permeability than the commercial capsaicin product. Moreover, this study succeeded in predicting and developing the microemulsions systems for transdermal delivery of capsaicin (Duangjit, Chairat, Opanasopit, Rojanarata, & Ngawhirunpat, 2016).

In this study, the effect of finasteride to human dermal papilla cells was investigated to study of the mechanism of finasteride in treatment of AGA. The toxicity test of finasteride to human dermal papilla cells was done. Then, the novel finasteride-

loaded microemulsion systems were developed for enhancing transdermal delivery of finasteride. The microemulsion formulations consist of oil phase, water phase, surfactant, and co-surfactant selected from finasteride solubility screening test for the suitable compositions. The microemulsion system which presented the largest area of microemulsions in pseudoternary phase diagram and had the microemulsion properties according to the theory (e.g. transparent liquid, droplet size < 150 nm, narrow size distribution) were selected to incorporate with finasteride. Microemulsions with or without finasteride were characterized for the physicochemical properties and tested the in vitro skin permeation study to investigate the penetration enhancing effect of microemulsion systems. Subsequently, microemulsions were optimized based on the computer program to predict the physicochemical properties.

1.2 Objectives of this research

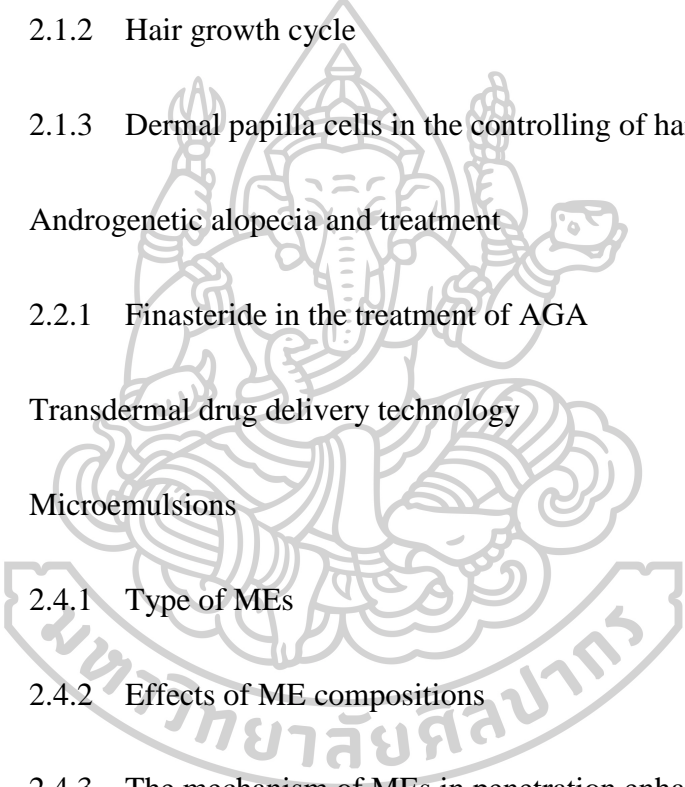
- 1.2.1 To examine the effect of finasteride to human dermal papilla cells.
- 1.2.2 To develop and optimize finasteride-loaded microemulsion formulations.
- 1.2.2 To evaluate the physicochemical properties, in vitro skin permeation of finasteride-loaded microemulsions.

1.3 The research hypothesis

- 1.3.1 Microemulsions can enhance the penetration of finasteride into the skin and human papilla cell.
- 1.3.2 The formulation compositions influence on the physicochemical properties and in vitro skin permeation enhancement.

CHAPTER 2

LITERATURE REVIEWS

- 2.1 Hair
 - 2.1.1 Hair morphology and function
 - 2.1.2 Hair growth cycle
 - 2.1.3 Dermal papilla cells in the controlling of hair growth cycle
 - 2.2 Androgenetic alopecia and treatment
 - 2.2.1 Finasteride in the treatment of AGA
 - 2.3 Transdermal drug delivery technology
 - 2.4 Microemulsions
 - 2.4.1 Type of MEs
 - 2.4.2 Effects of ME compositions
 - 2.4.3 The mechanism of MEs in penetration enhancement
 - 2.4.4 ME applications in pharmaceutical dosage forms
- 

2.1 Hair

2.1.2 Hair morphology and functions

Hair is a skin appendage that mainly develops from epidermis except for hair papilla which develop from dermis. In general, most mammals have hair covered on the skin and hair were used to classify animals. Skin is cover with hair all over the body except the mouth, other orifice and claw. Morphology of hair is shown in Figure 1. The composition of hair can be divided into two main parts, hair shaft and hair follicle.

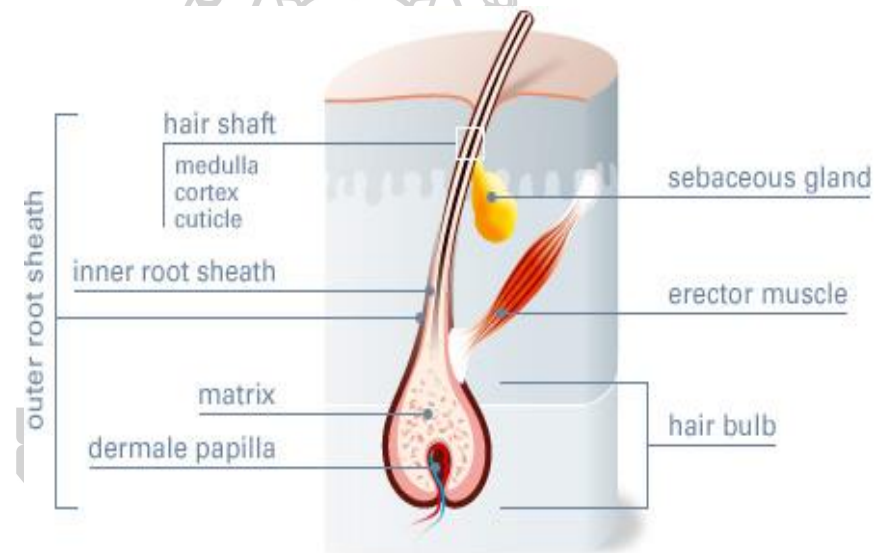


Figure 1 Morphology of human hair.

(http://www.revalid.com/uploads/pics/hair_bulb.jpg)

The manifest function of hair follicle is to control the production of hair shaft. Hair shaft is a part of fiber that grows above the scalp upper the skin. In humans the most important function of hair shaft is as a physical medium of social communication; in fact, scalp, facial, and body hairs are essentially the only body parts which an individual can shape to influence social intercourse (Stenn & Paus, 2001). Hair shaft

can be separated into three layers, the first outer layer is cuticle, the middle layer is cortex, and third inner layer is medulla as shown in Figure 2.

The cuticle layer of human hair is usually surrounded by 6 – 10 cuticle cells, each approximately 0.2-0.5 μm thick. The hair cuticle is formed from dead cell and overlapped on the skin surface and oriented liked the fish scales. Cuticle layers have an important role on hair's physical characteristics such as optical properties and feeling.

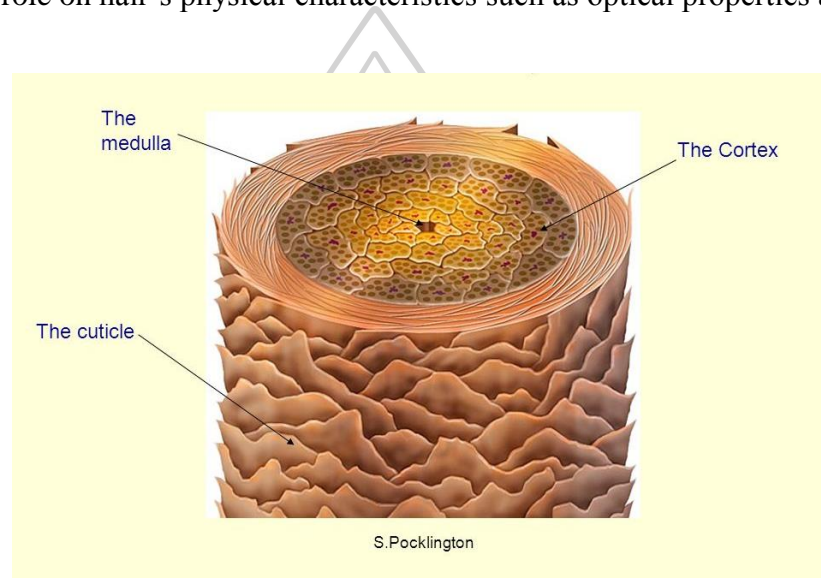


Figure 2 The cross section of hair shaft showing the cuticle layer, the cortex layer and the medulla layer.
(<https://slideplayer.com/slide/798224/3/images/2/The+Three+Layers+The+medulla+The+Cortex+The+cuticle+S.Pocklington.jpg>)

Cortex is the middle layer which has the bulk component of hair and supplies mechanical strength to hair. Cortex cells are closely-packed macrofibrils, which are targeted along the axis of the hair. Macrofibrils are composed of rodlike microfibril arranged in whorls shape and embedded in an intermicrofibrillar matrix in a parallel longitudinal oriented within microfibrils like a rope.

The innermost layer is medulla, which can be found only in terminal hair. Medulla is usually composed of various size of spongy keratin cells bounded with air spaces (Dawber, 1996).

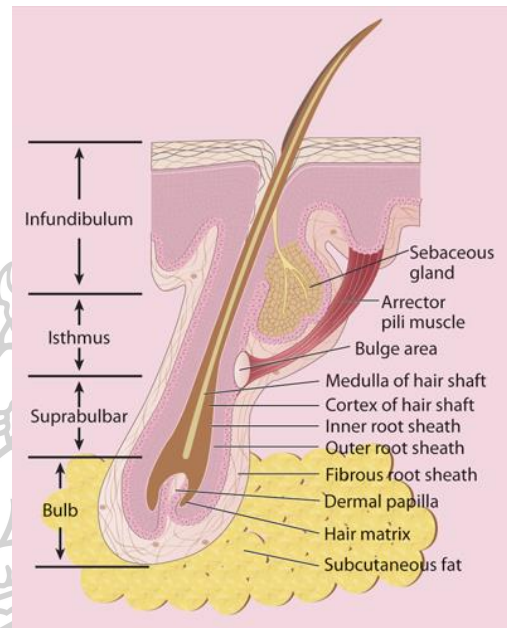


Figure 3 The compartment of hair follicle: infundibulum, isthmus, suprabulbar and bulb.

(https://accessmedicine.mhmedical.com/data/books/gold8/gold8_c088ef000.2.png)

Another part is hair follicle which is the most critical part of hair (Figure 3). The hair follicle develops from the embryonic epidermis as an epithelial finger (Stenn & Paus, 2001). It supplies nutrition and oxygen to hair and support hair fiber growth and elongation. Hair follicle contains the permanent superficial structure and transient cycling component which changes during the hair growth cycle. The permanent segment of the hair follicle can be divided into two sections namely, the infundibulum and isthmus of the permanent upper segment and the suprabulbar and bulb of the transient lower segment. The infundibulum which is the part between skin surface and

the opening of the duct from sebaceous gland. The isthmus, which is the part between the opening of the duct from sebaceous gland and the bulge region. The transient portion is the area extends from the bulge region to the base of hair follicle bulb. The epithelial hair bulb is situated around the papilla and contained the matrix cells and the germinative cells.

2.1.2 Hair growth cycle

In general, hair growth cycle can be categorized into the three major states, the anagen or active growth phase, the catagen or transition phase and the telogen or resting phase (Figure 4). The duration of each state depends on many factors such as location of hair and health status. 85% of hair growth cycle are in anagen phase (3-6 years). The major characteristic of anagen is the growing hair shaft and the

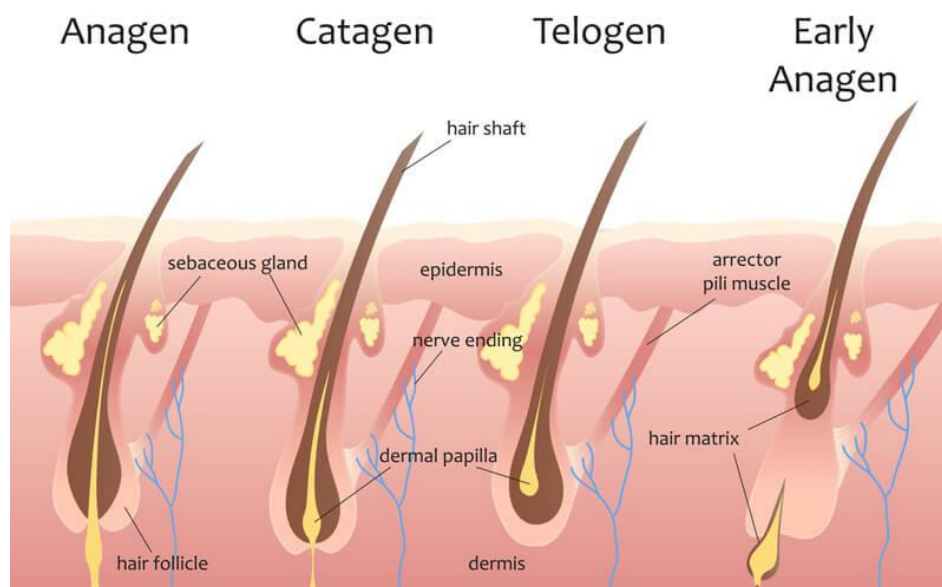


Figure 4 Hair growth cycle: anagen phase, catagen phase and telogen phase.
(<https://www.hairguard.com/wp-content/uploads/2017/10/hair-growth-phase-diagram-anagen-ccl.jpg>)

proliferation of epithelial hair follicle compartments, with the hair matrix keratinocytes located around the dermal papilla showing the highest proliferative activity. Also, the newly formed hair shaft is pigmented by the follicle pigmentary unit (Paus & Cotsarelis, 1999).

The short resting phase or catagen phase occur after the end of anagen phase. The duration of this phase is 1-2 weeks. The discontinuation of protein and pigment production is the characteristic of this phase, involution of the hair follicle and substantial extracellular matrix-remodeling, and condensation of the dermal papilla (Paus & Cotsarelis, 1999) resulting in upward movement of the dermal papilla within the connective tissue sheath of the follicle. In telogen phase (3-6 weeks), the hair shaft develops into a club hair, which is held tightly in the bulbous base of the follicular epithelium, before it is eventually shed from the follicle, usually as a result of combing or washing. After that, the hair growth cycle will return into anagen phase again.

2.1.3 Dermal papilla cells in the controlling of hair growth cycle

The dermal papilla cells (DPCs), specialized mesenchymal cell, are located at the base of hair follicle. DPCs have been recognized as functioning cells to secrete the signals that control hair follicle and these cells are hypothesized as the key targets of androgen in androgenetic alopecia (AGA) pathophysiology (Lai, Chang, Lai, Chen, & Chang, 2012; Randall, Thornton, Hamada, & Messenger, 1992). In the development of hair follicle, mesenchymal cell aggregate immediately below the epidermis. These aggregates locate the location of the new hair follicle. In anagen phase, the DPCs stay deep in the subcutaneous layer of the skin and is surrounded by hair matrix cells. In catagen, the DPCs move up to the dermis as the epithelial strand regresses. As the

secondary hair germ forms from the bottom of the bulge at the end of catagen, the DPCs come to rest immediately adjacent to these cells that will form the next lower hair follicle.

Hair regrowth cycle begins when the signals from DPCs reach the multipotent epidermal stem cells in the bulge region of hair follicle (Leiros, Attorresi, & Balana, 2012). The function and ability of DPCs to induce the regrowth of hair as well as to maintain the hair at growing phase were shown to depend on stem cell properties of DPCs. Sox-2 is one of stem cell-related transcription factors found in DPCs and functioning in the pluripotency maintenance. This Sox-2 plays the important role on hair growth demonstrated in transgenic animals and the lack of this transcription factor resulted in an impairment of hair shaft outgrowth (Clavel et al., 2012; Driskell, Giangreco, Jensen, Mulder, & Watt, 2009). Besides, the human stem cells protein

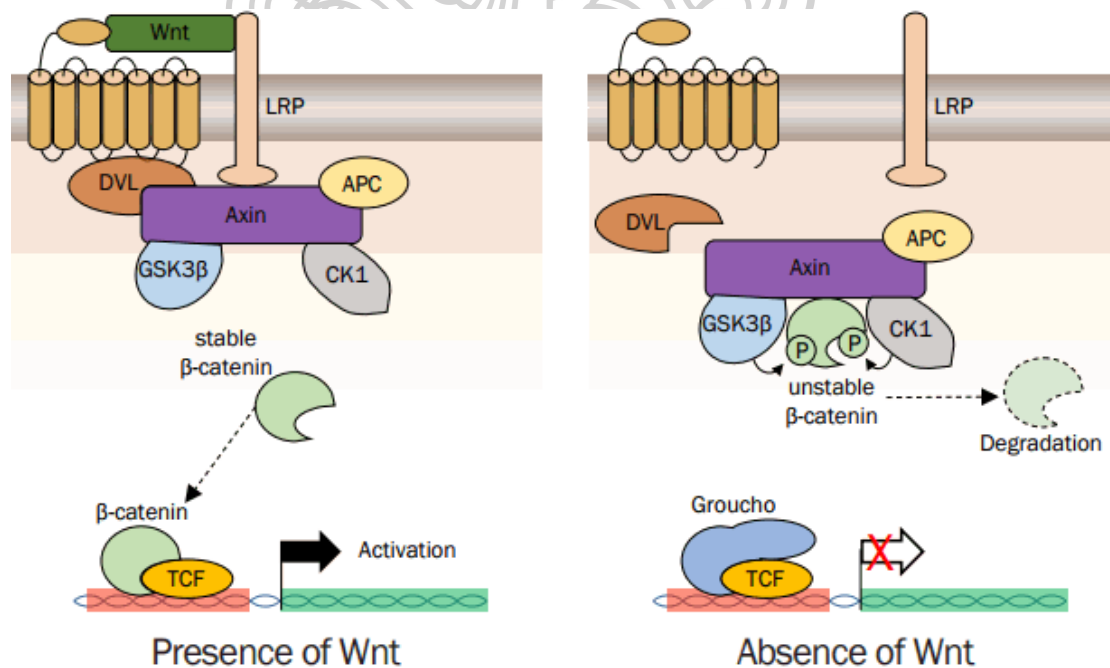


Figure 5 Schematic view of Wnt/β-catenin signaling.

marker such as CD133 implicate hair inductive property of DPCs (Driskell et al., 2009).

The activation of Wnt/ β -catenin signaling (Figure 5), especially Wnt10b is essential for hair development, hair cycling and hair regrowth (Kishimoto, Burgeson, & Morgan, 2000). Also, this signal was shown to regulate DPC inductive properties (Shimizu & Morgan, 2004). Wnt/ β -catenin has been shown to be the early trigger of DPCs in the induction and initiation of hair follicle formation (Lu, Wu, Chu, Bi, & Fan, 2016). Together, the active agents that induce or enhance stem cell signals and properties of DPCs may benefit the therapeutic treatment of hair loss

In 2016, Herman, et al. had reviewed the mechanism of action of herb and their active constituents use in hair loss treatment. There are many mechanism involving in control of hair growth cycle of herbs and their active constituent use in the treatment of hair loss and it may use to clarify some results in the study (Figure 6) (Herman & Herman, 2016).

In general, mechanisms involving in the stimulation of hair growth were

- (1) Insulin-like growth factor-1 (IGF-1)
- (2) Vascular endothelial growth factor (VEGF)
- (3) Epidermal growth factor (EGF)
- (4) Fibroblast growth factor-2 (FGF-2)
- (5) Endothelial nitric oxide synthase (eNOS)
- (6) Wnt/ β -catenin signaling pathway
- (7) Prostaglandin E (PGE),

(8) Prostaglandin F (PGF),

whereas the mechanism engaging to inhibit hair growth were

(1) 5 α -reductase

(2) Transforming growth factor beta (TGF- β)

(3) Fibroblast growth factor-5 (FGF-5)

(4) Prostaglandin D2 (PGD2)

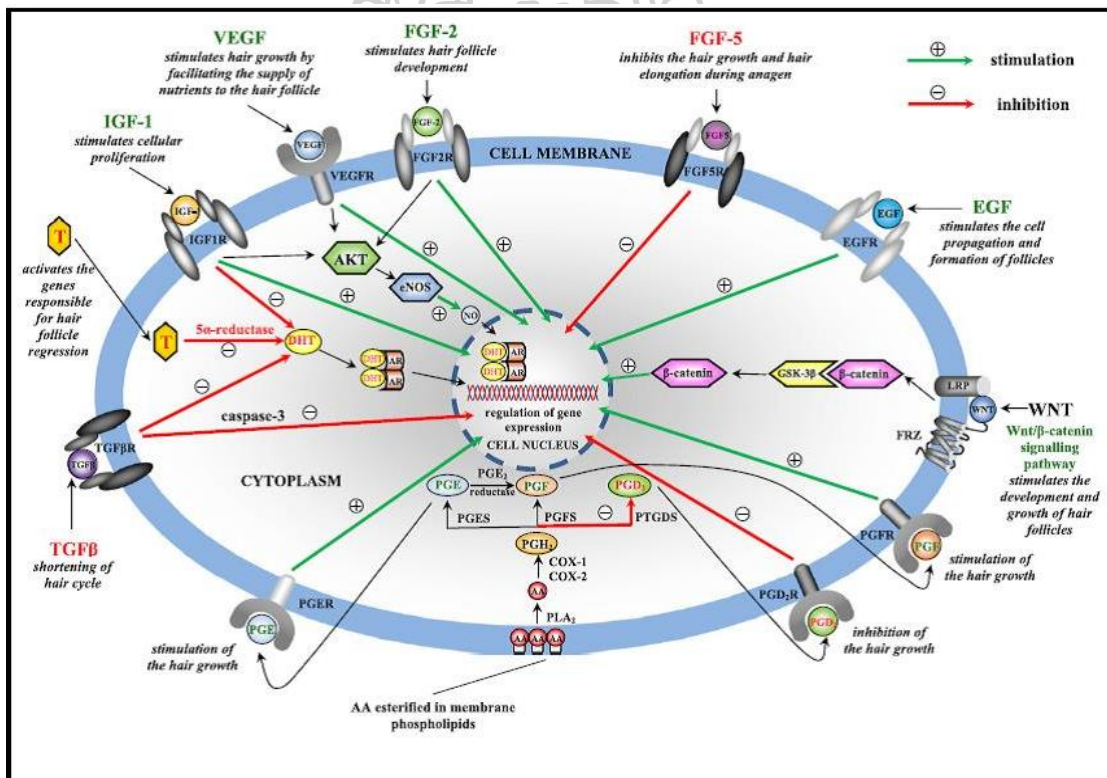


Figure 6 Different mechanism of action of herb and their active constituents

2.2 Androgenetic alopecia (AGA)

2.2.1 Pathophysiology of AGA

Androgenetic alopecia or AGA, which is the common type of alopecia, is a hereditary thinning of the hair induced by androgens in genetically susceptible men and women. This condition is also known as male-pattern hair loss or common baldness in men and as female-pattern hair loss in women. The thinning of hair usually begins

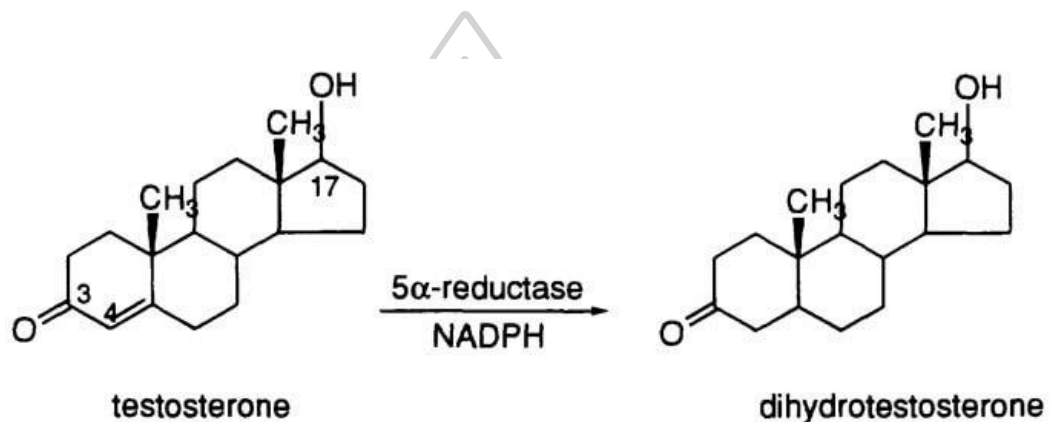


Figure 7 The conversion of testosterone to dihydrotestosterone by 5 α -reductase enzyme

(<https://selfhacked.com/app/uploads/2016/06/dht-1.jpg>)

between the ages of 12 and 40 years in both sexes, and approximately half the population expresses this trait to some degree before the age of 50.

The pathophysiology of AGA initiates with the androgenic hormones, testosterone (T) and dihydrotestosterone (DHT), which are the most important in regulating the anagen duration and hair matrix volume. DHT is formed by the peripheral conversion of testosterone by 5 α -reductase (Figure 7). DHT binds to androgen receptor on susceptible hair follicles and enlarges follicles in the beard, chest and limbs and miniaturizes follicles in the bitemporal region. In genetically susceptible

patients, DHT can cause miniaturization in the vertex and frontal hairline leading to AGA-patterned thinning. There are two isoforms of 5 α -reductase, Type 1 and type 2. 5 α -reductase type 1 can be found in sebaceous gland (skin and scalp) and liver while 5 α -reductase type 2 can be found in prostate gland, seminal vesicle, epididymis, hair follicle and also liver. The conversion of T to DHT in AGA occurs at the hair follicles and elicited by a type II 5 alpha-reductase enzyme type 2 (Kaufman & Dawber, 1999).

Currently there are two medications approved by the US FDA for hair regrowth and reversal of miniaturization of AGA, oral finasteride and topical minoxidil. Minoxidil is the current topical standard treatment of hair loss. Firstly, minoxidil is used as an oral antihypertensive medication, its association with hypertrichosis leading to its development as a topical therapy for AGA. The mechanism of action of minoxidil is unknown; however it is associated with vasodilation, angiogenesis and enhanced cell proliferation, probably mediated via potassium channel opening. Hypothetically, by widening blood vessels and opening potassium channels, it allows more oxygen, blood, and nutrients to the follicle. This may cause follicles in the telogen phase to shed, which are then replaced by thicker hairs in a new anagen phase. Oral finasteride is an inhibitor of 5 α -reductase type 2. Oral administration of finasteride 1 mg per day presents to decrease hair loss, increase hair growth, and improve the appearance of hair as compared to placebo.

2.2.2 Finasteride in the treatment of AGA

Finasteride (FN) is a synthetic 4-azasteroid compound, widely used for benign prostatic hyperplasia at low dose (1 mg/day) and for prostatic cancer at higher dose (5 mg/day). Recently, oral administration of FN has been used for the treatment of various

dermatological and follicular disorders such as acne, seborrhea and mostly male pattern baldness. 1 mg/day oral FN has been approved for the treatment of AGA (Monti, 2014).

The chemical structure and mechanism of FN presents in Figure 8.

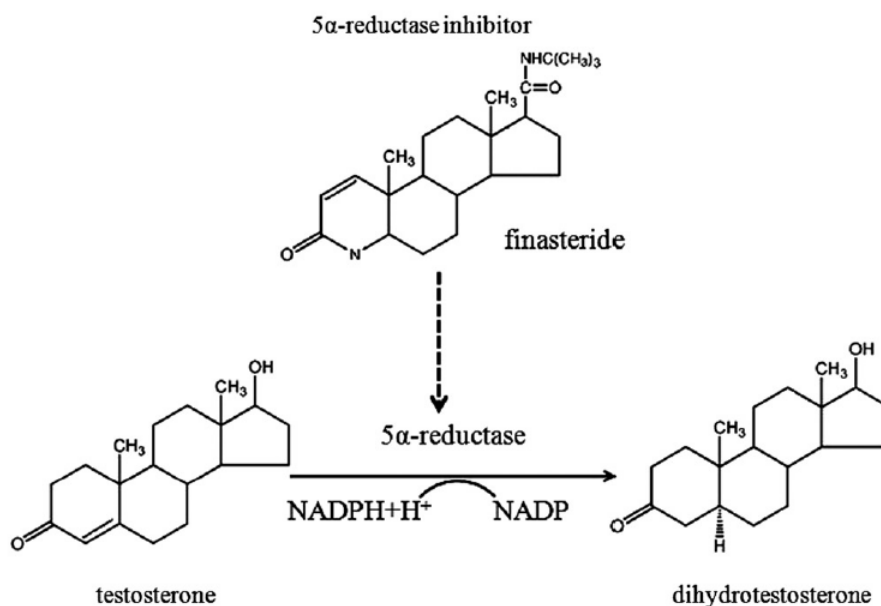


Figure 8 Structure of FN and mechanism of 5 α -reductase enzyme inhibitor

The chemical formula of FN is C₂₃H₃₆N₂O₂ with the molecular weight 372.6. This molecule is lipophilic drug with log P 3.03, and it is in the BCS class II (low solubility and high permeability). FN is weakly acidic drug with pKa 5.9. The mechanism of action is a competitive and selective inhibition of the 5 α -reductase type-2 isoenzyme (Libecco & Bergfeld, 2004; Tabbakhian et al., 2006). In 1999, Drake et al., reported that 1 mg oral administration of FN daily can decrease the scalp DHT and serum DHT concentration at 64% and 68%, respectively, and inhibit the miniaturization of hair follicle.

However, oral administration of FN has many undesirable systemic side effects such as mood disturbance, gynecomastia, decreased libido, erectile dysfunction and

ejaculation disorder. In the clinical studies, 2% of patients reported sexual side effects that can be resolved with discontinuation of the drug. With these reason, FN topical formulation is preferable to oral.

Many recent year, FN has been investigated and developed to use for topical and transdermal delivery. Many attempts have been made to enhance drug deposition in the hair follicle using delivery systems such as liposomes, niosomes (Tabbakhian et al., 2006), liquid crytaline nanoparticles (Madheswaran et al., 2013), polymersomes (Caon et al., 2014), ethosomes (Sujatha S et al., 2016). Many researchers reported about novel delivery systems that aim to enhance the penetration of the drug in to the skin and pilosebaceous unit and control the release of the drug in hair follicle.

In 2006, Tabbakhian et al. evaluated the effects of composition and physical state of liposome and niosome on the extent of FN permeation through and deposition into the different strata of the hamster flank and ear skin. The study presented that the MLVs (multilamella vesicles, liposome and niosome) had a significantly greater retaining effect on FN permeation compared to hydroalcoholic solution, and negatively charged MLVs facilitated the deposition of FN into sebaceous gland region.

The other novel carriers for topical delivery of FN had been developed in 2014 by Caon et al. FN had been loaded in polymersome made from chitosan-decorated polystyrene-b-poly (acrylic acid) to provide high FN retention in the dermis and epidermis while allowing some control of drug release. The results of this study presented that this FN-loaded polymersomes represent a promising alternative for topical administration of FN since they improve the drug penetration in the skin and increase its accumulation in the skin layer. Moreover, polymersomes decorated with

chitosan seem to be more appropriate option since they provided greater drug retention in the skin and better control over the drug release profile.

Many studies demonstrated many transdermal drug delivery systems and microemulsions (MEs) are another one system that is interested by the researchers because of the uncomplicated preparation with thermodynamic stability. Moreover they can enhance the solubility of lipophilic drug including FN.

2.3 Transdermal drug delivery technology

Transdermal drug delivery system (TDDS) is the passage of therapeutic quantities of drug substances through the skin by intracellular, intercellular or transfollicular pathway (Figure 9), into the general circulation for their systemic effect. The advantages of transdermal delivery include convenience, improved patient compliance, and prompt termination of dosing and avoidance of the first-pass effect. In addition, transdermal systems are non-invasive and can be self-administered. Nowadays, TDDS is the alternative route to oral administration and injection.

The first generation of TDDS is transdermal patch that have thus far been in clinical use. First-generation delivery drug substance must have low-molecular weight, lipophilic and efficacious at low doses.

The second generation of TDDS aim to enhance skin permeability by

- (i) reversibly disrupting stratum corneum structure
- (ii) provide an added driving force for transport into the skin
- (iii) avoid injury to deeper, living tissues

Therefore, the enhancement methods developed in this generation are conventional chemical enhancers, iontophoresis and non-cavitation ultrasound. Liposomes and microemulsions have been used as chemical enhancers of high molecular

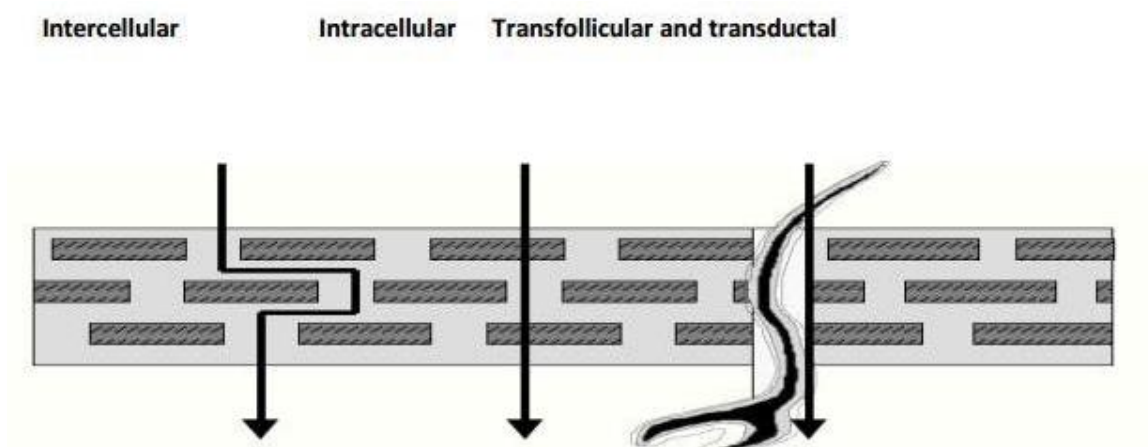


Figure 9 Transdermal delivery pathway of the substances
<http://advancejournals.org/Advances-in-Biology-and-BioMedicine/wp-content/uploads/sites/5/2016/03/b6.jpg>

The third generation of TDDS aim to make significant impact on drug delivery because it targets its effects to the stratum corneum. TDDS in this generation include the combination of chemical enhancer, biochemical enhancer, electroporation and microneedles (Prausnitz & Langer, 2008).

2.4 Microemulsions

Microemulsions (MEs) were developed by Hoar and Schulma in 1940s by titrating the milky emulsions with hexanol then the transparent water-in-oil dispersions were obtained. MEs consist of oil phase which is the most important component of MEs because it can solubilize the required dose of the lipophilic drug, aqueous phase which contains hydrophilic active ingredients and preservatives, and

surfactant which usually combines with co-surfactant (alcohol or non-alcohol) using for stabilizing the MEs. Various types of surfactants can be used in MEs i.e. cationic, anionic, non-ionic and zwitterionic.

Microemulsion systems have the advantages over conventional emulsions. They are thermodynamically stable liquid systems and spontaneously formed. In addition, preparation of MEs requires no energy use, therefore it is easy to prepare. At low or high temperature, MEs may become unstable but it is the reversible reaction when the temperature returns in stable range it becomes as it is. The use of MEs as delivery systems can improve the efficacy of a drug, allowing the total dose to be reduced and thus minimizing side effects. However, large amount of surfactant are used in MEs to stabilize the system, skin irritation study should be concerned. The differences between macroemulsion and microemulsion are presented in Table 1.

Table 1 The differences between macroemulsions and microemulsions

Macroemulsion	Microemulsion
They are lyophobic in nature	They are the border between lyophilic and lyophobic
Droplet diameter 1 to 20 mm.	Droplet diameter 10 to 100 nm.
Macroemulsion droplets exist as individual entities.	Microemulsion droplets disappear within fraction of seconds.
Emulsion droplets are roughly spherical droplets of one phase dispersed into the other phase.	Microemulsions are the structures of various droplets like bi-continuous to swollen micelles.
Macroemulsions requires quick agitation for their formation.	Microemulsions are obtained by gentle mixing of ingredients.
Most of the emulsions are opaque (white) in appearance.	Microemulsions are transparent or translucent in nature.

2.4.1 Type of MEs

According to Winsor, there are four types of microemulsion phases exists in equilibria, these phases are also referred as Winsor phases. They are,

1. *Oil- in- water (O/W) microemulsion or winsor I*: oil droplets surrounded by a surfactant (and may be co-surfactant) film that forms the internal phase dispersed in the continuous aqueous phase.

2. *Water –in- oil (W/O) microemulsion or winsor II*: water droplets are dispersed in the continuous oil phase. These can call “reverse micelles”, where the polar-headgroups of the surfactant are facing into the droplets of water and non-polar tails facing into the oil phase.

3. *Bicontinuous microemulsion or winsor III*: the amount of water phase and oil phase are similar, both water and oil exist as a continuous phase. Transitions from O/W to W/O microemulsions may pass through this bicontinuous state.

4. *Single phase homogeneous mixture or winsor IV*: oil, water and surfactants mixture are homogenously mixed.

2.4.2 Effects of ME compositions

Oil phase

Many substances have been used in oil phase such as ester of fatty acid or fatty alcohol, digestible oil from the family of triglyceride, including soybean oil, sesame seed oil, cotton seed oil and safflower oil. Other than the conventional oils (neutral, non-polar substances), many oils that have skin penetration- enhancing properties were selected. Isopropyl myristate and oleic acid are the most frequency used in

microemulsion. Terpene group substance such as limonene which has skin penetration-enhancing properties is one of favorite substance used in oil phase of microemulsion. The component of oil phase influence the three main parameter of microemulsion: drug release, drug solubilization (drug loading capacity) and the skin permeability (Djekic & Primorac, 2008). However, oil phase most chooses from drug solubilization, some previous study suggests that maximum concentration of drug solubility did not indicate the maximum skin penetration of the drug but the composition in oil may be have more affect to microemulsion properties (Rhee, Choi, Park, & Chi, 2001; Zhang & Michniak-Kohn, 2011).

Surfactant and co-surfactant mixture (S_{mix})

Of course that the concentration and ratio between surfactant and co-surfactant influence to the microemulsion properties, size, shape of aggregates and water solubility (Djekic & Primorac, 2008; Heuschkel, Goebel, & Neubert, 2008; Hosmer, Reed, Bentley, Normoo, & Lopes, 2009; Lawrence & Rees, 2000). The structure and the lipophilic of surfactant most affect to drug release of microemulsion and it can influence to skin permeation if the release is the limiting step of penetration. Surfactant and co-surfactant can enhance the skin penetration by disrupt the stratum corneum and increasing the ratio of S_{mix} content in microemulsion can enhance the transport across the skin (Hosmer et al., 2009; Huang et al., 2008). Co-surfactant often used in MEs are short-length alcohols but the skin permeability effect of them are not clear. In 2008, Maghraby had study the flux of hydrocortisone microemulsion across rabbit skin and presented that ethanol showed the greatest effect followed by propylene glycol (PG) and isopropanol (El Maghraby, 2008). Another study indicated that the increasing of

chain length of the co-surfactant from ethanol to isopropanol (Figure 10) can decrease the flux of curcumin and increase in the number of hydroxyl groups from isopropanol to propylene glycol (Figure 10) increased the skin permeation flux (Liu, Chang, & Hung, 2011).

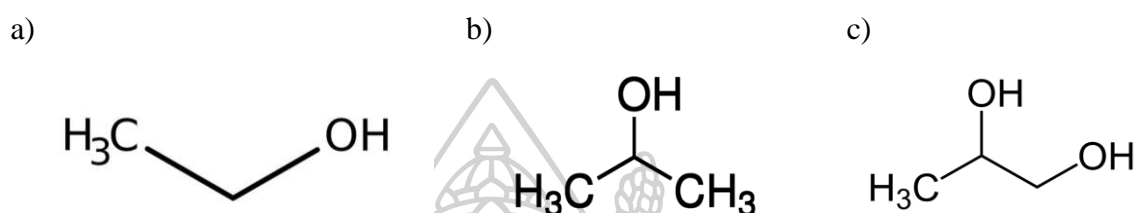


Figure 10 Molecular structure of a) Ethanol, b) Isopropanol and c) PG

Water phase

The content of water can affect the internal structure of MEs which influenced the drug delivery to the skin. The increasing of water content in microemulsion formulation can transform W/O to O/W and lead to:

- i) changing in the thermodynamic activity of the drug especially lipophilic drug
- ii) improved the skin hydration
- iii) changing in skin permeability

However it depends on the various concentration of the penetration enhancer included in oil phase and Smix. Delgado-Charro et al, 1997., presented that MEs with high content of water phase and O/W structure also improved sucrose delivery, while ketoprofen and lidocaine which are lipophilic drugs showed the enhancement of steady-state permeation flux and cumulative permeation when the water content was increased

(the microstructure was transformed from W/O to O/W) (Zhang & Michniak-Kohn, 2011).

2.4.3 The mechanism of MEs in penetration enhancement

Various mechanisms have been used to describe the skin penetration enhancement of MEs, mostly are combination mechanisms. The first most important property is the small droplet size and large area to volume ratio of MEs. With the small droplet size range between 100-300 nm could enhance transdermal delivery of diazepam-loaded MEs compared to standard emulsions (Schwarz, Weisspapir, & Friedman, 1995).

Another mechanism is the action of individual components of MEs. Surfactant, oil phase and other skin penetration enhancer in the formulation can increase the skin permeation of the drug by disruption the lipid structure of stratum corneum or increasing the solubility of the drug concentration in the skin.

In addition, increasing in skin hydration is used to describe the the skin penetration enhancement of MEs. The hydration of stratum corneum is increased by the increasing of percentage of water content in MEs (Williams & Barry, 2004). Moreover, high drug loading capacity is another one important property which has been used to explain the enhancement in skin penetration of MEs.

2.4.4 Microemulsion applications in pharmaceutical dosage forms

Microemulsion systems can be used in various types of pharmaceutical dosage forms including such as:

- (1) parenteral dosage form especially intravenous route
- (2) oral delivery to improve the absorption of the drug
- (3) topical delivery which can avoid the hepatic first-pass metabolism, salivary and degradation of the drug in stomach and related toxicity effects.
- (4) ocular and pulmonary delivery to attain prolong release profile of the drug
- (5) other pharmaceutical applications (nasal delivery and brain targeting)

In 2013, Fouad et al. developed and optimized microemulsions and poloxamer microemulsion-based gel (PMBG) to enhance transport of diclofenac epolamine (DE) into the skin forming in-skin drug depot for sustained transdermal delivery of drug. The optimized ME formulation was composed of 30% Capryol[®], 50% S_{mix} (a mixture of Labrasol[®]/Transcutol[®], 1:2 w/w) and 20% water. PMBG and Flector[®] gel, the optimized ME showed the highest cumulative amount of DE permeated after 8 h and the release of DE from the skin was observed even after removal of ME applied to the skin (Fouad, Basalious, El-Nabarawi, & Tayel, 2013).

For parenteral administration, Pineros et al., developed the analgesic and anti-inflammatory controlled-released injectable microemulsions utilizing lysine clonixinate (LC) as model drug and generally regarded as safe (GRAS) excipients. The results showed that the MEs consisting of Labrafil[®]/Lauroglycol[®]/Polysorbate 80/water with LC (56.25/18.75/15/10, w/w) could be a promising formulation after buccal surgery due to their abilities to control the drug release and significantly achieve greater analgesic and anti-inflammatory effect over 24 h (Pineros, Slowing, Serrano, de Pablo, & Ballesteros, 2017).

CHAPTER 3

MATERIAL AND METHODS

3.1 Materials

3.2 Equipment

3.3 Methods

3.3.1 Effect of finasteride to human dermal papilla cells

3.3.1.1 Cell culture

3.3.1.2 Cell viability assay

3.3.1.3 Nuclear staining assay

3.3.1.4 Aggregation behavior evaluation

3.3.1.5 Scanning Electron Microscope (SEM)

3.3.1.6 Western blot analysis

3.3.1.7 Immunocytochemistry

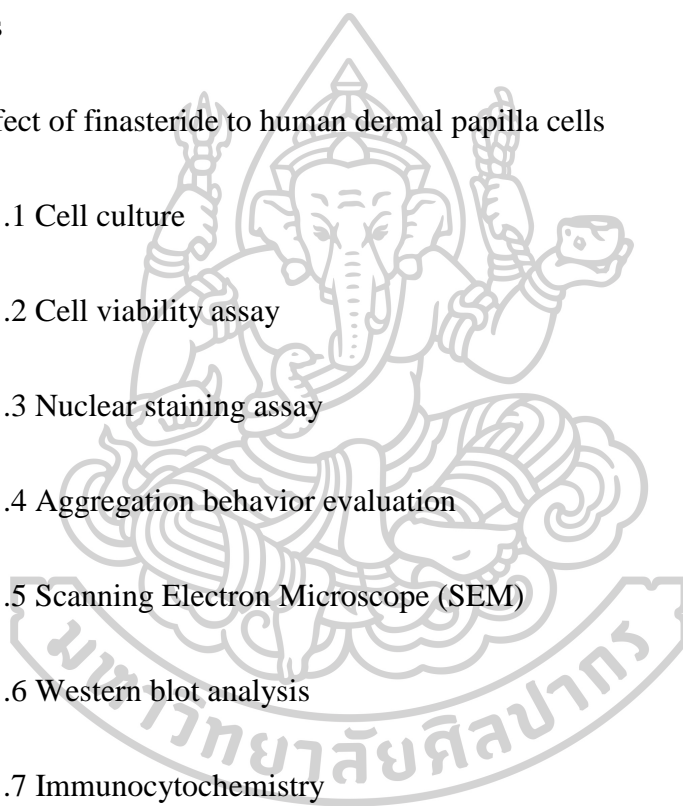
3.3.2 Preparation of FN-loaded MEs

3.3.2.1 Screening of ME ingredients by solubility study

3.3.2.2 Construction of pseudoternary phase diagram

3.3.2.3 Preparation of FN-loaded MEs

3.3.2.4 Optimization of FN-loaded MEs



3.3.3 Characterization of FN-loaded MEs

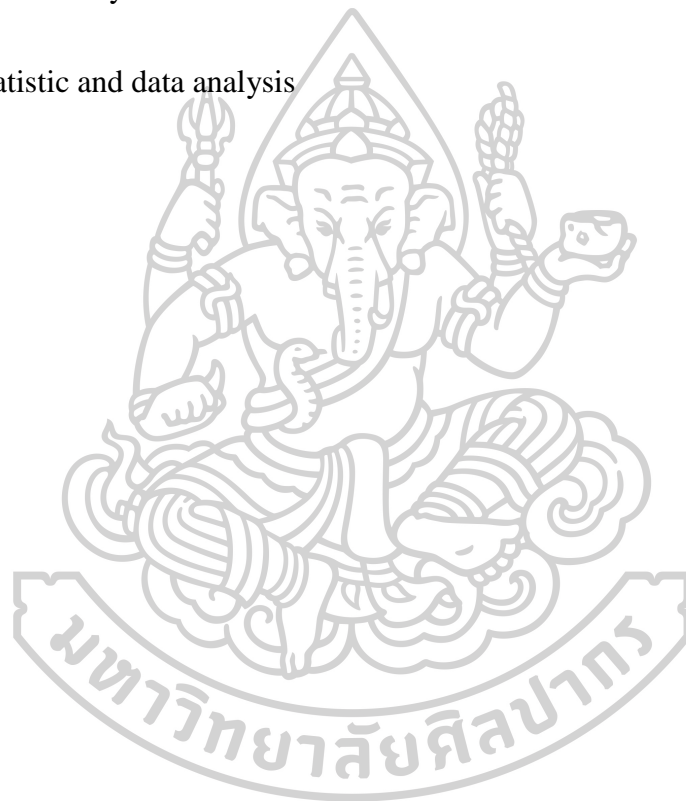
3.3.3.1 Droplet size, size distribution conductivity and pH

3.3.3.2 Drug loading efficiency

3.3.4 *In vitro* skin permeation study

3.3.5 HPLC analysis

3.3.6 Statistic and data analysis



3.1 Materials

1. 3- (4,5- Dimethylthiazol- 2- yl) - 2,5- diphenyltetrazolium bromide; MTT (Invitrogen, Carlsbad, CA, USA).
2. Alexa Fluor 488/594 conjugated secondary antibody (Invitrogen, Carlsbad, CA, USA).
3. Bergamot oil (Namsiang Ltd., Bangkok, Thailand)
4. Carjuput oil (Namsiang Ltd., Bangkok, Thailand)
5. Cinnamon oil (New Sang Thong Trading L.P., Bangkok, Thailand)
6. Dimethylsulfoxide; DMSO (Sigma (St. Louis, MO, USA)
7. Dulbecco's Modified Eagle's Medium;DMEM (Gibco Grand Island, NY, USA)
8. Fetal bovine serum; FBS (Life technologies, MD, USA)
9. Finasteride; FN (Sigma, St. Louis, MO, USA)
10. Hoechst 33342 and propidium iodide (PI) were obtained from (Molecular Probes Inc., Eugene, OR, USA).
11. Human dermal papilla primary cells culture 1 (Applied Biological Materials Inc., Richmond, BC, Canada)
12. Human dermal papilla primary cells culture 2 (Celprogen Inc., CA, USA)
13. Immortalized dermal papilla cells (Applied Biological Materials Inc, Richmond, BC, Canada)
14. Immobilon Western Chemiluminescent HRP substrate (Thermo Fisher Scientific Inc., Rockford, IL, USA)
15. Lavender oil (Namsiang Ltd., Bangkok, Thailand)

16. Medium chain triglyceride: MCT
17. Olive oil (Namsiang Ltd., Bangkok, Thailand)
18. Penicillin/Streptomycin sterile solution (Life technologies, MD, USA)
19. Polyethylene glycol 400 (Namsiang Ltd., Bangkok, Thailand)
20. Polyethylene glycol sorbitan monolaurate 20
21. Propylene glycol (Namsiang Ltd., Bangkok, Thailand)
22. Rabbit monoclonal antibodies for integrin- β 1, β -catenin, phosphorylated ATP-dependent tyrosine kinase (p-Akt, Ser 473), Nanog, Sox-2, CD44, β -actin, and HRP-conjugated secondary antibodies (Cell Signaling, Denver, MA, USA)
23. All other chemicals were commercially available and analytical grade.
 - Disodium hydrogen phosphate dodecahydrate; $\text{Na}_2\text{HPO}_4 \cdot 12\text{H}_2\text{O}$ (Ajax Finchem, Australia)
 - Chloroform; CHCl_3 (RCI Labscan, Bangkok, Thailand)
 - Methanol; MeOH (Fisher Scientific UK, Loughborough, Leicester, UK)
 - Potassium chloride; KCl (Ajax Finchem, Australia)
 - Potassium dihydrogenphosphate; KH_2PO_4 (Ajax Finchem, Australia)
 - Sodium chloride; NaCl (Ajax Finchem, Australia)
 - Triton[®] X-100 (Amresco[®], Solon, Ohio, USA)
24. Sprague Dawley Rat, Female, 5-6 weeks (National Laboratory Animal Center, Mahidol University, Nakhon Pathom, Thailand)

3.2 Equipments

1. Aluminium foil (Diamond, VA, USA)
2. Analytical balance (Model CP224S and CP3202S, SARTORIOUS, Germany)
3. Bath-type sonicator (5510J-DTH Branson Ultrasonics, CL, USA)
4. Beaker (PYREX[®], USA and Duran[®], Germany)
5. Cellulose acetate filter 0.45 μm , 47 mm (Tokyo Roshi Kaisha, Tokyo, Japan)
6. Cellulose n filter 0.45 μm , 47 mm (Sartorius AG, Goettinaen, Germany)
7. Centrifuge (MULTIFUGE 1S-R, Kendro laboratory product, Hanau, Germany)
8. Cylinder (PYREX[®], USA)
9. Desiccator
10. Fine forceps
11. Fluorescence microscope (Olympus IX 51 with DP70, Olympus America Inc., Central valley, PA)
12. High-performance liquid chromatography, HPLC (Agilent 1100 series with Diode Array System, USA)
13. HPLC analytical column; ReproSil-Pur Basic C18, 5 μm , 250 x 4.6 mm (Dr, Maisch GmbH, Germany)
14. Incubated shaker
15. Labnet VX100 Vortex (MO BIO Laboratories, Carlsbad, CA)
16. Microcentrifuge tube; Eppendorf[®] tubes (CORNING[®]; Corning Incorporated, NY, USA) and holder

17. Microplate reader (Anthos, Durham, NC)
18. Multi flask shaker
19. Multi magnetic stirrer and magnetic bar (Becthai Bangkok equipment and chemical, Bangkok, Thailand)
20. Nylon membrane; 0.45 μm (Nuclepore, Whatman Inc., MA, USA)
21. Parafilm (BEMIS[®], WI, USA)
22. pH Meter (Satorious Professional Meter)
23. Photon correlation spectroscopy; PCS (Zetasizer Nano series, Malvern Instrument, UK)
24. Shell Lab shaking incubator (Sheldon Manufacturing, Cornelius, OR, USA)
25. Stirring rod
26. Scanning electron microscopy; SEM (JEOL, model JSM6400, Japan)
27. Test tube (PYREX[®], USA)
28. Thermo-regulated water bath (WiseCircu[®] Fuzzy Control System; Model WCR-P6, DAIHAN Scientific Co., Ltd., Korea)
29. Twin compact pH meter B-212 (Horiba, Chiyoda-ku, Tokyo, Japan)
30. Vertical diffusion cell (Franz diffusion cell) 5 mL
31. Volumetric flask (PYREX[®], USA)
32. Western Blotting Equipment; Mini-Trans Blot[®] Cell (Bio-Rad Laboratories, Inc., USA)

3.3 Methods

3.3.1 Effect of finasteride to human dermal papilla cells

3.3.1.1 Cell culture

Immortalized dermal papilla cells (DPCs) were obtained from Applied Biological Material Inc (Richmond, BC). Human primary dermal papilla cells 1 (HDPCs1) were obtained from Applied Biological Materials Inc. (Richmond, BC, Canada) and human dermal papilla primary cells culture 2 (HDPCs2) was purchased from Celprogen (Celprogen Inc., CA, USA). The culture method modified from Kiratipaiboon, 2015. Briefly, the cells were cultured in Dulbecco's Modified Eagle's Medium (DMEM, Gibco Grand Island, NY, USA) supplemented with 10% fetal bovine serum (FBS) and 100 units/mL of penicillin/streptomycin (Life technologies, MD, USA) at 37 °C in a 5% CO₂ atmosphere (C. Kiratipaiboon, P. Tengamnuay, & P. Chanvorachote, 2015). The cells were maintained in medium containing bovine pituitary extract 4 µl/mL, fetal calf serum 0.05 mL/mL, basic fibroblast growth factor 1 ng/mL, recombinant human insulin 5 µg/mL and phenol red 0.62 ng/mL, and 100 units/mL of penicillin/streptomycin at 37 °C in a 5% CO₂ atmosphere.

3.3.1.2 Cell Viability Assay

The cytotoxicity of FN in DPCs and HDPCs was determined by MTT assay modified from Kiratipaiboon, 2015 (Chayanin Kiratipaiboon, Parkpoom Tengamnuay, & Pithi Chanvorachote, 2015). Briefly, 1 x 10⁴ cells/well of DPCs and HDPCs were

seeded in 96 well plates and incubated overnight. Cells were treated with different concentrations of FN (0.01-100 μM) for 24 h. After indicated treatments, Cells were incubated with MTT for 3 h at 37°C. The intensity of MTT product was measured at 570 nm using a microplate reader. Cell viability was calculated as percentage relative to non-treated (control) value using the formula (1).

$$\text{Cell viability (\%)} = \frac{\text{A570 of treatment}}{\text{A570 of control}} \times 100 \quad (1)$$

3.3.1.3 Nuclear Staining Assay

Apoptotic and necrosis cell deaths were detected by Hoechst 33342 and PI co-staining. Cells (1×10^4 cells/well) were seeded onto each well of a 96 well plate and incubated overnight. Then, Cells were treated with various concentrations of FN for 24 h. After treatments, Cells were stained with 10 $\mu\text{g/ml}$ of Hoechst 33342 and 5 $\mu\text{g/ml}$ of PI for 30 min at 37°C and visualized by a fluorescence microscope (Olympus IX 51 with DP70; Olympus America Inc., Centerville, PA, USA).

3.3.1.4 Aggregation Behavior Evaluation of DPCs

DPCs were seeded at a density of 3×10^5 cells/well onto each 6 cm dishes and incubated overnight for cell attachment. Cells were cultured in the presence or absence of FN (10-100 μM). Aggregation behavior of DPCs was observed at 5 days by a phase-contrast microscope (Olympus IX 51 with DP70; Olympus America Inc., Centerville, PA, USA).

3.3.1.5 Scanning Electron Microscope (SEM)

DPCs treated with various concentration of FN (100 μ M) were fixed in 2.5% glutaraldehyde in phosphate buffer pH 7.2 for 2 hours. Cells were washed two times with phosphate buffer and once with distilled water. DPCs were dehydrated with 30%, 50%, 70%, 95% and 100% ethanol for 5 minutes/each, dried, mount and coat with gold (sputter caoter, Balzers model SCD 040, Germany). Coated cells were observed under SEM (JEOL, model JSM6400, Japan).

3.3.1.6 Western Blot Analysis

Cells were seeded at a density of 3×10^5 cells/dish onto each 6 cm dishes overnight and cultured in various concentrations of FN for 24 h. Afterward, Cells were incubated in lysis buffer containing 20 mM Tris-HCl (pH7.5), 0.5% Triton X, 150 mM sodium chloride, 10% glycerol, 1 mM sodium orthovanadate, 50 mM sodium fluoride, 100 mM phenylmethylsulfonyl fluoride and commercial protease inhibitor cocktail (Roche Molecular Biochemicals) for 30 min on ice. Cell lysates were then collected and determined for protein concentration using the Bradford method (Bio-Rad, Hercules, CA). Equal amount of proteins of each sample (70 μ g) are heated in Laemmli loading buffer at 95°C for 5 min and subsequently loaded on 10% SDS-polyacrylamide electrophoresis. After separation, proteins were transferred onto 0.45 μ m nitrocellulose membranes (Bio-Rad). Subsequently, the membranes were blocked with 5% non-fat milk in TBST (25 mM Tris HCl (pH7.5), 125 mM NaCl, 0.05% Tween-20) at 4°C overnight, membranes were incubated with specific primary antibodies at 4°C overnight. Membranes are washed 3 times with TBST for 5 min and

incubated with horseradish peroxidase coupled secondary antibodies for 2 h at room temperature. The immune complexes are detected with chemiluminescence substrate (Supersignal West Pico; Pierce, Rockford, IL, USA) and quantified using Image J software (NIH, Bethesda, MD, USA).

3.3.1.7 Immunocytochemistry (ICC)

Cells were seeded at a density of 1×10^4 cells/well in 96-well plate and incubated overnight. Cells were cultured in various concentration of FN (10-100 μM) for 24 and 48 h. Cells were fixed with 4% paraformaldehyde for 15 min and permeabilized with 0.5% Triton-X for 5 min at room temperature. After that, cells were incubated with 10% FBS and 0.1% Triton-X (blocking solution) for 1 h at room temperature. Cells were washed and incubated with specific primary antibodies (β -catenin, Nanog, and Sox-2) at 4°C overnight. Secondary antibodies at dilution 1:100 were added after washed cells with 10% FBS and 0.1% Triton-X. Hoechst 33342 in blocking solution at 1:1,000 dilution were added and incubated for 1 h at room temperature. Cells were fixed again with 4% paraformaldehyde for 10 min and were mounted with 50% glycerol. Samples were examined with fluorescence microscope (Olympus IX 51 with DP70; Olympus America Inc., Centerville, PA, USA).

3.3.2 Preparation of FN-loaded MEs

3.3.2.1 Screening of ME ingredients by solubility study

Excess amount of FN was added to each oil, surfactant or co-surfactant in tightly closed test tube. The mixture was sonicated for 1 h and then equilibrated at 25 ± 0.5 °C in a shaker for 72 h to achieve the concentration equilibrium. The mixture was filtered

through a membrane filter (0.45 μ m, 13 mm) and analyzed for FN concentration by high performance liquid chromatography (HPLC).

3.3.2.2 Construction of pseudoternary phase diagram

The pseudoternary phase diagrams of MEs were constructed by the water titration method. Three components of ME were composed of oil phase, water phase and mixture of surfactant and co-surfactant (S_{mix}). The surfactant mixtures were prepared in different weight ratio, 1:1, 2:1 and 3:1, of surfactant and co-surfactant. Then the S_{mix} was dissolved in oil phase in the vial at weight ratios of 1:9, 2:8, 3:7, 4:6, 5:5, 6:4, 7:3, 8:2 and 9:1 (oil: S_{mix}). Each vial of mixture was titrated drop-wisely with purified water from burette, and stirred with magnetic until the mixture became turbid (Cha & Shariat). The quantity of water required was recorded then the percentage of each component was calculated. The pseudoternary phase diagram was established to delineate the area of ME and plotted by using Prosim[®] ternary diagram software.

3.3.2.3 Preparation of FN-loaded MEs

From the ME area of pseudoternary phase diagram, FN was dissolved together with selected seven different ratios (Duangjit et al., 2016). Finasteride was dissolved in oil, then S_{mix} and water were added, and stirred with a magnetic stirrer. FN-loaded MEs were stored in airtight containers.

3.3.2.4 Optimization of FN-loaded MEs

Design Expert[®] software with a simplex lattice design was utilized to optimize the ME system. The casual factor consists of oil phase (X_1), surfactant system (X_2) and water phase(X_3), based on the area under the pseudo-ternary phase diagram. The upper and lower limits of each component were assigned as follows:

$$5 \leq X_1 \leq 25 (\%)$$

$$55 \leq X_2 \leq 75 (\%)$$

$$10 \leq X_3 \leq 30 (\%)$$

$$X_1 + X_2 + X_3 = 100 (\%)$$

The physicochemical characteristics of MEs such as droplet size (Y_1), size distribution (Y_2), electrical conductivity (Y_3), pH (Y_4), % EE (Y_5) and skin permeation flux (Y_6) were defined as response variables. The seven model formulations of FN-loaded MEs were prepared from ME having the biggest area of pseudo-ternary phase diagram.

3.3.3 Characterization of FN-loaded MEs

3.3.3.1 Droplet size, size distribution, electrical conductivity and pH

Droplet size, size distribution, electrical conductivity and pH of free MEs and FN-loaded MEs were characterized. The dynamic light scattering technique (Zetasizer Nano ZS, Malvern Instruments Worcestershire, UK) was used to evaluate droplet size and size distribution. Mean droplet size and PDI (Polydispersity Index) were recorded. The electrical conductivity was measured using a conductivity meter (S230 SevenCompact[™], Mettler Toledo, Switzerland). The pH of MEs was determined using

pH meter (S220 SevenCompact™, Mettler Toledo, Switzerland). Each measurement was determined in triplicate at 25° C, and then the average and standard deviation were calculated.

3.3.3.2 Drug loading efficiency

Drug loading capacity was studied by adding excess amount of FN to the ME formulations and stirring for 48 h at 25° C. The formulations were centrifuged, and the supernatant was collected. HPLC was used to analyze the concentration of saturate FN in ME formulations. The % entrapment efficiency of FN-loaded MEs was calculated.

$$\% \text{ Entrapment efficiency} = \frac{\text{The amount of drug content}}{\text{The amount of drug added to formulation}} \times 100$$

3.3.4 *In vitro* skin permeation studies

3.3.4.1 Skin preparations

Female Sprague Dawley rats (5-6 weeks old) were used for *in vitro* skin permeation study. The hair shafts were trimmed before the collection of the skin. Then, the upper part of full-thickness skin was carefully excised from the dorsal region of the rats under anesthesia of intraperitoneally injection of sodium pentobarbital (100 mg/kg). The subcutaneous fatty layer and connective tissues were carefully removed from the dermis. The prepared skins were washed with phosphate buffer saline (PBS; pH 7.4), wrapped in aluminum foil, stored at -20° C, and defrosted immediately prior to use.

3.3.4.2 Diffusion cells experiment

The rat skins were mounted between donor chamber and receptor chamber of Franz diffusion cells. The stratum corneum side was faced upward into donor chamber. The receptor chamber was filled with 6.0 mL of 50% ethanol in phosphate buffer pH 7.4, the receptor solution did not interfere the skin permeability (Charoenputtakun, Pamornpathomkul, Opanasopit, Rojanarata, & Ngawhirunpat, 2014), and then the temperature at 32°C (the temperature of the skin) (Jaipakdee et al., 2016) was controlled using water jacket. The donor chamber was filled with 1 g FN-loaded ME formulations after that 1.0 mL of the receptor medium was withdrawn from the receptor chamber at 0.5, 1, 2, 4, 6, 8 and 24 h, and the same volume of fresh medium was replaced. HPLC was used to analyze the amount of FN penetrating through the skin. The skin permeation profiles were plotted and the skin permeation flux was calculated.

3.3.5 HPLC analysis

FN in each experiment is determined by HPLC system (Agilent 1100 series, Germany) with isocratic pump, UV-vis detector at 210 nm and autosampler. The column was Reprosil-Pur Basic (C18, 5 μ m, 250x4.6 mm, Dr-Maisch, Germany) and mobile phase consists of methanol and water (70:30 (v/v)) with flow rate of 1.0 mL/min.

3.3.6 Statistically analysis

Each experiment is repeated at least three time, and the results were expressed as mean \pm S.D. Statistical analysis of all determination was performed using one-way analysis of variance (ANOVA) and Duncan's multiple range test. The *P* Values less than 0.05 was considered as statistically significant.

CHAPTER 4

RESULTS AND DISCUSSIONS

4.1 Effect of FN to DPCs

4.1.1 Effect of FN on viability of DPCs and HDPCs.

4.1.2 FN enhances aggregation pattern in DPCs.

4.1.3 Effect of FN on Wnt/ β -catenin signaling in DPCs

4.1.4 Effect of FN on stem cell markers and transcription factors

4.1.5 FN maintains the stem cell phenotypes in HDPCs.

4.2 Formulations of FN-loaded MEs

4.2.1 Screening of ME ingredients by solubility study

4.2.2 Construction of pseudoternary phase diagrams

4.2.3 Preparation of FN-loaded MEs

4.3 Characterization of FN-loaded MEs

4.3.1 Droplet size, size distribution, electrical conductivity and pH

4.3.2 Drug loading efficiency

4.4 *In vitro* skin permeation study of FN -loaded MEs

4.5 Optimization of FN -loaded MEs by computer design

4.1 Effect of FN on DPCs

4.1.1 Effect of FN on viability of DPCs and HDPCs.

Cells were treated with various concentrations of FN (0.01-100 μM) for 24 h. Cell viability and cell death were evaluated by MTT and Hoechst 33342/propidium iodide (PI) co-staining assay. FN in the concentration ranging from 0.01 to 100 μM had no significant effect on DPCs viability (Figure 11a).

Corresponding with the Hoechst/ PI apoptosis assay in Fig. 11b and 11c, FN treatment (0.01-100 μM) caused neither apoptosis nor necrosis cell death. Therefore, the non-toxic doses of FN (10-100 μM) were selected and used for the following experiments.

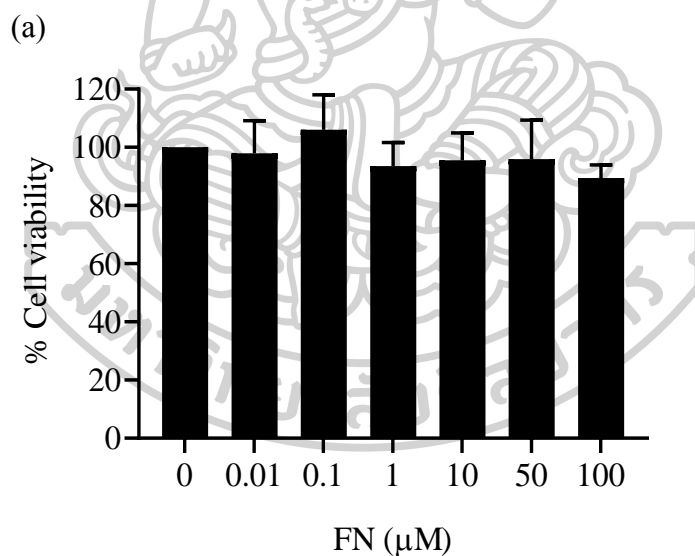


Figure 11 continue.

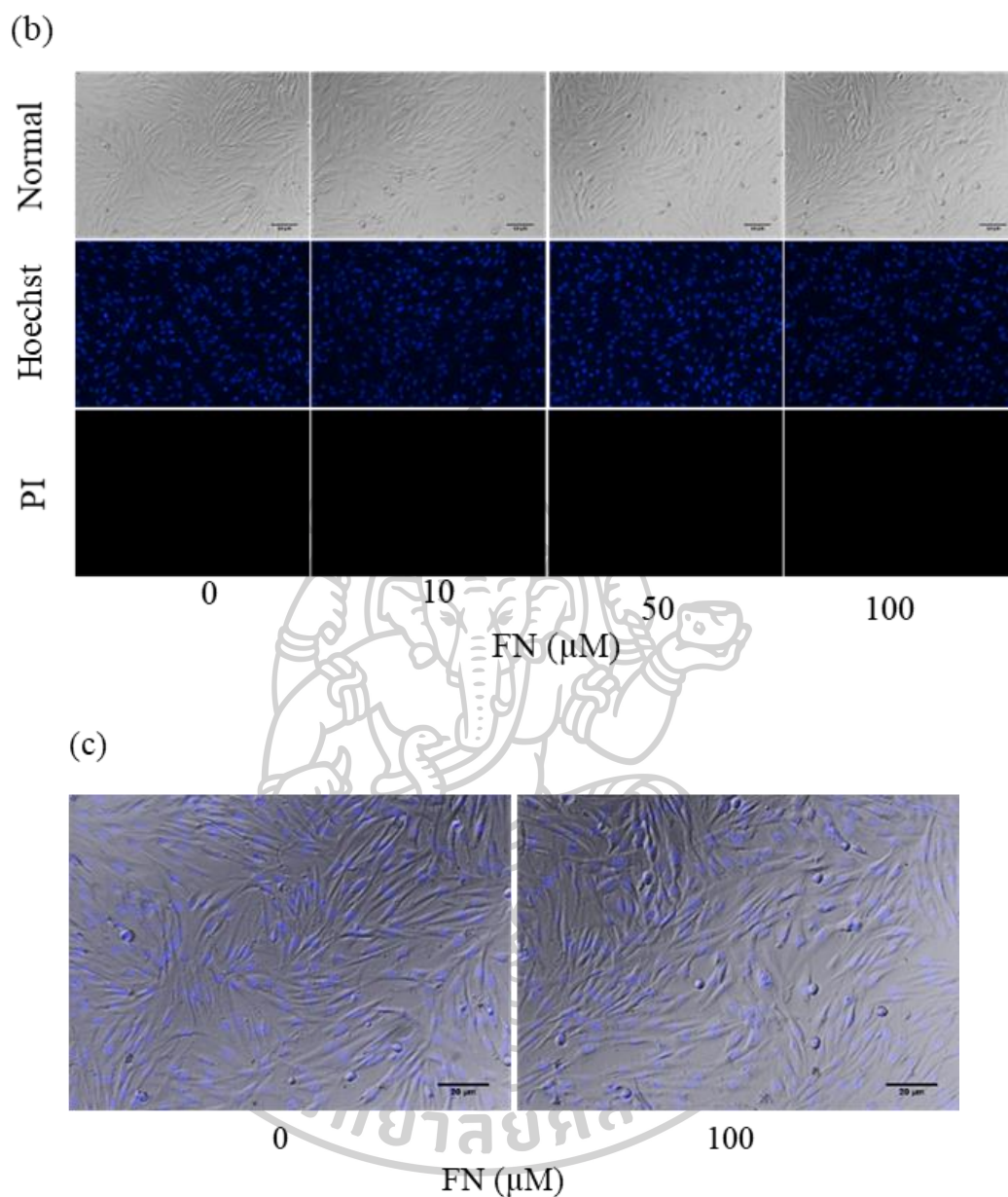


Figure 11 Cytotoxicity of FN (0.01-100 μM) on DPCs. (a) DPCs was treated for 24 h and determined by MTT assay. The data represent the means of three independent samples \pm SD. (b) Hoechst 33342/PI apoptosis assay for investigation mode of cell death after treatment for 24 h. (c) Morphology of DPCs.

For HDPCs, 2 different sources of cells were treated with various concentrations of FN (0.01-100 μM) for 24 h and cell viability was determined by MTT assay. The results showed that FN in the concentrations ranging from 0.01 to 100 μM had no significant effect on cell viability of both HDPCs (Figure 12a-b).

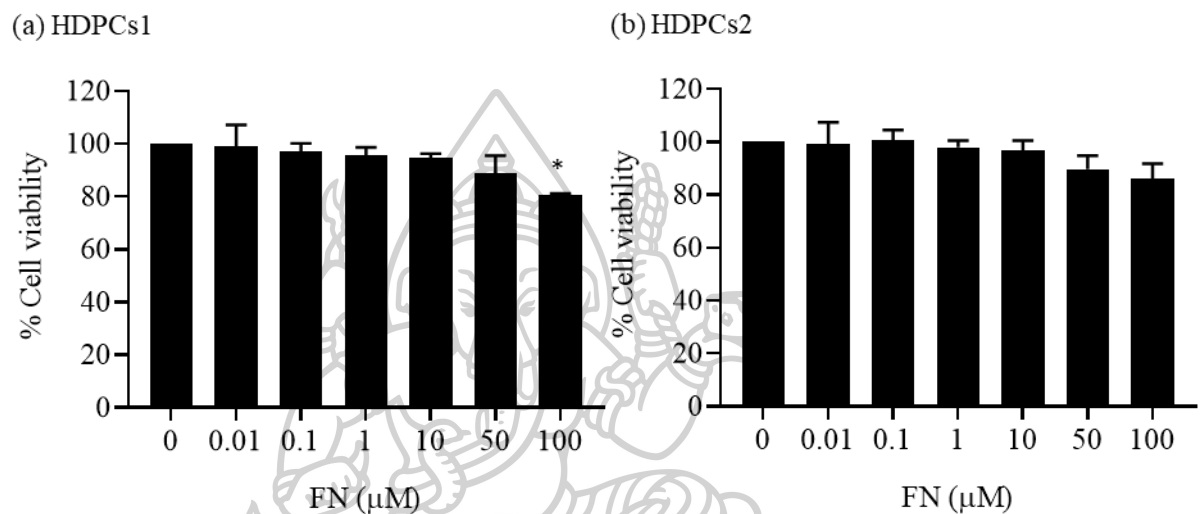


Figure 12 Cytotoxicity of FN on 2 different sources of HDPCs. Cells were treated with FN (0.01-100 μM) for 24 h and determined the cytotoxicity by MTT assay.

4.1.2 FN enhances aggregation pattern in DPCs.

DPCs have been known as multipotent stem cells and they had the ability to control hair growth (Clavel et al., 2012; Driskell et al., 2009; Driskell et al., 2012; Ito et al., 2007). Here, we explored the effect of FN on the stem cell-like aggregation behavior in DPCs. Cells were treated with FN (10-100 μM) for 5 days and the aggregation pattern of the cells was determined at day 5. The aggregation patterns of DPCs are shown in Figure 13a (by a phase-contrast microscope) and Figure 13b (by SEM).

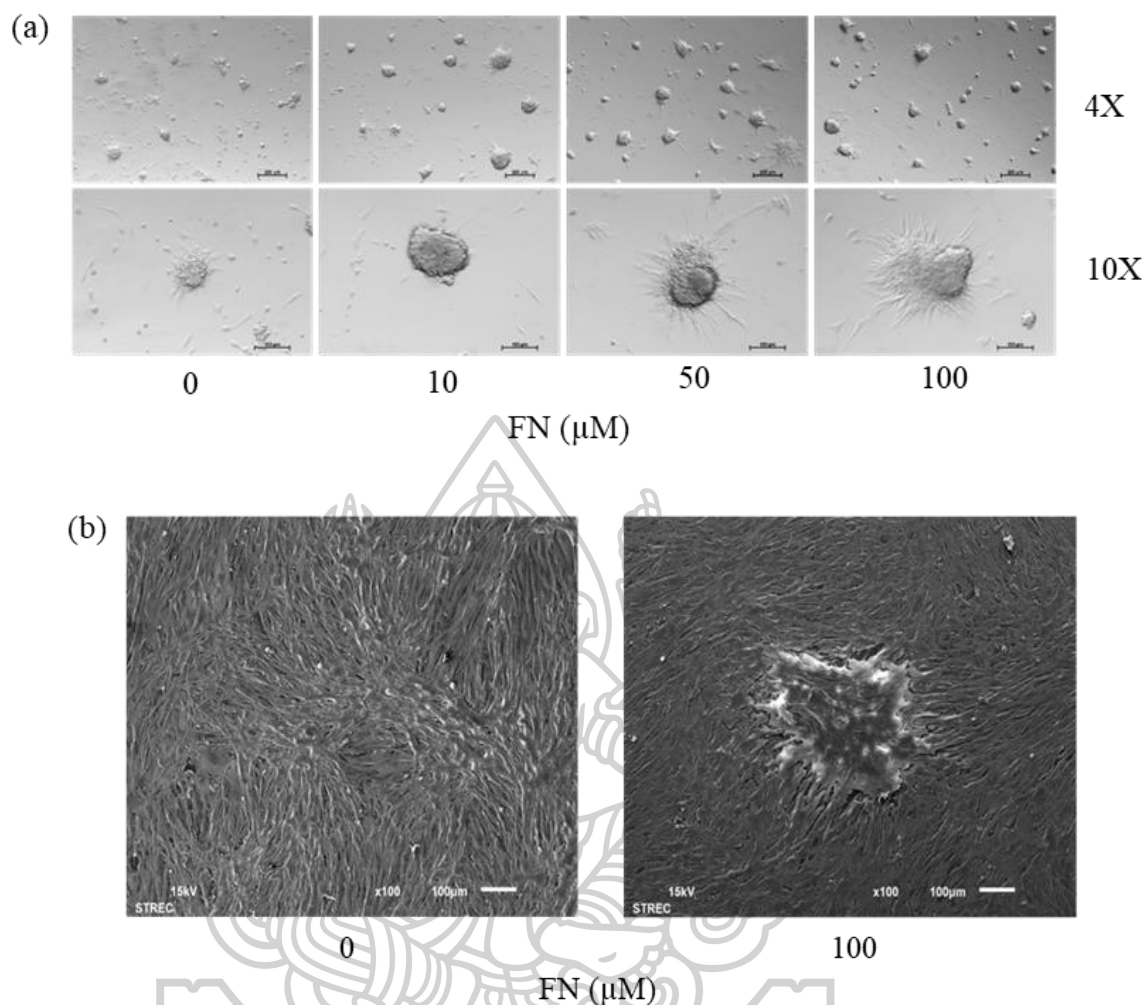


Figure 13 Aggregation behavior of DPCs. (a) Aggregation behavior of DPCs after indicated treatment with FN (10-100 μM) for five days. (b) The SEM image for aggregation behavior of DPCs after indicated treatment with FN (100 μM) for five days.

The size of aggregation cells in Figure 14a was slightly decreased in response to FN treatment when compared with the control. FN at the concentrations of 50 and 100 μM significantly increased the aggregation number of DPCs when compared with the control (Figure 14b).

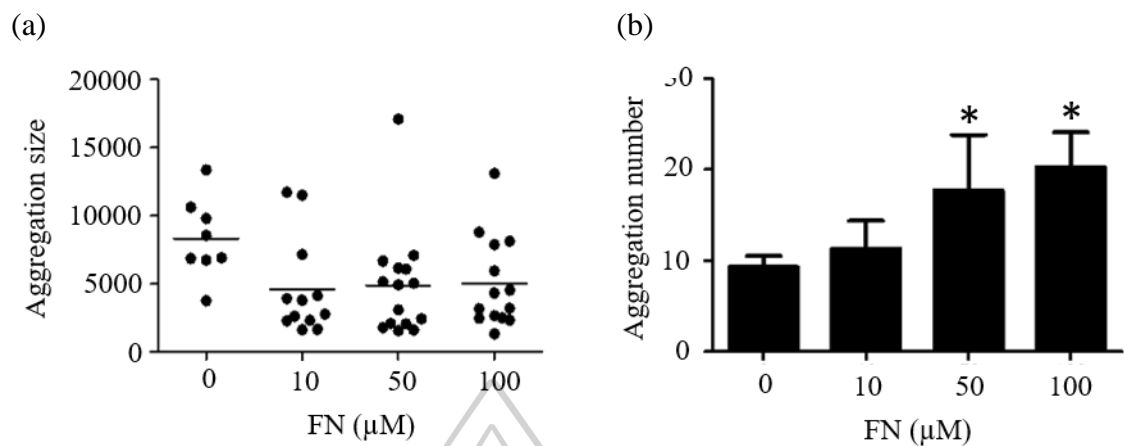


Figure 14 Effect of FN on aggregation behavior of DPCs (a) Aggregation size and (b) Aggregation number were determined by image analyzer. The data represent the mean of three independent samples \pm SD. * $P < 0.05$ versus non-treated control.

4.1.3 Effect of FN on Wnt/ β -catenin signaling in DPCs

The Wnt/ β -catenin signaling plays an important role to maintain stemness in stem cell including hair growth and hair regeneration (Merrill, 2012). Activation of Wnt/ β -catenin leads to the increase of stem cell compartment (Kretschmar & Clevers, 2017) and stimulates DPCs to induce hair growth through the induction and initiation of hair follicle formation and prolongation of anagen phase. To determine whether FN affects Wnt/ β -catenin pathway in DPCs, the signaling proteins related to Wnt/ β -catenin including activated AKT (phosphorylated AKT (p-AKT) at Ser 473) and β -catenin were analyzed by western blot analysis. FN at the concentrations of 10-100 μ M significantly increased the level of p-AKT (Figure 15a). In addition, 100 μ M FN significantly increased the protein expression level of β -catenin. The induction of cellular β -catenin level was confirmed by immunocytochemistry.

Immunocytochemistry detected by β -catenin antibody showed that FN-treated cells had an augmented level of β -catenin compared with the non-treated control (Figure 15b).

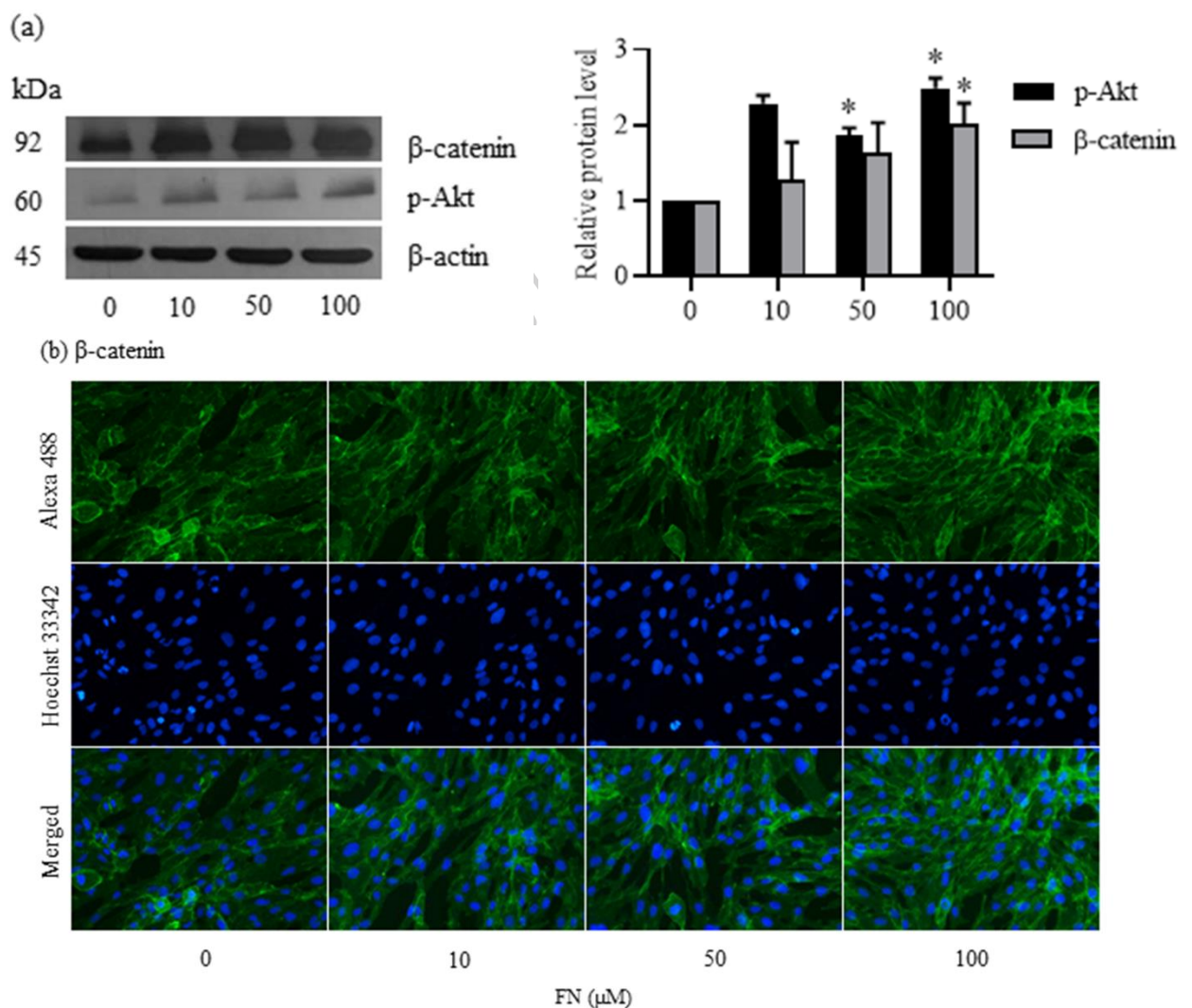


Figure 15 Effect of FN on Wnt/ β -catenin signaling in DPCs. Cells were culture in the various concentration of FN (10- 100 μ M) for 24 h. (a) After treatment, the levels of Wnt/ β -catenin signaling (p-Akt (Ser473) and β -catenin) were analyzed by western blot. β -actin was served as the loading control. The immunoblot signals were quantified by densitometry and the mean data from independent experiments were normalized to the results. The data represent the means of three

independent samples \pm SD. * $P < 0.05$ versus non-treated control. (b) Expression of β -catenin was analyzed by immunofluorescence staining.

4.1.4 Effect of FN on stem cell markers and transcription factor

Having shown that FN treatment could induce the increase of stem cell signals in DPCs. We further confirmed the above results by determining the effect of FN treatment on the stem cell markers in DPCs. Integrin- β 1 and CD44 were widely used to monitor stem cell phenotype of DPCs. The cells were cultured for 24 h in the presence or absence of non-toxic concentrations of FN. Then, the protein markers were analyzed by western blot analysis. Figure 16a shows that 100 μ M FN increased the protein level of integrin- β 1 in a dose-dependent manner, however, FN had only slightly effect on the level of CD44.

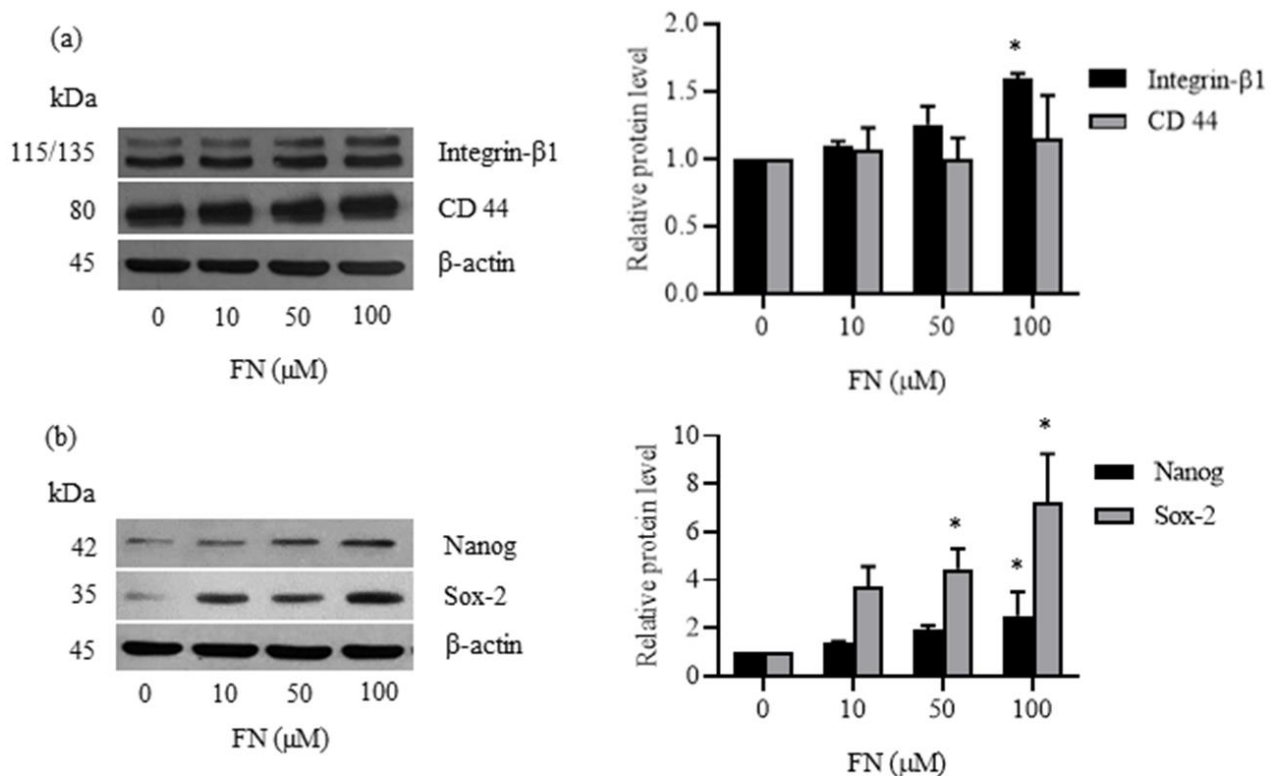
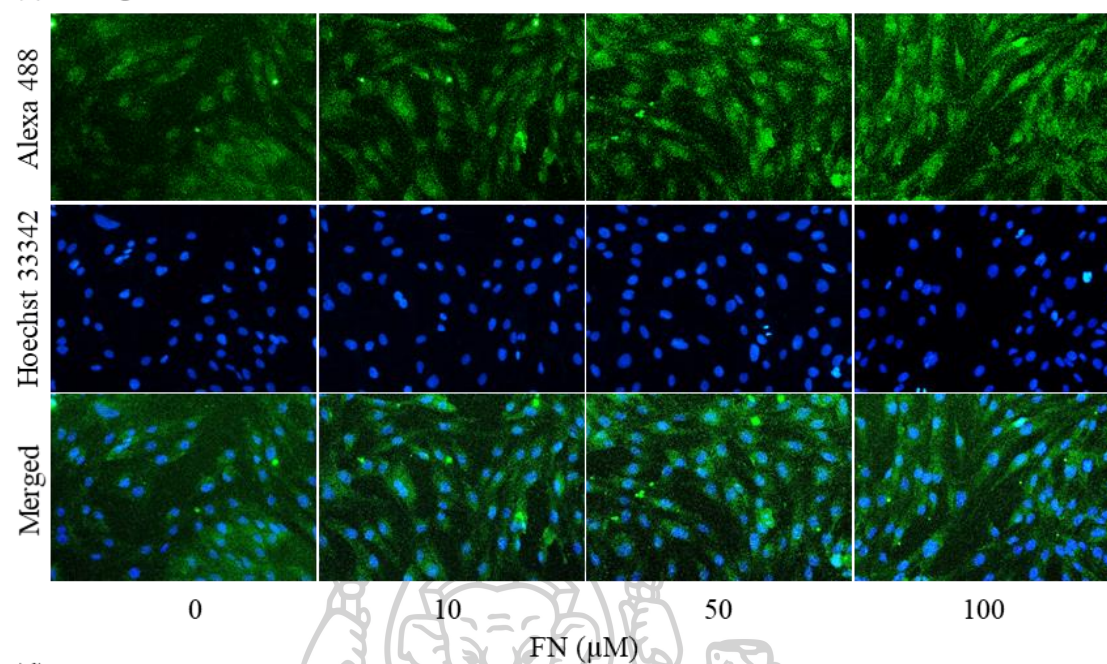


Figure 16 continue.

(c) Nanog



(d) Sox-2

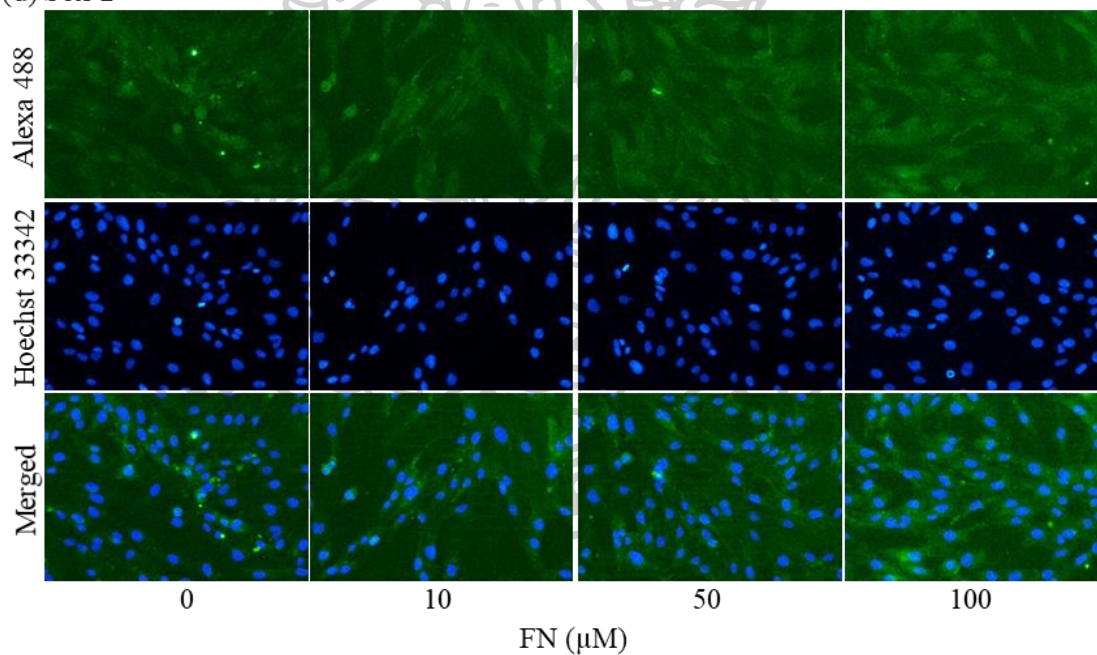


Figure 16 Effect of FN on stem cell-like phenotype and self-renewal transcription factors in DPCs. Cells were culture in the various concentration of FN (10-100 μM) for 24 h. (a and b) After treatment, the levels of integrin β -1, CD44, Nanog, Sox-2 were analyzed by western blot. β -actin was served as the loading control. The immunoblot signals were quantified by densitometry and the mean data from independent experiments were

normalized to the results. The data represent the means of three independent samples \pm SD. * $P < 0.05$ versus non-treated control. (c and d) Expression of Nanog and Sox-2 was analyzed by immunofluorescence staining.

Self-renewal transcription factors like Nanog and Sox-2 have been shown to play a major role on stem cell properties (He, Nakada, & Morrison, 2009). We therefore investigated whether treatment of the DPCs with FN could increase the cellular levels of Nanog and Sox-2. Western blot results showed that FN increased the protein level of Nanog and Sox-2 in a dose-dependent manner (Figure 16b). The induction of Nanog and Sox-2 was confirmed by immunocytochemistry. As shown in Figure 16c and d, FN increased the expression of Nanog and Sox-2 when compared with the non-treated control.

4.1.5 FN maintains the stem cell phenotypes in HDPCs.

To confirm the stem cell induction of FN in other DPCs, the human primary dermal papilla cells (HDPCs) from 2 different donors were used. HDPCs were treated with various concentrations of FN (0.01-100 μ M) for 24 h. FN at 100 μ M slightly decreased viability of HDPCs1 (Figure 12a). Meanwhile, FN (0.01-100 μ M) had no effect on cell viability in HDPCs2 (Figure 12b). We next tested the characteristics of stem cells in these primary cells after treatment with FN (10-100 μ M). The expression of stem cell proteins was determined by immunocytochemistry. Consistently, the expression of β -catenin, Nanog, and Sox-2 was increased in response to FN treatment in a dose-dependent manner in HDPCs1 and HDPCs2 (Figure 17a-f).

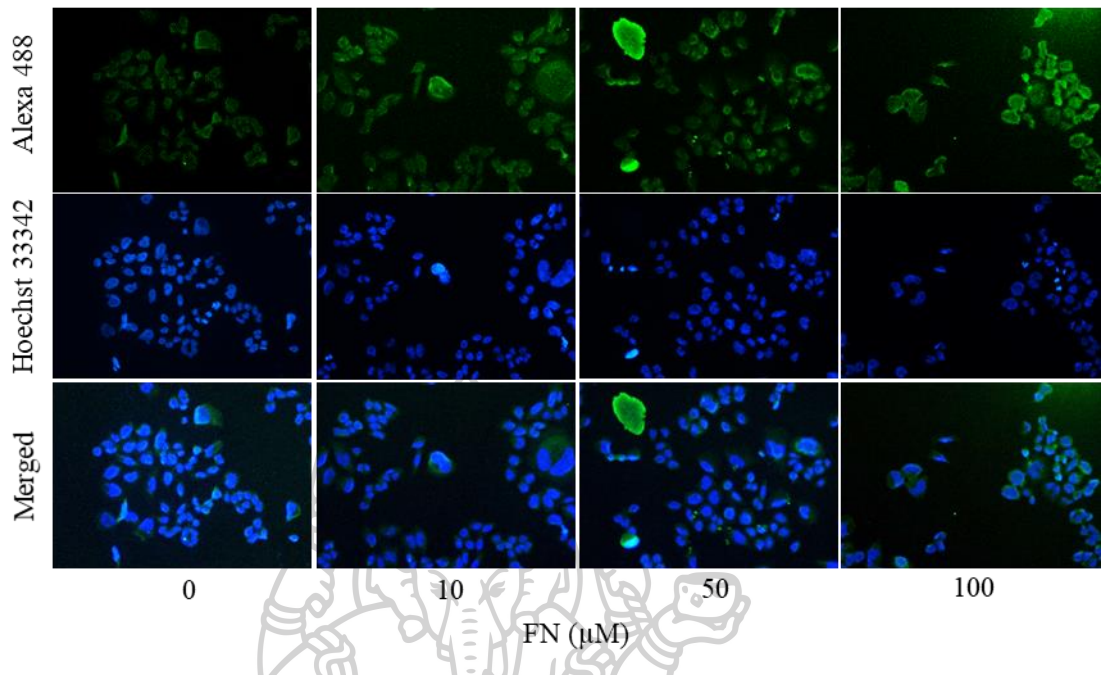
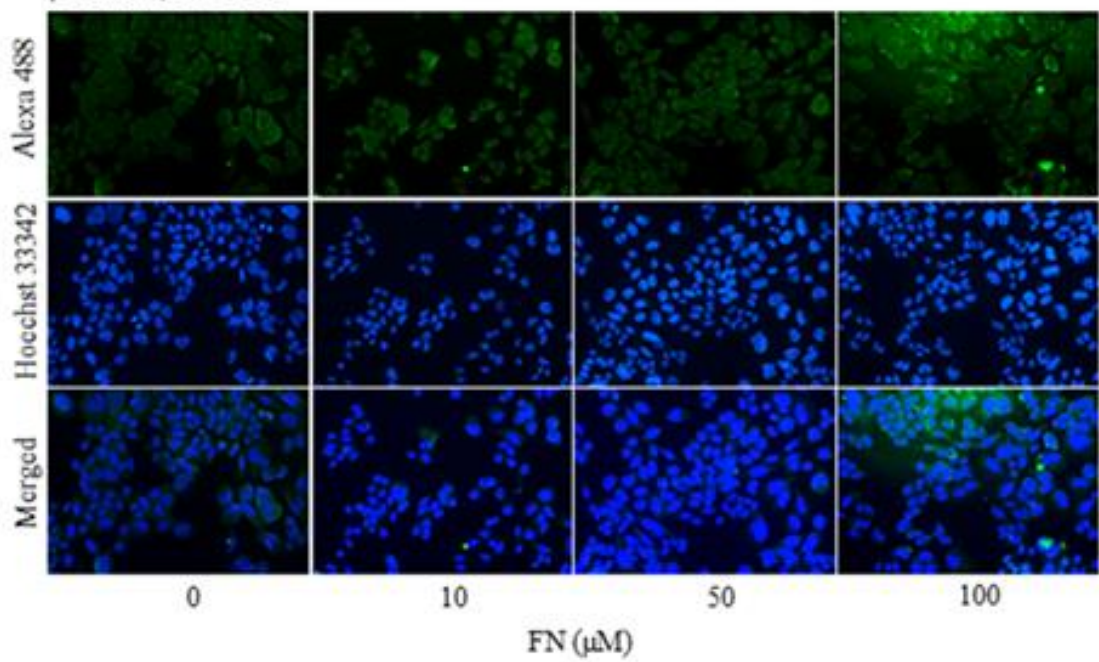
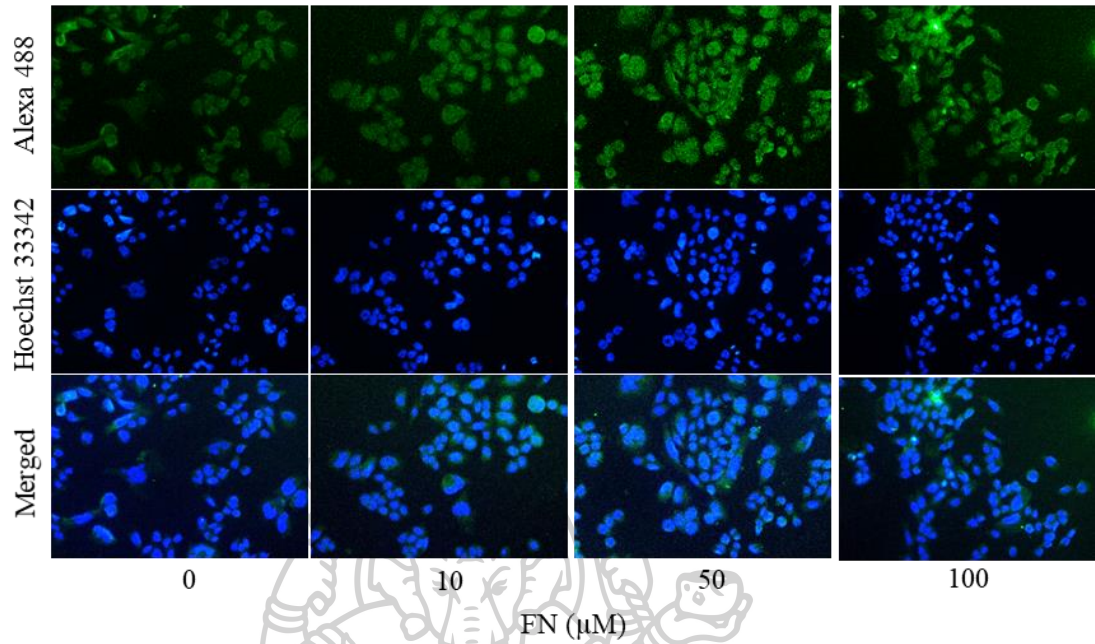
(a) β -catenin, HDPCs1(b) β -catenin, HDPCs2

Figure 17 continue.

(c) Nanog, HPDCs1



(d) Nanog, HPDCs2

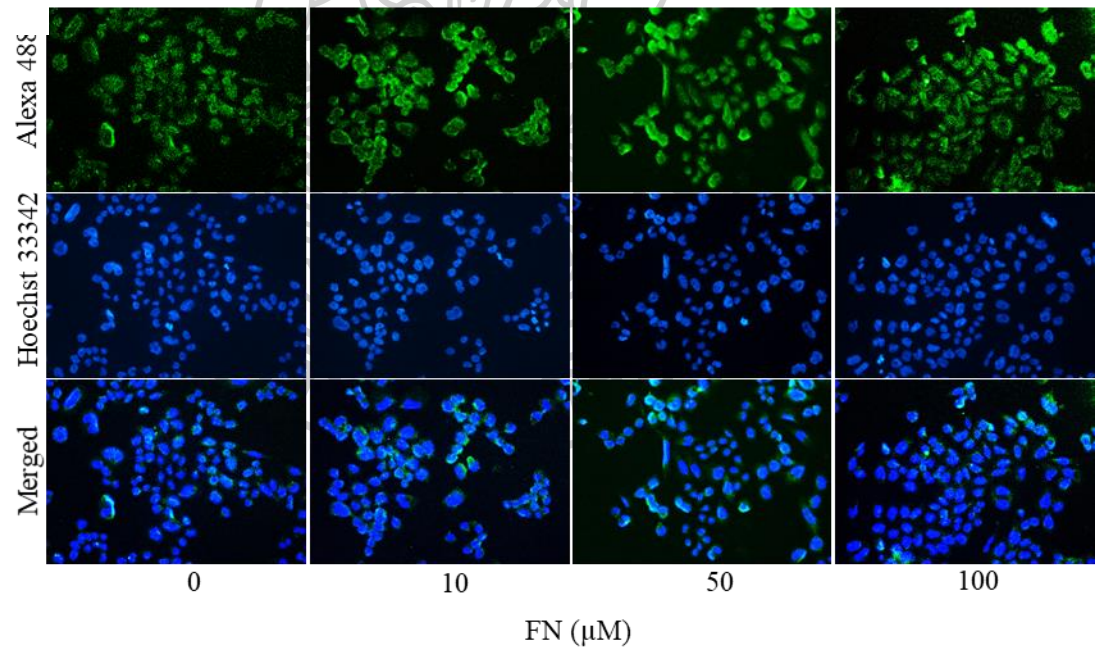
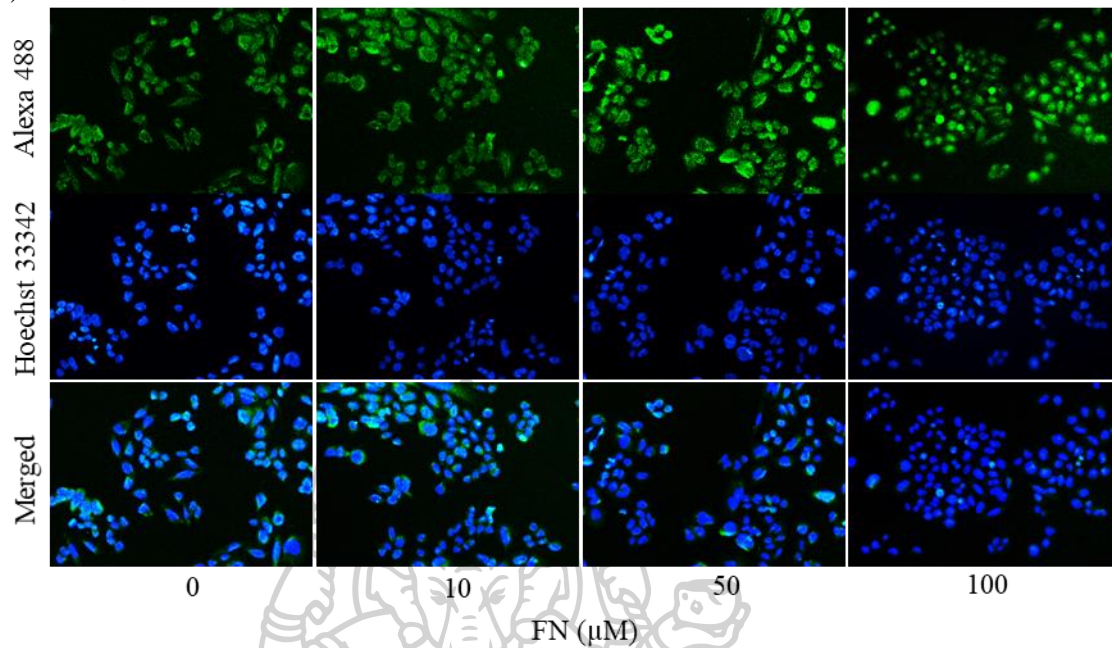


Figure 17 continue.

(e) Sox-2, HPDCs1



(f) Sox-2, Primary DP #2, 24 h

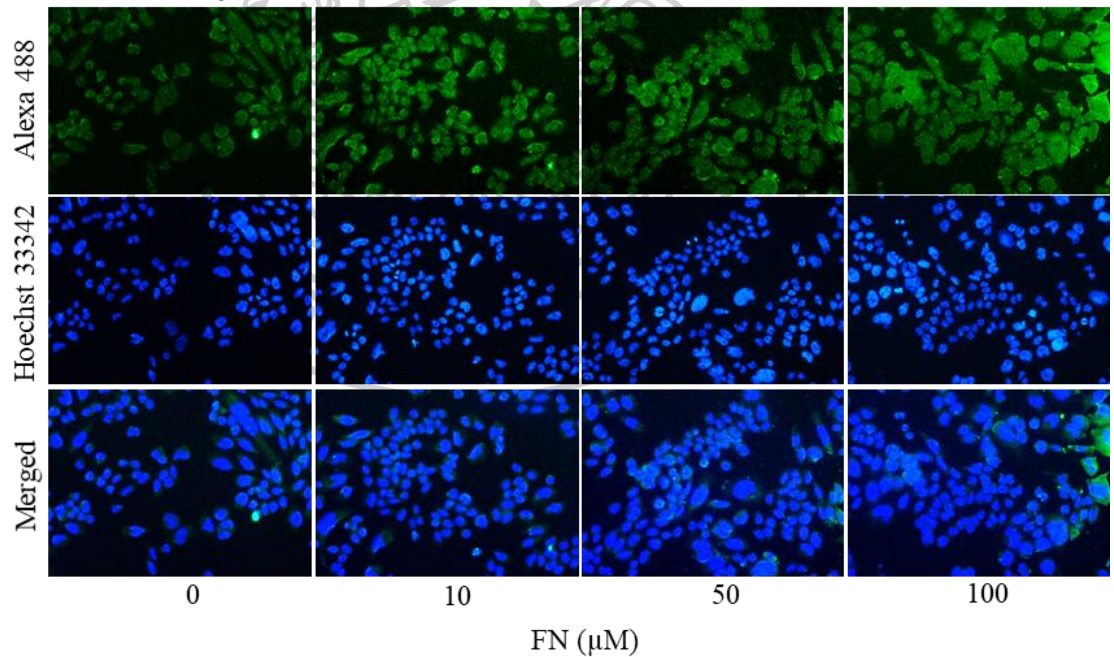


Figure 17 Effect of FN on Wnt/ β -catenin signaling and self-renewal transcription factors in HDPCs were investigated. Expression of β -catenin, Nanog and Sox-2 was analyzed by immunofluorescence staining.

Stem cell property of DPCs plays an important role in hair growth cycle and hair follicle formation (Armstrong et al., 2006). Thus, the augmentation of stemness in DPCs may increase the rate of hair growth and benefit hair loss control. Here we have reported for the first time that FN, a widely prescribed drug for the treatment of hair loss, have a potentiating effects on stem cell properties in DPCs.

The hair follicle formation of DPCs is related to stem cell behaviors including aggregate behaviors (Osada, Iwabuchi, Kishimoto, Hamazaki, & Okochi, 2007). Treatment of the DPCs with non-toxic concentrations of FN significantly increased the number of cell aggregation in comparison to the non-treated control cells (Figure 14b). Also, we found the effect of FN in augmenting the stem cell signals in DPCs by increasing the stem cell markers and transcription factors (Figure 16a-c and figure 17). Wnt/ β -catenin is known to regulate stem cell characteristics and functions (Merrill, 2012; Miki, Yasuda, & Kahn, 2011). Inactivation of β -catenin in DPCs causes the reduction of developing hair growth and impaired hair regeneration (Enshell-Seijffers, Lindon, Wu, Taketo, & Morgan, 2010). In contrast, the activation of such a β -catenin signal resulted in an expansion and formation of hair follicle (Huelsen, Vogel, Erdmann, Cotsarelis, & Birchmeier, 2001). β -catenin is known to be controlled by several cellular mechanisms and the AKT signaling has been recognized as one key regulator of β -catenin. The activated AKT protein increases cellular level of β -catenin by inhibiting GSK3 β -mediated ubiquitination and proteasomal degradation of β -catenin protein (Fukumoto et al., 2001). We found that in response to FN treatment the activated AKT was increased together with the increase in cellular β -catenin (Figure 15), suggesting that FN could maintain stem cell signaling through AKT/ β -catenin-dependent mechanism. Likewise, integrin- β 1 was shown to play a role in hair follicle

formation and stem cell maintenance (Conti, Rudling, Robson, & Hodivala-Dilke, 2003; Raghavan, Bauer, Mundschau, Li, & Fuchs, 2000). Hair follicle bulge stem cells was shown to have high integrin- β 1 expression (Akiyama, Smith, & Shimizu, 2000). We also found that treatment of the DPCs with FN induced the high expression of integrin- β 1 (Figure 16a).

The transcription factors that are important for self-renewal property of stem cells, namely, Sox-2 and Nanog were widely used as biomarkers for human stem cells detection (Boyer et al., 2005). Sox-2 plays an important role in maintaining pluripotency of stem cells (Arnold et al., 2011). Sox-2 interacts and cooperates with other transcription factors, such as Nanog and Oct-4, for regulating of stem cell pluripotency (Boyer et al., 2005). Sox-2, Nanog, and Oct-4 form a core protein for regulating in pluripotent stem cells to maintain their self-renewal. For DPCs and hair follicle stem cells, it was shown that these stem cells contain high level of Sox-2 (Rendl, Lewis, & Fuchs, 2005) and this transcription factor regulates hair growth (Clavel et al., 2012). The Sox-2 and Nanog were significantly upregulated in the FN-treated DPCs, supporting our conclusion that FN may potentiate stemness and stem cell function of DPCs. Besides, we have confirmed the key evidence of FN accentuates stem cell signal in human primary dermal papilla cells from 2 different sources.

4.2 Formulations of FN-loaded MEs

4.2.1 Screening of oil and co-surfactant of MEs by solubility study

ME formulations consisted of water, oil, surfactant and co-surfactant. To select the ingredients of MEs, the solubility study was determined. The solubility of FN in 5 oils and 2 co-surfactants are shown in Table 2. Among the oils, cinnamon oil showed the highest FN solubility (54.78 ± 0.07 mg/mL). While co-surfactants, propylene glycol

(PG) showed higher FN solubility (20.26 ± 0.48 mg/mL) than polyethylene glycol 400 (PEG 400) (4.27 ± 0.02 mg/mL). From these results, cinnamon oil and PG were selected to formulate the MEs as oil and co-surfactant, respectively.

Table 2 Solubility of FN in various oils and co-surfactants (n=3)

	Components	Solubility of FN (mg/mL)
		mean \pm SD
Oil	MCT oil	0.66 ± 0.001^d
	Bergamot oil	17.78 ± 0.16^b
	Cinnamon oil	54.78 ± 0.07^a
	Lavender oil	10.88 ± 0.77^c
	Cajuput oil	1.97 ± 0.07^d
Co-surfactant	PG	20.26 ± 0.48
	PEG 400	4.27 ± 0.02

Cinnamon oil is essential oil from *Cinnamomum zeylanicum* and *Cinnamomum cassia*, mainly extract from leave and bark of the tree. Cinnamon oil usually use in fragrance industry which can be mix in various food, perfume, cosmetic and medicinal products. Cinnamon oil has many pharmacological activity such as antioxidant, anti-inflammatory, antimicrobial, antidiabetic, etc., that make this oil has high value. The main constituent of cinnamon oil was cinnamaldehyde (Figure 18a) and eugenol (Figure 18b), however, cinnamon oil from different part of the tree has different ratio of the compounds (P. V. Rao & Gan, 2014).

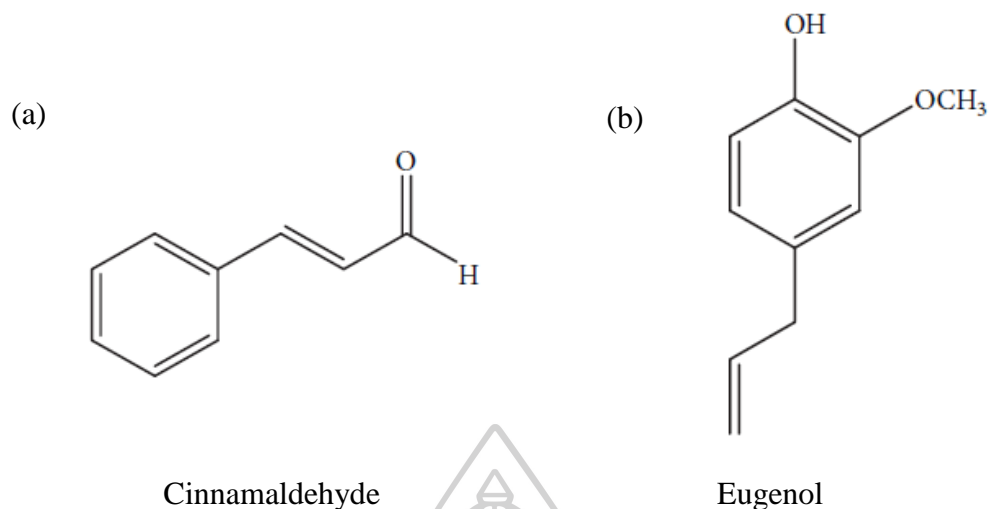


Figure 18 Chemical structure of the main constituents of cinnamon oil

(a) cinnamaldehyde and (b) eugenol

The chemical structure of cinnamaldehyde and eugenol have the core benzene ring and hydrocarbon chain which showed the lipophilic properties the same as FN. Therefore, this reason could support the result of high solubility of FN in cinnamon oil. In addition, cinnamon oil presented the skin penetration enhancement property in vitro. Cinnamon oil showed the higher skin penetration of ibuprofen than azone which is the synthetic penetration enhancer (Chen et al., 2015). These result can expected that cinnamon oil would be enhanced the skin penetration of FN by increased the solubility in formulation and increased the retention of the drug into the skin.

4.2.2 Construction of pseudoternary phase diagram of MEs

After oil and co-surfactant were selected, pseudoternary phase diagram of MEs was constructed. Different surfactants were mixed with PG (co-surfactant) at 1:1 ratio by weight. Then, pseudoternary phase diagram were constructed by water titration

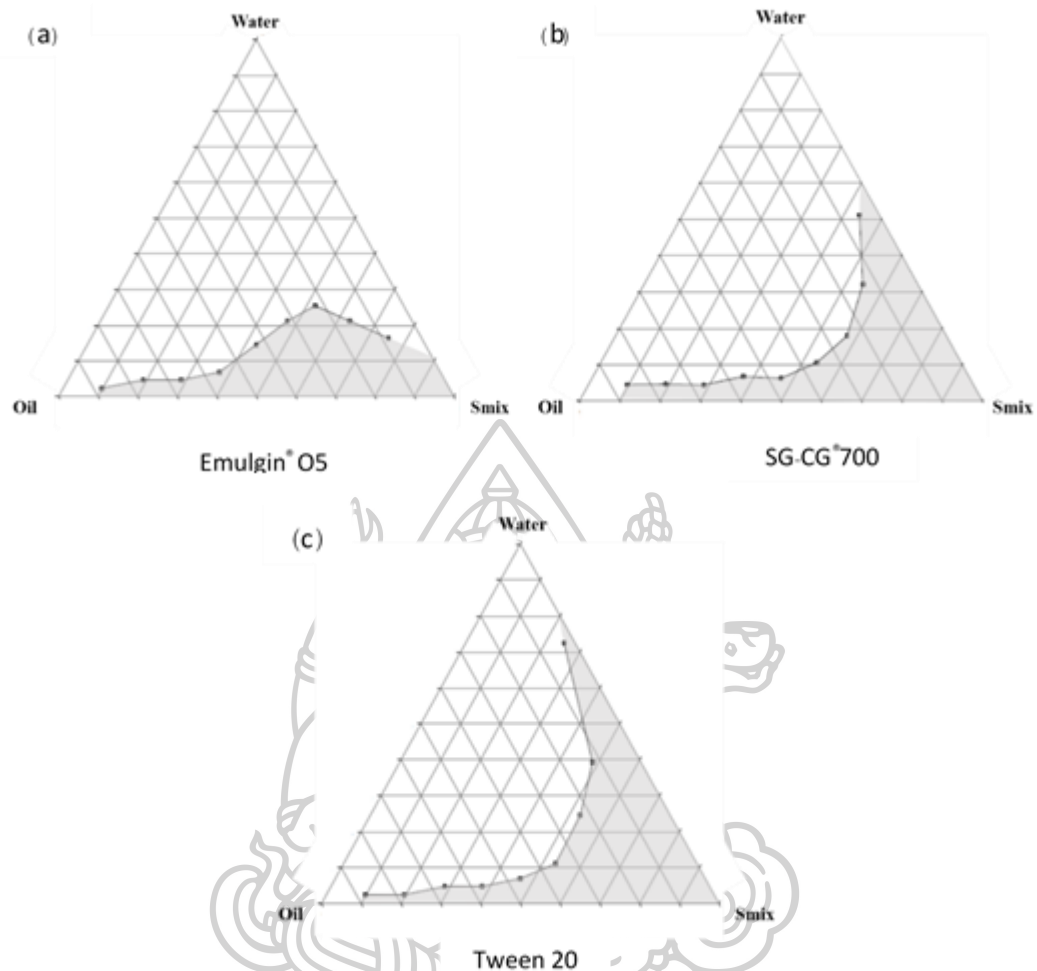


Figure 19 Pseudoternary phase diagram of cinnamon oil MEs with different surfactants mixed with PG at 1:1 ratio by weight.; (a) Emulgin[®] O5, (b) SG-CG[®]700, and (c) Tween 20 method. Emulgin[®]O5 (polyoxyethylene cetyl/oleyl ether), SG-CG[®]700 (PEG-7 glyceryl cocoate) and Tween 20 (polyoxy ethylene sorbitane monolaurate) were the non-ionic surfactant used in this study. Figure 19 showed the area of MEs (gray area) in pseudoternary phase diagram of each surfactant and Tween 20 presented the biggest area of MEs. With this reason, Tween 20 was used as surfactant in the formulation.

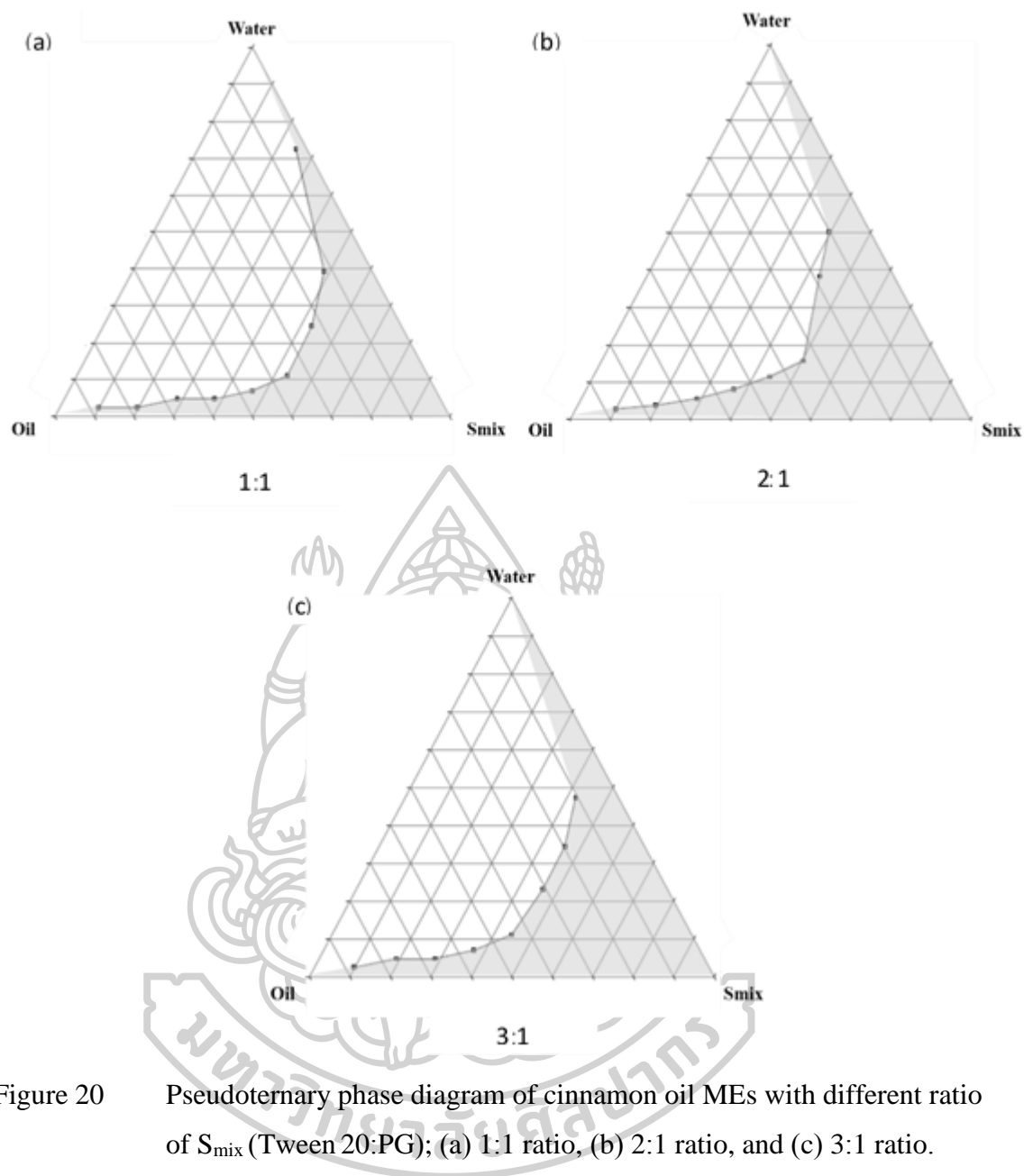


Figure 20 Pseudoternary phase diagram of cinnamon oil MEs with different ratio of S_{mix} (Tween 20:PG); (a) 1:1 ratio, (b) 2:1 ratio, and (c) 3:1 ratio.

To find out the optimize ratio of surfactant and co-surfactant mixture, Tween 20 and PG mixture was prepared at different weight ratios (1:1, 2:1 and 3:1) then mixed with cinnamon oil and water titration method was used to construct pseudoternary phase diagram.

The ME area in pseudoternary phase diagram of each S_{mix} ratio is shown in Figure 20, it was apparent that the increasing in weight ratio of Tween 20 and PG (3:1)

resulted in increasing of isotropic ME region. Therefore, S_{mix} with weight ratio 3:1 was selected for FN-loaded ME formulations.

4.2.3 Preparation of FN-loaded ME formulations

From the ME area of pseudoternary phase diagram, FN was dissolved together with selected seven different ratios (Figure 21) as the formulation model (Duangjit et al., 2016). The amount of each component in the formulation is presented in Table 3. FN was dissolved in cinnamon oil, then S_{mix} and water were added, and stirred with a magnetic stirrer for 15 min. FN-loaded MEs were stored in airtight containers.

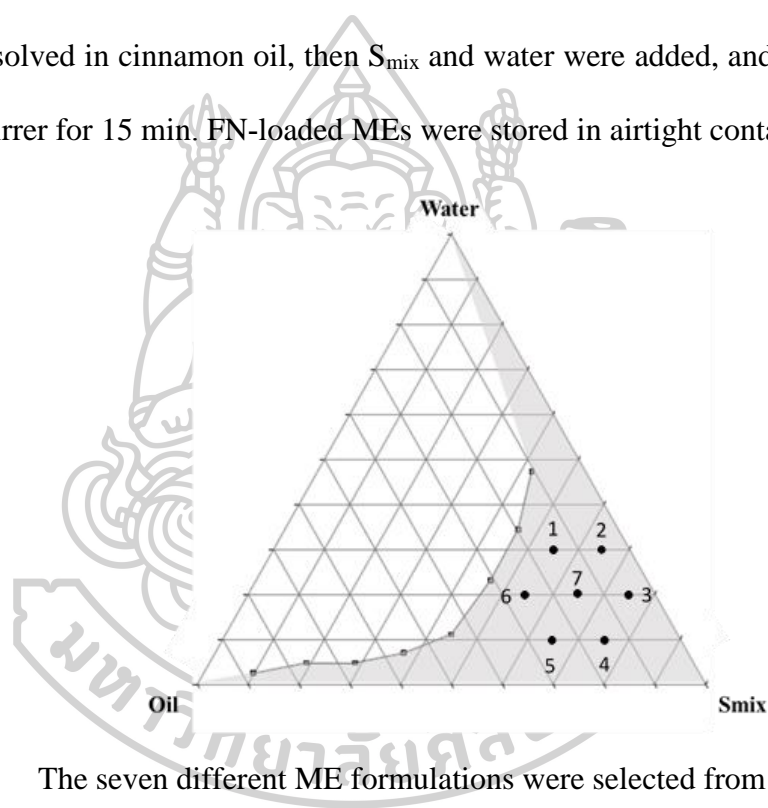


Figure 21 The seven different ME formulations were selected from ME region of pseudoternary phase diagram with S_{mix} at 3:1 ratio.

0.1% w/w of FN preparation can be found in the topical formulation in some countries. In 2014, Monti et al. formulated the hydroxypropyl chitosan based aqueous formulations with 0.25% w/w of FN for topical use (Monti et al., 2014). With this reason, 0.1% and 0.3% w/w of FN were selected to incorporate in MEs by dissolving the drug in oil phase then mixed with S_{mix} and finally added water into the formulations,

then FN was loaded in MEs. The physical appearance of 0.1% and 0.3% w/w FN-loaded MEs was clear and translucent.

Table 3 The amount of each component of seven ME formulations (%w/w) with S_{mix} at 3:1 ratio

Formulation	Oil phase	S_{mix}	Water phase
1	15	55	30
2	5	65	30
3	5	75	20
4	15	75	20
5	25	65	10
6	25	55	10
7	15	65	20

4.3 Characterization of FN-loaded MEs

4.3.1 Droplet size, size distribution, conductivity and pH

The appearance of finish blank MEs and FN-loaded MEs were clear solutions. The average droplet size of seven ME formulations evaluated by using dynamic light scattering technique are presented in Figure 22. The blank MEs had droplets size ranging from 232.67 to 361.89 nm while in 0.1% and 0.3% FN-loaded MEs had droplets size ranging from 207.53 to 337.36 nm and 176.91 to 355.57, respectively. For the average droplet size, FN-loaded MEs showed significantly smaller droplet size than blank MEs. 0.3% FN-loaded MEs presented smaller droplet size than 0.1% FN-loaded MEs.

The effect of different ratio of composition (Oil : Smix : Water) in ME formulations were studied. ME1 and ME6 having high water ratio showed smaller size than other formulations while ME4 having high ratio of Smix presented the largest droplet size. In addition, the small droplet size of FN-loaded MEs may be influenced from the interaction between the drug and the constituents in MEs such as the chemical compound in cinnamon oil, therefore these may cause the tight of inner droplet.

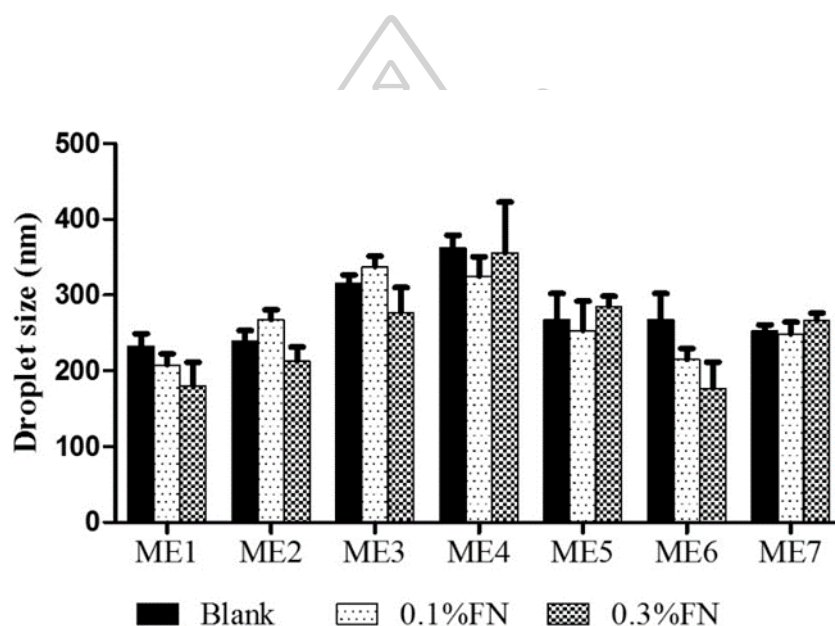


Figure 22 Droplet size of seven formulations of FN-loaded MEs at three concentrations of FN (Blank, 0.1% and 0.3%w/w).

However, all MEs showed the droplet size larger than 150 nm which might be caused from the composition of PG, long chain alcohol, in the formulation (El Maghraby, 2008). In 2010, Ramesh et al. reported the droplet size of aceclofenac topical MEs was larger than 200 nm, however the evaluation of other properties such as optical birefringence by polarized light microscopy indicated isotropic system of ME.

Size distribution of blank MEs and FN-loaded MEs presented by using the poly dispersity index (PDI) and evaluated by using dynamic light scattering technique. The

results are shown in Figure 23. All three groups of MEs showed the narrow size distribution and the homogeneity of droplet size supported by PDI ranging from 0.34 to 0.46.

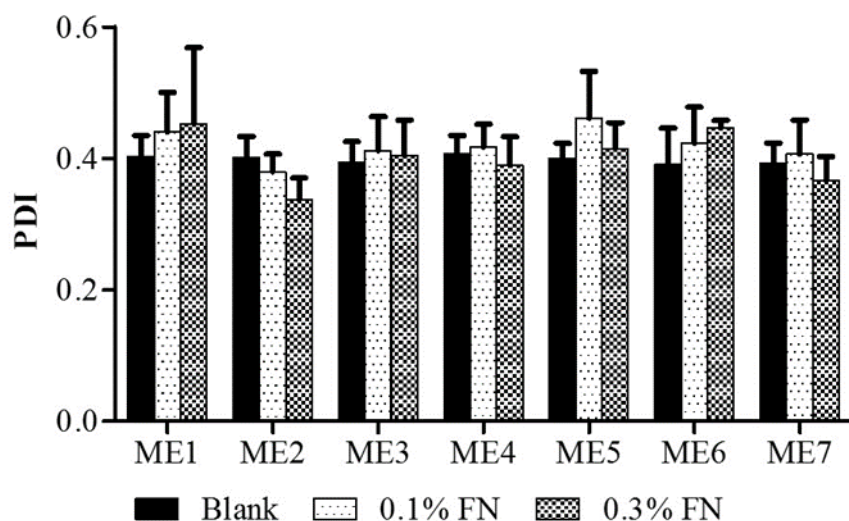


Figure 23 Size distribution of seven formulations of FN-loaded MEs at three concentrations of FN (Blank, 0.1% and 0.3%w/w).

PDI is used to describe the degree of non-uniformity of a size distribution of particles. PDI was dimensionless parameter such that the smaller value than 0.05 represent the highly monodispers but if the PDI value larger than 0.7 it means that the sample had broad size distribution and not suitable to analyzed by dynamic light scattering (DLS) technique (Danaei et al., 2018).

Electrical conductivity is the parameter used to indicate the type of ME, O/W, bicontinuous and W/O type. Figure 24 presents the conductivity of blank ME and FN-loaded MEs. 0.3% FN-loaded MEs had conductivity value ranging from 0.016-0.058 mS/cm. They showed the significantly higher conductivity than blank MEs (0.15-0.50 mS/cm) and 0.1% FN-loaded MEs (0.015-0.047 mS/cm). ME1 had high water ratio

(30%) in formulation, therefore it had higher conductivity than other formulations. The results of conductivity value (>0.01 mS/cm) indicated that these MEs were classified as oil-in-water ME (Duangjit et al., 2016).

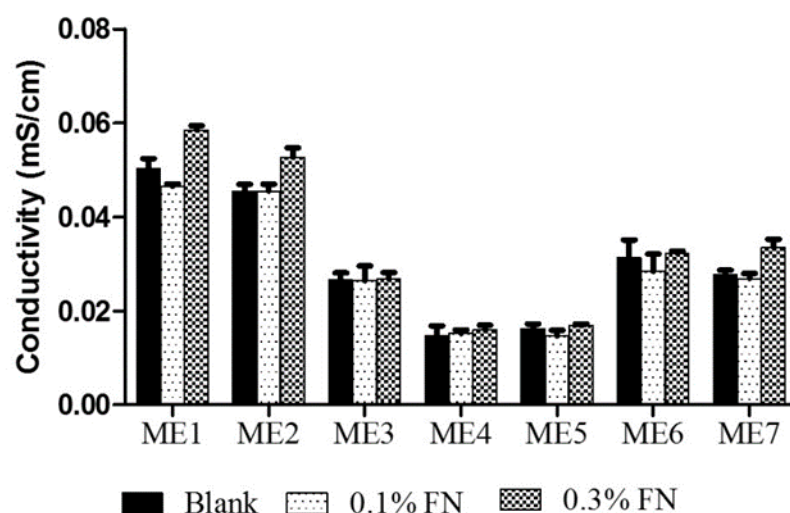


Figure 24 Conductivity of seven formulations of FN-loaded MEs at three concentrations of FN (Blank, 0.1% and 0.3%w/w).

pH value of blank ME and FN-loaded MEs presented in Figure 25. All three groups ME formulations had pH ranging from 5.2 to 7.7. 3% FN-loaded MEs showed the lowest average pH value (6.0) while blank MEs and 0.1% FN-loaded MEs had the average pH value 7.0 and 6.9, respectively. These results indicated that high concentration of FN caused slightly decreasing in pH value of MEs because FN was the weakly acidic drug with pKa 5.9. However, the pH value of FN-loaded MEs was in the range of human skin pH (5.5-6.5, therefore these formulations can be used as topical formulation.

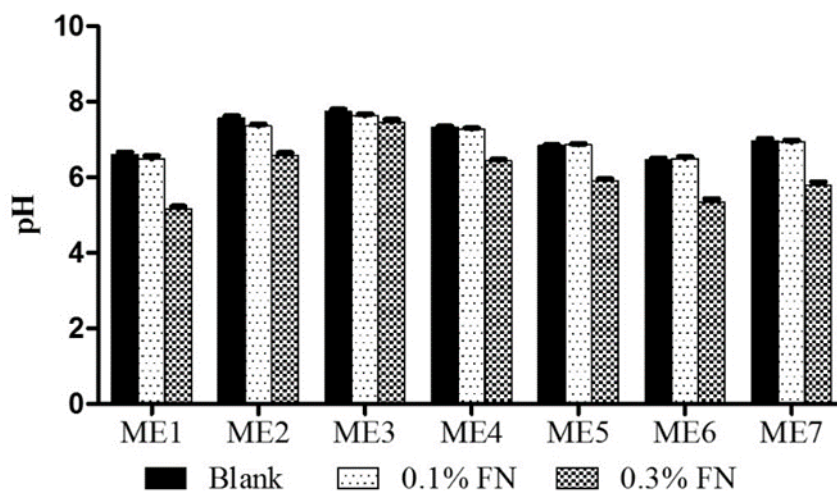


Figure 25 pH of seven formulations of FN-loaded MEs at three concentrations of FN (Blank, 0.1% and 0.3%w/w).

4.3.2 Drug loading efficiency

The percentage of entrapment efficiency (%EE) was used to describe the drug loading efficiency of ME determined by using HPLC.

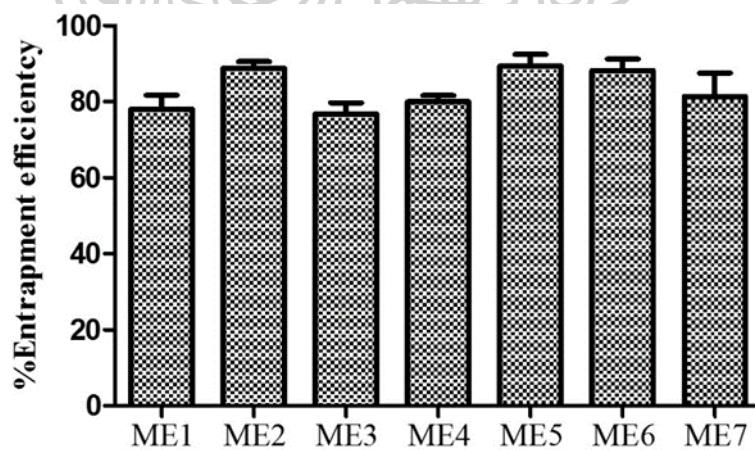


Figure 26 % Entrapment efficiency of FN-loaded MEs.

Figure 26 presented the %EE of ME1-ME7 formulations. ME1-ME7 had the %EE ranging from 76.81% to 89.41%. ME5 with high ratio of oil (25%) showed the highest %EE closely to ME2 (88.7%) and ME6 (88.2%) whereas the ME3, the

formulation with low concentration of oil (5%) had the lowest %EE (76.8). These results indicated that FN which is the lipophilic drug had high solubility in oil phase therefore ME formulations with high ratio of oil can loaded the high content of FN.

4.4 *In vitro* skin permeation study

The skin permeation profile of ME1- ME7 were shown in Figure 27. The cumulative amount profile was plotted against time. The release kinetics and steady-state flux value were determined as the slope of linear portion of the plot. The skin permeation flux of the FN-loaded MEs were presented in Figure 28. FN-loaded ME1 presented the highest skin permeation flux (2.32 $\mu\text{g}/\text{cm}^2/\text{h}$) but it was not significantly different from FN-loaded ME3 (1.94 $\mu\text{g}/\text{cm}^2/\text{h}$) and FN-loaded ME6 (1.49 $\mu\text{g}/\text{cm}^2/\text{h}$). The flux of FN-loaded ME5 was significantly lower than another formulation at $p < 0.05$. The water content in the formulation affected skin permeation of drug. The FN-loaded ME5 had the same amount of water (10% w/w) as FN-loaded ME4. The skin permeation flux of FN-loaded ME5 was low and close to FN-loaded ME4. Whereas FN-loaded ME1 having 30% w/w of water showed higher skin permeation. These results indicated that high concentration of water can enhance the skin permeation of FN-loaded MEs due to the increasing of skin hydration. In addition, the small droplet size of FN-loaded ME1 might support the increasing of skin permeation flux.

However, the skin permeation flux was affected by various factors such as the type and concentration of oil, surfactant and co-surfactant. Therefore, other factor affecting skin permeation and skin permeation mechanism of ME should be investigated.

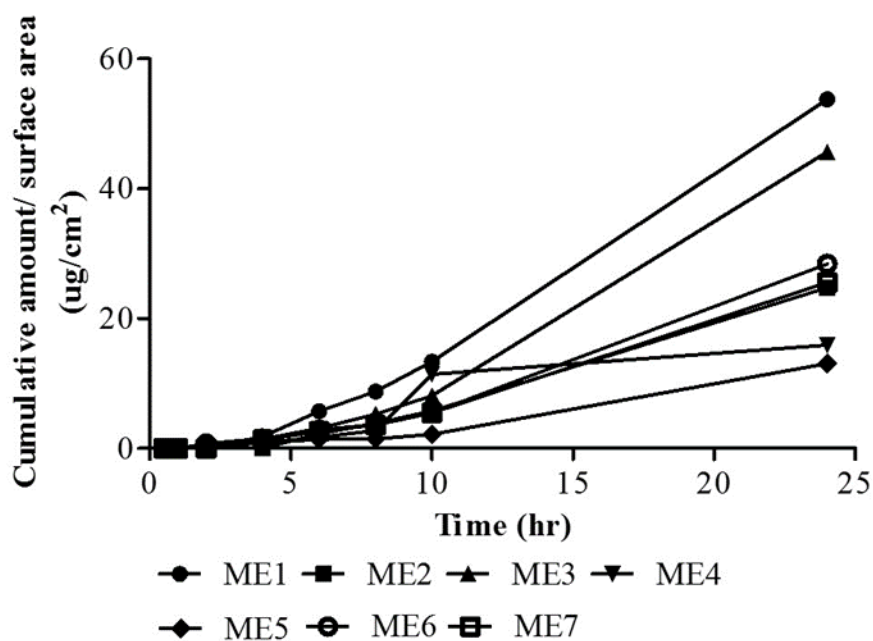


Figure 27 The skin permeation profile of seven formulations of 0.3% w/w FN-loaded MEs.

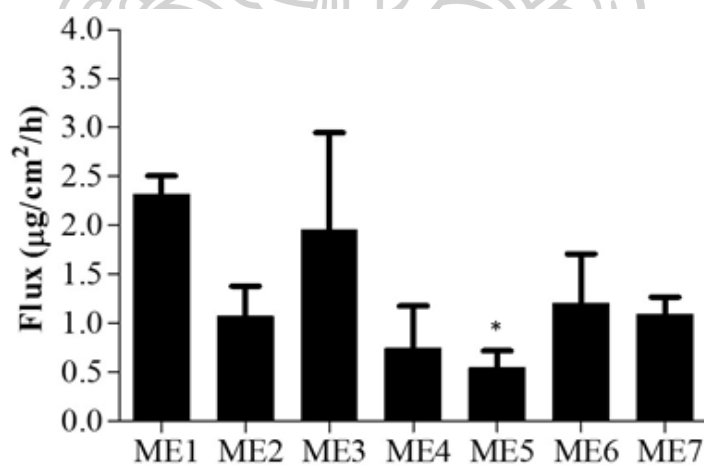


Figure 28 The skin permeation flux of 0.3% w/w FN-loaded ME formulations.

* $P < 0.05$

The different ratio of the compositions in MEs presented the different in physicochemical properties and in vitro skin permeation. Droplet size and electrical conductivity were the two properties that obviously influenced by the ratio of MEs

composition. The large amount of water phase in ME1 presented the small droplet size and high electrical conductivity which could be affected to the skin permeation flux. In general, small droplet size was the main factor promoted the increasing in skin penetration and the electrical conductivity indicated that the MEs were O/W type. The results from this part of the study can be summarized that the increasing in skin permeation flux of FN-loaded ME1 were influenced by the small droplet size and high electrical conductivity from the large amount of water phase. However, FN-loaded ME3 was the second formulation with high skin permeation flux but this formulation had a large amount of S_{mix} . The droplet size of FN-loaded ME3 was larger than FN-loaded ME1 and electrical conductivity was lower than FN-loaded ME1, too. Therefore, maybe more relevant factors can affect to the skin permeation flux of the drug in MEs and the optimal formulations should be further investigated.

4.5 Optimization of FN-loaded ME formulations by computer design

In the development of FN-loaded MEs for topical use, many properties of the formulation had been investigated. To obtain the optimal ratio of ME formulation, the simplex lattice design was used to optimize the FN-loaded ME systems. The ratio of oil phase, water and surfactant mixture obtained from the model of MEs. The response surface comparing between blank ME and FN-loaded MEs are presented in Figure 28. All of response variables were evaluated and sketched using the Design Expert[®] Software (Version 8), Approved No 009503 (Stat-Ease, Inc., Minneapolis, MN). The ratio of cinnamon oil (X_1), surfactant mixture (X_2) and water (X_3) were defined as causal factors, while the physicochemical characteristics such as droplet size (Y_1), size distribution (Y_2), conductivity (Y_3), pH (Y_4), %EE (Y_5) and skin permeation flux (Y_6)

were defined as response variables. The results of response surface exhibited uncomplicated relationships between the causal factors and the response variables.

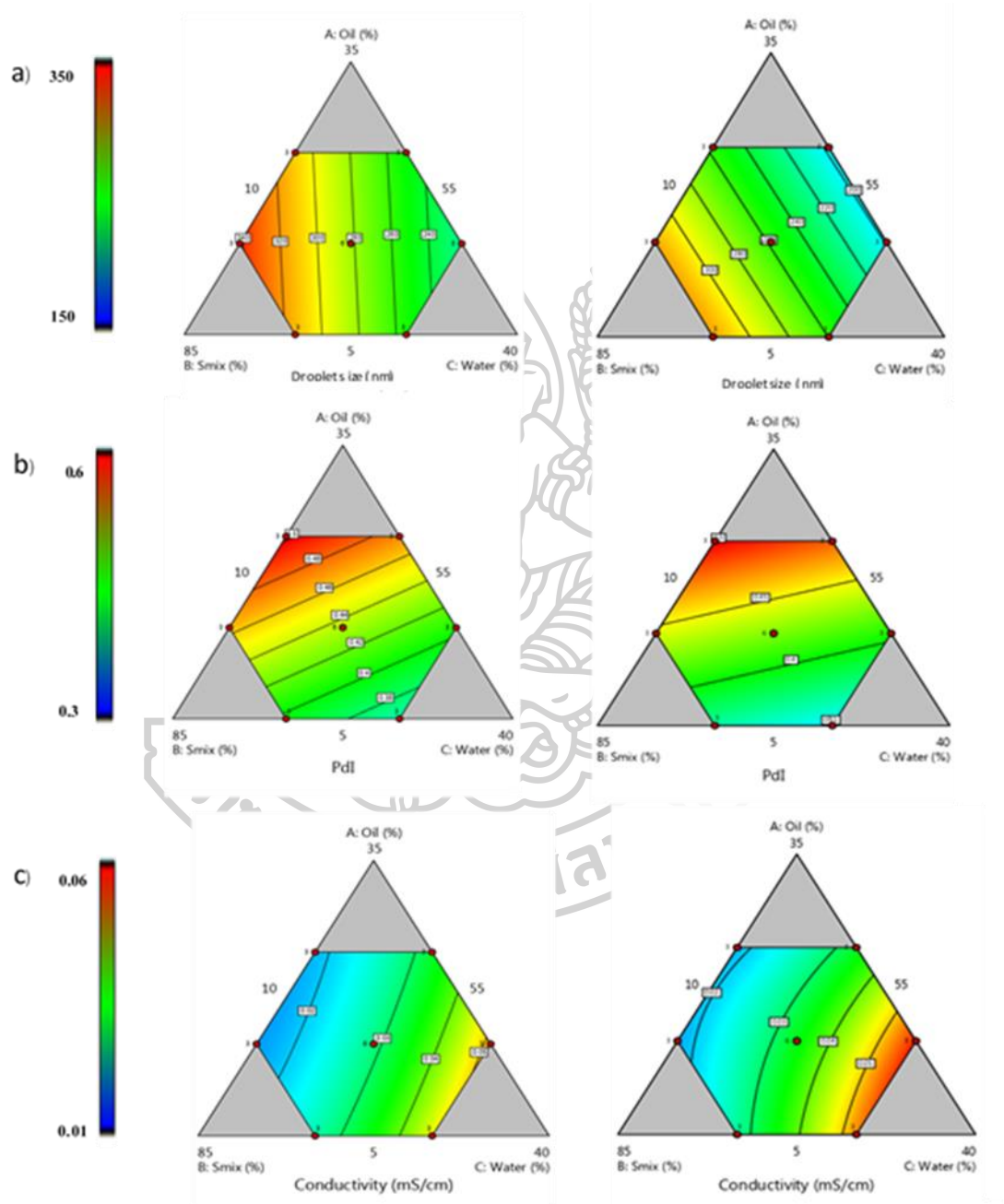


Figure 29 continue.

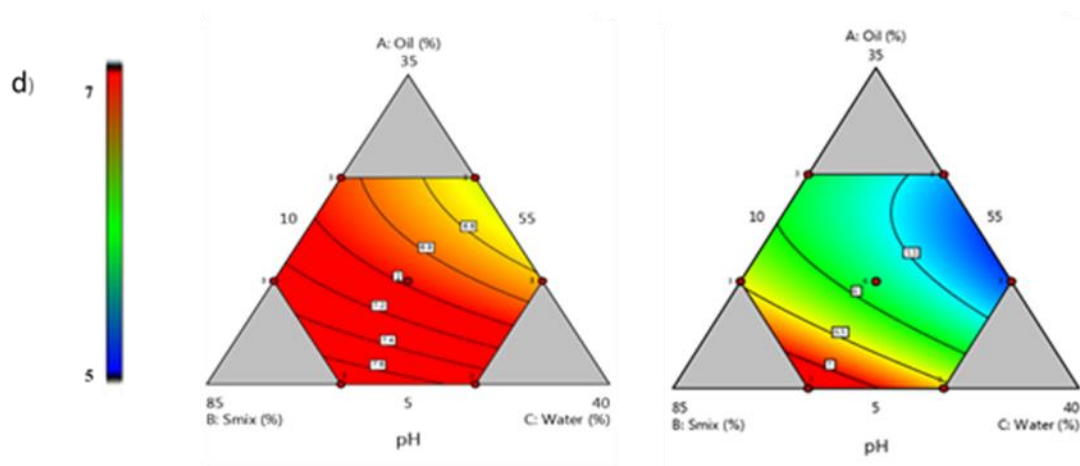


Figure 29 The response surface of a) droplet size, b) PDI, c) conductivity and d) pH for blank ME (left column) and 0.3% w/w FN-loaded MEs (right column).

The influences of the formulation factor on the physicochemical properties of blank MEs and FN-loaded MEs are shown in Figure 28. The droplet size (Y_1) of blank MEs and 0.3% FN-loaded MEs increased when the concentration of surfactant mixture were increased and incorporation of 0.3% FN into MEs showed significantly affect the droplet size of ME (Figure 29a). The size distribution (Y_2) of FN-loaded MEs present in PDI was not significantly different from blank ME. However, both blank ME and FN-loaded MEs showed the narrow size distribution when the formulation had high percentage of water (Figure 29b). In the response surface of conductivity (Y_3) prediction, both blank ME and FN-loaded MEs had high electrical conductivity (>0.01 mS/cm), so they could be classified as water-in-oil MEs (Duangjit, 2015). The conductivity of ME was influenced by the composition of the ME. When the water content was increased, the electrical conductivity increased (Figure 29c). The response surface of pH (Y_4) presented that the pH of MEs depended on the composition of MEs. The pH of both blank MEs and FN-loaded MEs was ranging from 5.2-7.7 and the formulation became weak base when it had high percentage of oil and water (Figure

29d). The incorporation of 0.3% FN into MEs decreased pH value to weak acid but it was also safety to use as topical formulation.

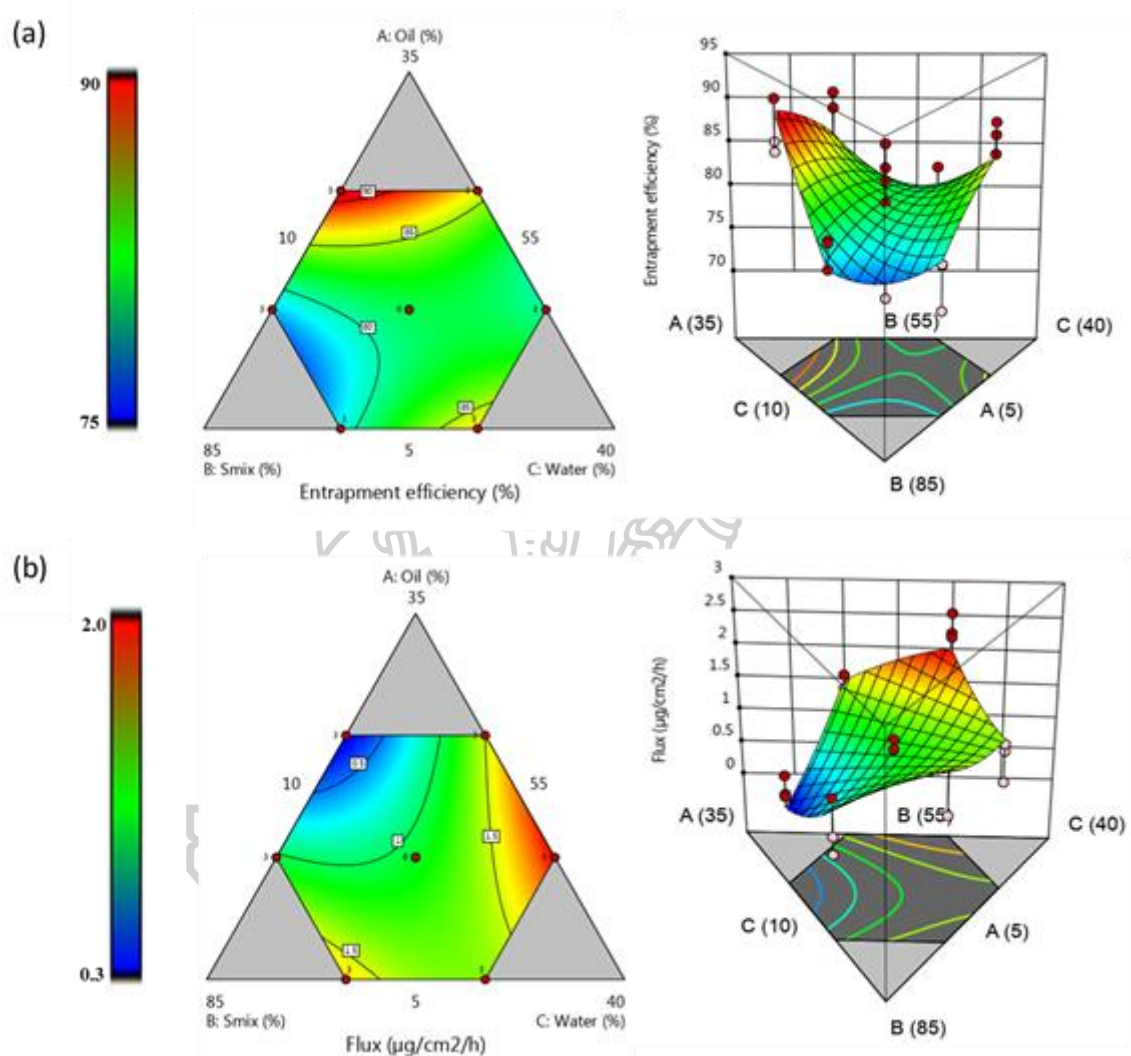


Figure 30 The response surface of a) % Entrapment efficiency (EE) and b) Skin permeation flux of 0.3% w/w FN-loaded MEs.

The contour plot and 3D response surface of %EE and the skin permeation flux were presented in Figure 30. The increasing of oil phase in ME formulations can enhance the entrapment efficiency of MEs. Moreover, if ME formulations had high S_{mix}

ratio, the entrapment of the drug would be decreased because FN was the lipophilic drug and had high solubility in oil or non-polar substance then the ME formulations with high oil phase provided high entrapment efficiency. Whereas, ME formulations with high ratio of oil decreased the skin permeation flux but high water content can enhance the skin permeation flux of FN.

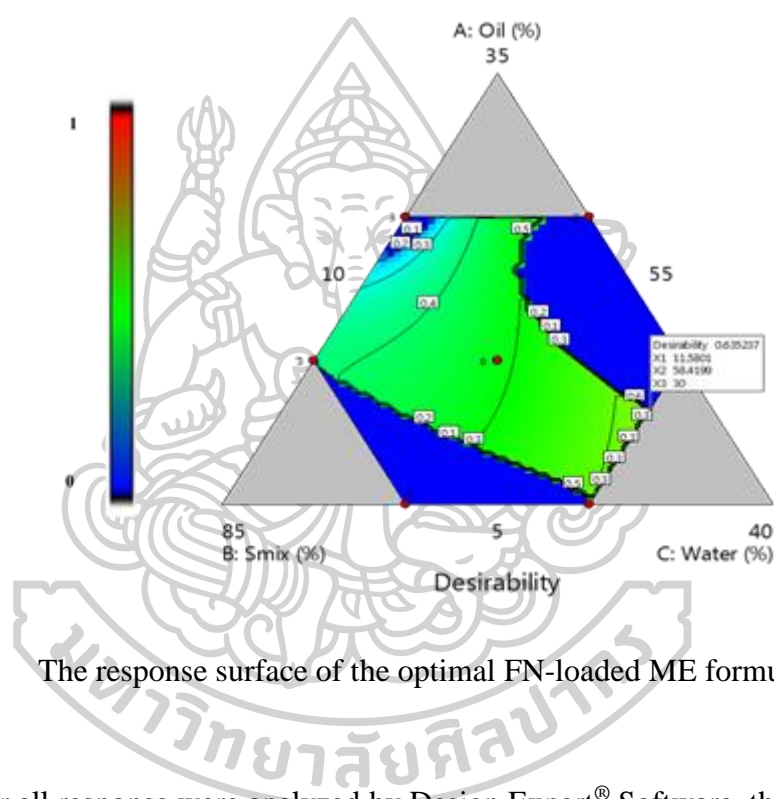


Figure 31 The response surface of the optimal FN-loaded ME formulation

After all response were analyzed by Design Expert[®] Software, the optimal FN-loaded MEs was predicted with the reasonable physicochemical properties. Minimum droplet size and size distribution with maximum entrapment efficiency and skin permeation flux were the important requirement properties for the optimal formulation because these can affect to the therapeutic efficacy of the drug. Figure 31 presented the prediction of the optimal FN-loaded ME formulations with the requirement of physicochemical properties and the desirability value was 0.635. At the prediction point, the optimal ratio of each component was 11.58% of oil phase, 58.42% of S_{mix}

and 30% of water phase. With this optimal formulation, the physicochemical characteristic would be predicted and presented in Table 4.

Table 4 The prediction value of the physicochemical characteristic from the optimal FN-loaded MEs.

Physicochemical characteristics	Constraint	Prediction value
Droplet size (nm)	minimize	216.61
PDI	minimize	0.386
Conductivity (mS/cm)	in range	0.058
pH	in range	5.5
%EE	maximize	82.13
Flux ($\mu\text{g}/\text{cm}^2/\text{h}$)	maximize	1.691

However, the optimal formulation can be adjusted for the suitable physicochemical properties and the prediction value from the computer program should be verified by the experiment again.

CHAPTER 5

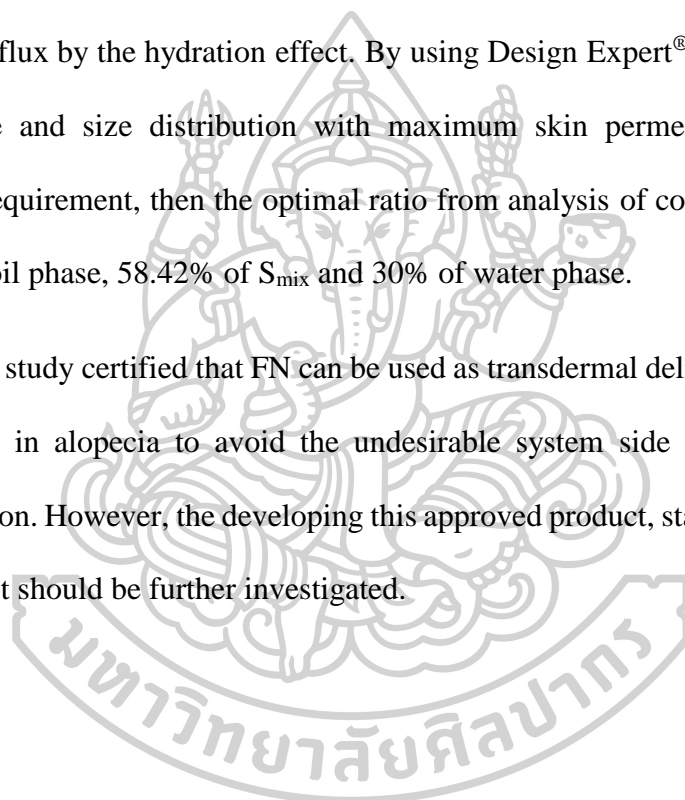
CONCLUSIONS

This study was divided into two parts, first part was the novel regulatory activity and mechanism how FN regulates stem cell signal in DPCs. The results indicated that treatment of the DPCs and HDPCs with 10-100 μ M of FN did not cause toxicity to cells. With this non-toxic concentration, FN significantly increased the number of cell aggregation when compared with non-treated cells. Moreover, FN can expand the stem cell signal by increasing the stem cell markers and transcription factors through Wn/ β -catenin signaling partway which regulate characteristics and functions of stem cells. FN demonstrated the activation of AKTt protein which increased the cellular β -catenin level. With this reason, FN could maintain stem cell signaling through AKT/ β -catenin-dependent mechanism. In addition, FN also presented the increasing of integrin- β 1 (stem cell marker) expression. Furthermore, Sox-2 and Nanog, the important transcription factors for self-renewal property of stem cells and regulation of hair growth cycle, illustrated significantly upregulated in the FN-treated DPCs. With all these results confirm that FN had the ability to maintain stemness and stem cell function of DPCs.

The second part of this study was formulation and optimization of FN-loaded MEs on the purpose of transdermal delivery. The components of ME system consisted of cinnamon oil as oil phase, Tween 20 as surfactant, PG as co-surfactant and water. The influence of the component ratio to the physicochemical characteristic, entrapment efficiency and skin permeation flux of FN-loaded MEs was investigated. The study presented that the different ratio of the components in ME formulations affected the

physicochemical characteristic. The incorporation of 0.1% and 0.3% w/w of FN into ME system affected the physicochemical characteristic. Both two concentrations (0.1 and 0.3 %) of FN-loaded MEs showed significantly decrease in droplet size and pH which were the good point to be used as transdermal formulation. FN-loaded MEs with high ratio of oil phase increased the entrapment efficiency of the drug result from the high lipid solubility of the drug whereas that high ratio of water increased the skin permeation flux by the hydration effect. By using Design Expert® Software, minimum droplet size and size distribution with maximum skin permeation flux were the important requirement, then the optimal ratio from analysis of computer program was 11.85% of oil phase, 58.42% of S_{mix} and 30% of water phase.

This study certified that FN can be used as transdermal delivery formulation for hair growth in alopecia to avoid the undesirable system side effect from the oral administration. However, the developing this approved product, stability study and skin irritation test should be further investigated.



REFERENCES

- Akiyama, M., Smith, L. T., & Shimizu, H. (2000). Changing patterns of localization of putative stem cells in developing human hair follicles. *J Invest Dermatol*, *114*(2), 321-327. doi:10.1046/j.1523-1747.2000.00857.x
- Armstrong, L., Hughes, O., Yung, S., Hyslop, L., Stewart, R., Wappler, I., . . . Lako, M. (2006). The role of PI3K/AKT, MAPK/ERK and NFkappabeta signalling in the maintenance of human embryonic stem cell pluripotency and viability highlighted by transcriptional profiling and functional analysis. *Hum Mol Genet*, *15*(11), 1894-1913. doi:10.1093/hmg/ddl112
- Arnold, K., Sarkar, A., Yram, M. A., Polo, J. M., Bronson, R., Sengupta, S., . . . Hochedlinger, K. (2011). Sox2(+) adult stem and progenitor cells are important for tissue regeneration and survival of mice. *Cell Stem Cell*, *9*(4), 317-329. doi:10.1016/j.stem.2011.09.001
- Azzouni, F., Godoy, A., Li, Y., & Mohler, J. (2012). The 5 alpha-reductase isozyme family: a review of basic biology and their role in human diseases. *Adv Urol*, *2012*, 530121. doi:10.1155/2012/530121
- Biruss, B., Kahlig, H., & Valenta, C. (2007). Evaluation of an eucalyptus oil containing topical drug delivery system for selected steroid hormones. *Int J Pharm*, *328*(2), 142-151. doi:10.1016/j.ijpharm.2006.08.003
- Boyer, L. A., Lee, T. I., Cole, M. F., Johnstone, S. E., Levine, S. S., Zucker, J. P., . . . Young, R. A. (2005). Core transcriptional regulatory circuitry in human embryonic stem cells. *Cell*, *122*(6), 947-956. doi:10.1016/j.cell.2005.08.020
- Brown, C. J., Goss, S. J., Lubahn, D. B., Joseph, D. R., Wilson, E. M., French, F. S., & Willard, H. F. (1989). Androgen receptor locus on the human X chromosome: regional localization to Xq11-12 and description of a DNA polymorphism. *Am J Hum Genet*, *44*(2), 264-269.
- Caon, T., Porto, L. C., Granada, A., Tagliari, M. P., Silva, M. A., Simoes, C. M., . . . Soldi, V. (2014). Chitosan-decorated polystyrene-b-poly(acrylic acid) polymersomes as novel carriers for topical delivery of finasteride. *Eur J Pharm Sci*, *52*, 165-172. doi:10.1016/j.ejps.2013.11.008
- Cha, E. K., & Shariat, S. F. (2011). The use of 5alpha-reductase inhibitors for the prevention and treatment of prostate cancer. *Eur Urol*, *59*(4), 515-517. doi:10.1016/j.eururo.2011.01.028
- Charoenputtakun, P., Pamornpathomkul, B., Opanasopit, P., Rojanarata, T., & Ngawhirunpat, T. (2014). Terpene composited lipid nanoparticles for enhanced dermal delivery of all-trans-retinoic acids. *Biol Pharm Bull*, *37*(7), 1139-1148.
- Chen, J., Jiang, Q. D., Wu, Y. M., Liu, P., Yao, J. H., Lu, Q., . . . Duan, J. A. (2015). Potential of Essential Oils as Penetration Enhancers for Transdermal Administration of Ibuprofen to Treat Dysmenorrhoea. *Molecules*, *20*(10), 18219-18236. doi:10.3390/molecules201018219
- Clavel, C., Grisanti, L., Zemla, R., Rezza, A., Barros, R., Sennett, R., . . . Rendl, M. (2012). Sox2 in the dermal papilla niche controls hair growth by fine-tuning BMP signaling in differentiating hair shaft progenitors. *Dev Cell*, *23*(5), 981-994. doi:10.1016/j.devcel.2012.10.013

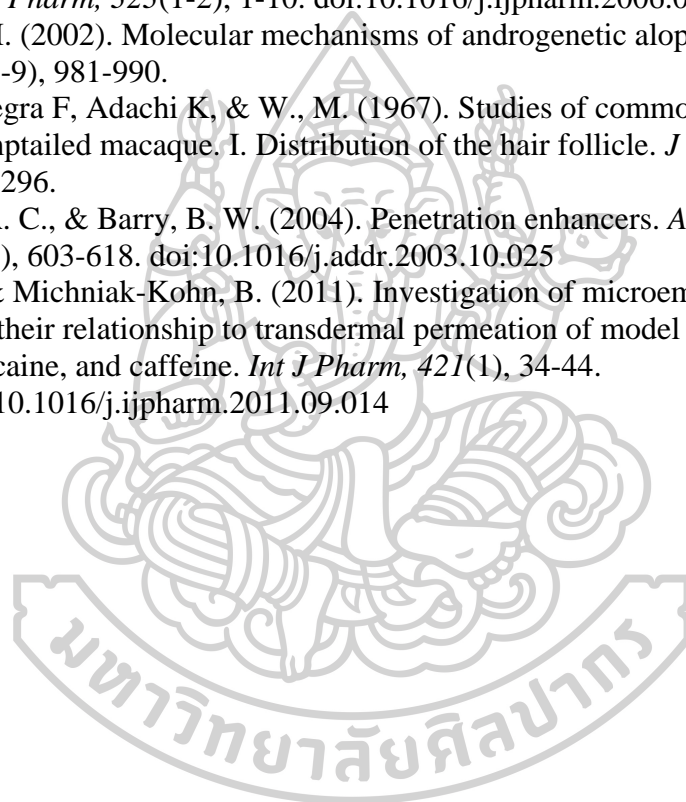
- Conti, F. J., Rudling, R. J., Robson, A., & Hodivala-Dilke, K. M. (2003). $\alpha 3\beta 1$ -integrin regulates hair follicle but not interfollicular morphogenesis in adult epidermis. *J Cell Sci*, *116*(Pt 13), 2737-2747. doi:10.1242/jcs.00475
- Danaei, M., Dehghankhold, M., Ataei, S., Hasanzadeh Davarani, F., Javanmard, R., Dokhani, A., . . . Mozafari, M. R. (2018). Impact of Particle Size and Polydispersity Index on the Clinical Applications of Lipidic Nanocarrier Systems. *Pharmaceutics*, *10*(2). doi:10.3390/pharmaceutics10020057
- Dawber, R. (1996). Hair: its structure and response to cosmetic preparations. *Clin Dermatol*, *14*(1), 105-112.
- Djekic, L., & Primorac, M. (2008). The influence of cosurfactants and oils on the formation of pharmaceutical microemulsions based on PEG-8 caprylic/capric glycerides. *Int J Pharm*, *352*(1-2), 231-239. doi:10.1016/j.ijpharm.2007.10.041
- Drake, L., Hordinsky, M., Fiedler, V., Swinehart, J., Unger, W. P., Cotterill, P. C., . . . Waldstreicher, J. (1999). The effects of finasteride on scalp skin and serum androgen levels in men with androgenetic alopecia. *J Am Acad Dermatol*, *41*(4), 550-554.
- Driskell, R. R., Giangreco, A., Jensen, K. B., Mulder, K. W., & Watt, F. M. (2009). Sox2-positive dermal papilla cells specify hair follicle type in mammalian epidermis. *Development*, *136*(16), 2815-2823. doi:10.1242/dev.038620
- Driskell, R. R., Juneja, V. R., Connelly, J. T., Kretzschmar, K., Tan, D. W., & Watt, F. M. (2012). Clonal growth of dermal papilla cells in hydrogels reveals intrinsic differences between Sox2-positive and -negative cells in vitro and in vivo. *J Invest Dermatol*, *132*(4), 1084-1093. doi:10.1038/jid.2011.428
- Duangjit, S., Chairat, W., Opanasopit, P., Rojanarata, T., & Ngawhirunpat, T. (2016). Application of Design Expert for the investigation of capsaicin-loaded microemulsions for transdermal delivery. *Pharm Dev Technol*, *21*(6), 698-705. doi:10.3109/10837450.2015.1048552
- El Maghraby, G. M. (2008). Transdermal delivery of hydrocortisone from eucalyptus oil microemulsion: effects of cosurfactants. *Int J Pharm*, *355*(1-2), 285-292. doi:10.1016/j.ijpharm.2007.12.022
- Ellis, J. A., & Sinclair, R. D. (2008). Male pattern baldness: current treatments, future prospects. *Drug Discov Today*, *13*(17-18), 791-797. doi:10.1016/j.drudis.2008.05.010
- Enshell-Seijffers, D., Lindon, C., Wu, E., Taketo, M. M., & Morgan, B. A. (2010). Beta-catenin activity in the dermal papilla of the hair follicle regulates pigment-type switching. *Proc Natl Acad Sci U S A*, *107*(50), 21564-21569. doi:10.1073/pnas.1007326107
- Fouad, S. A., Basalious, E. B., El-Nabarawi, M. A., & Tayel, S. A. (2013). Microemulsion and poloxamer microemulsion-based gel for sustained transdermal delivery of diclofenac epolamine using in-skin drug depot: in vitro/in vivo evaluation. *Int J Pharm*, *453*(2), 569-578. doi:10.1016/j.ijpharm.2013.06.009
- Fukumoto, S., Hsieh, C. M., Maemura, K., Layne, M. D., Yet, S. F., Lee, K. H., . . . Lee, M. E. (2001). Akt participation in the Wnt signaling pathway through Dishevelled. *J Biol Chem*, *276*(20), 17479-17483. doi:10.1074/jbc.C000880200
- Gomes, M. J., Martins, S., Ferreira, D., Segundo, M. A., & Reis, S. (2014). Lipid nanoparticles for topical and transdermal application for alopecia treatment:

- development, physicochemical characterization, and in vitro release and penetration studies. *Int J Nanomedicine*, 9, 1231-1242. doi:10.2147/IJN.S45561
- Haber, R. S. (2004). Pharmacologic management of pattern hair loss. *Facial Plast Surg Clin North Am*, 12(2), 181-189. doi:10.1016/j.fsc.2003.12.008
- Hajheydari, Z., Akbari, J., Saeedi, M., & Shokoohi, L. (2009). Comparing the therapeutic effects of finasteride gel and tablet in treatment of the androgenetic alopecia. *Indian J Dermatol Venereol Leprol*, 75(1), 47-51.
- He, S., Nakada, D., & Morrison, S. J. (2009). Mechanisms of stem cell self-renewal. *Annu Rev Cell Dev Biol*, 25, 377-406. doi:10.1146/annurev.cellbio.042308.113248
- Herman, A., & Herman, A. P. (2016). Mechanism of action of herbs and their active constituents used in hair loss treatment. *Fitoterapia*, 114, 18-25. doi:10.1016/j.fitote.2016.08.008
- Heuschkel, S., Goebel, A., & Neubert, R. H. (2008). Microemulsions--modern colloidal carrier for dermal and transdermal drug delivery. *J Pharm Sci*, 97(2), 603-631. doi:10.1002/jps.20995
- Hosmer, J., Reed, R., Bentley, M. V., Nornoo, A., & Lopes, L. B. (2009). Microemulsions containing medium-chain glycerides as transdermal delivery systems for hydrophilic and hydrophobic drugs. *AAPS PharmSciTech*, 10(2), 589-596. doi:10.1208/s12249-009-9251-0
- Huang, Y. B., Lin, Y. H., Lu, T. M., Wang, R. J., Tsai, Y. H., & Wu, P. C. (2008). Transdermal delivery of capsaicin derivative-sodium nonivamide acetate using microemulsions as vehicles. *Int J Pharm*, 349(1-2), 206-211. doi:10.1016/j.ijpharm.2007.07.022
- Huelsken, J., Vogel, R., Erdmann, B., Cotsarelis, G., & Birchmeier, W. (2001). beta-Catenin controls hair follicle morphogenesis and stem cell differentiation in the skin. *Cell*, 105(4), 533-545.
- Imperato-McGinley, J., Guerrero, L., Gautier, T., German, J. L., & Peterson, R. E. (1975). Steroid 5alpha-reductase deficiency in man. An inherited form of male pseudohermaphroditism. *Birth Defects Orig Artic Ser*, 11(4), 91-103.
- Inui, S., Nakajima, T., & Itami, S. (2009). Scalp dermoscopy of androgenetic alopecia in Asian people. *J Dermatol*, 36(2), 82-85. doi:10.1111/j.1346-8138.2009.00593.x
- Ito, M., Yang, Z., Andl, T., Cui, C., Kim, N., Millar, S. E., & Cotsarelis, G. (2007). Wnt-dependent de novo hair follicle regeneration in adult mouse skin after wounding. *Nature*, 447(7142), 316-320. doi:10.1038/nature05766
- Jaipakdee, N., Limpongsa, E., & Pongjanyakul, T. (2016). Optimization of minoxidil microemulsions using fractional factorial design approach. *Pharm Dev Technol*, 21(1), 86-97. doi:10.3109/10837450.2014.971375
- Kaufman, K. D., & Dawber, R. P. (1999). Finasteride, a Type 2 5alpha-reductase inhibitor, in the treatment of men with androgenetic alopecia. *Expert Opinion on Investigational Drugs*, 8(4), 403-415. doi:10.1517/13543784.8.4.403
- Kiratipaiboon, C., Tengamnuay, P., & Chanvorachote, P. (2015). Glycyrrhizic acid attenuates stem cell-like phenotypes of human dermal papilla cells. *Phytomedicine*, 22(14), 1269-1278. doi:10.1016/j.phymed.2015.11.002
- Kiratipaiboon, C., Tengamnuay, P., & Chanvorachote, P. (2015). Glycyrrhizic acid attenuates stem cell-like phenotypes of human dermal papilla cells.

- Phytomedicine*, 22(14), 1269-1278.
doi:<https://doi.org/10.1016/j.phymed.2015.11.002>
- Kishimoto, J., Burgeson, R. E., & Morgan, B. A. (2000). Wnt signaling maintains the hair-inducing activity of the dermal papilla. *Genes Dev*, 14(10), 1181-1185.
- Kogan, A., & Garti, N. (2006). Microemulsions as transdermal drug delivery vehicles. *Adv Colloid Interface Sci*, 123-126, 369-385. doi:10.1016/j.cis.2006.05.014
- Kretzschmar, K., & Clevers, H. (2017). Wnt/beta-catenin signaling in adult mammalian epithelial stem cells. *Dev Biol*, 428(2), 273-282.
doi:10.1016/j.ydbio.2017.05.015
- Kumar, R., Singh, B., Bakshi, G., & Katare, O. P. (2007). Development of liposomal systems of finasteride for topical applications: design, characterization, and in vitro evaluation. *Pharm Dev Technol*, 12(6), 591-601.
doi:10.1080/10837450701481181
- Lai, J. J., Chang, P., Lai, K. P., Chen, L., & Chang, C. (2012). The role of androgen and androgen receptor in skin-related disorders. *Arch Dermatol Res*, 304(7), 499-510. doi:10.1007/s00403-012-1265-x
- Lawrence, M. J., & Rees, G. D. (2000). Microemulsion-based media as novel drug delivery systems. *Adv Drug Deliv Rev*, 45(1), 89-121.
- Leiros, G. J., Attorresi, A. I., & Balana, M. E. (2012). Hair follicle stem cell differentiation is inhibited through cross-talk between Wnt/beta-catenin and androgen signalling in dermal papilla cells from patients with androgenetic alopecia. *Br J Dermatol*, 166(5), 1035-1042. doi:10.1111/j.1365-2133.2012.10856.x
- Libecco, J. F., & Bergfeld, W. F. (2004). Finasteride in the treatment of alopecia. *Expert Opinion on Pharmacotherapy*, 5(4), 933-940. doi:10.1517/14656566.5.4.933
- Liu, C. H., Chang, F. Y., & Hung, D. K. (2011). Terpene microemulsions for transdermal curcumin delivery: effects of terpenes and cosurfactants. *Colloids Surf B Biointerfaces*, 82(1), 63-70. doi:10.1016/j.colsurfb.2010.08.018
- Lu, G. Q., Wu, Z. B., Chu, X. Y., Bi, Z. G., & Fan, W. X. (2016). An investigation of crosstalk between Wnt/beta-catenin and transforming growth factor-beta signaling in androgenetic alopecia. *Medicine (Baltimore)*, 95(30), e4297. doi:10.1097/MD.00000000000004297
- Madheswaran, T., Baskaran, R., Thapa, R. K., Rhyu, J. Y., Choi, H. Y., Kim, J. O., . . . Yoo, B. K. (2013). Design and in vitro evaluation of finasteride-loaded liquid crystalline nanoparticles for topical delivery. *AAPS PharmSciTech*, 14(1), 45-52. doi:10.1208/s12249-012-9888-y
- Merrill, B. J. (2012). Wnt pathway regulation of embryonic stem cell self-renewal. *Cold Spring Harb Perspect Biol*, 4(9), a007971. doi:10.1101/cshperspect.a007971
- Messenger, A. G., & Rundegren, J. (2004). Minoxidil: mechanisms of action on hair growth. *Br J Dermatol*, 150(2), 186-194.
- Miki, T., Yasuda, S. Y., & Kahn, M. (2011). Wnt/beta-catenin signaling in embryonic stem cell self-renewal and somatic cell reprogramming. *Stem Cell Rev*, 7(4), 836-846. doi:10.1007/s12015-011-9275-1
- Monti, D., Tampucci, S., Burgalassi, S., Chetoni, P., Lenzi, C., Pirone, A., & Mailland, F. (2014). Topical formulations containing finasteride. Part I: in vitro permeation/penetration study and in vivo pharmacokinetics in hairless rat. *J Pharm Sci*, 103(8), 2307-2314. doi:10.1002/jps.24028

- Norwood, O. T. (1975). Male pattern baldness: classification and incidence. *South Med J*, 68(11), 1359-1365.
- Olsen, E. A., & Weiner, M. S. (1987). Topical minoxidil in male pattern baldness: effects of discontinuation of treatment. *J Am Acad Dermatol*, 17(1), 97-101.
- Olsen, E. A., Whiting, D., Bergfeld, W., Miller, J., Hordinsky, M., Wanser, R., . . . Kohut, B. (2007). A multicenter, randomized, placebo-controlled, double-blind clinical trial of a novel formulation of 5% minoxidil topical foam versus placebo in the treatment of androgenetic alopecia in men. *J Am Acad Dermatol*, 57(5), 767-774. doi:10.1016/j.jaad.2007.04.012
- Osada, A., Iwabuchi, T., Kishimoto, J., Hamazaki, T. S., & Okochi, H. (2007). Long-term culture of mouse vibrissal dermal papilla cells and de novo hair follicle induction. *Tissue Eng*, 13(5), 975-982. doi:10.1089/ten.2006.0304
- Paus, R., & Cotsarelis, G. (1999). The biology of hair follicles. *N Engl J Med*, 341(7), 491-497. doi:10.1056/NEJM199908123410706
- Pineros, I., Slowing, K., Serrano, D. R., de Pablo, E., & Ballesteros, M. P. (2017). Analgesic and anti-inflammatory controlled-released injectable microemulsion: Pseudo-ternary phase diagrams, in vitro, ex vivo and in vivo evaluation. *Eur J Pharm Sci*, 101, 220-227. doi:10.1016/j.ejps.2016.12.030
- Prausnitz, M. R., & Langer, R. (2008). Transdermal drug delivery. *Nat Biotechnol*, 26(11), 1261-1268. doi:10.1038/nbt.1504
- Raghavan, S., Bauer, C., Mundschau, G., Li, Q., & Fuchs, E. (2000). Conditional ablation of beta1 integrin in skin. Severe defects in epidermal proliferation, basement membrane formation, and hair follicle invagination. *J Cell Biol*, 150(5), 1149-1160. doi:10.1083/jcb.150.5.1149
- Randall, V. A., Thornton, M. J., Hamada, K., & Messenger, A. G. (1992). Mechanism of androgen action in cultured dermal papilla cells derived from human hair follicles with varying responses to androgens in vivo. *J Invest Dermatol*, 98(6 Suppl), 86S-91S.
- Randall, V. A., Thornton, M. J., Hamada, K., & Messenger, A. G. (1994). Androgen action in cultured dermal papilla cells from human hair follicles. *Skin Pharmacol*, 7(1-2), 20-26.
- Rao, P. V., & Gan, S. H. (2014). Cinnamon: a multifaceted medicinal plant. *Evid Based Complement Alternat Med*, 2014, 642942. doi:10.1155/2014/642942
- Rao, Y., Zheng, F., Liang, X., Wang, H., Zhang, J., & Lu, X. (2015). Penetration profile and human cadaver skin distribution of finasteride from vesicular nanocarriers. *Drug Deliv*, 22(8), 1003-1009. doi:10.3109/10717544.2013.839128
- Rendl, M., Lewis, L., & Fuchs, E. (2005). Molecular dissection of mesenchymal-epithelial interactions in the hair follicle. *PLoS Biol*, 3(11), e331. doi:10.1371/journal.pbio.0030331
- Rhee, Y. S., Choi, J. G., Park, E. S., & Chi, S. C. (2001). Transdermal delivery of ketoprofen using microemulsions. *Int J Pharm*, 228(1-2), 161-170.
- Schmidt, L. J., & Tindall, D. J. (2011). Steroid 5 alpha-reductase inhibitors targeting BPH and prostate cancer. *J Steroid Biochem Mol Biol*, 125(1-2), 32-38. doi:10.1016/j.jsbmb.2010.09.003
- Schwarz, J. S., Weisspapir, M. R., & Friedman, D. I. (1995). Enhanced transdermal delivery of diazepam by submicron emulsion (SME) creams. *Pharm Res*, 12(5), 687-692.

- Shimizu, H., & Morgan, B. A. (2004). Wnt signaling through the beta-catenin pathway is sufficient to maintain, but not restore, anagen-phase characteristics of dermal papilla cells. *J Invest Dermatol*, 122(2), 239-245. doi:10.1046/j.0022-202X.2004.22224.x
- Stenn, K. S., & Paus, R. (2001). Controls of hair follicle cycling. *Physiol Rev*, 81(1), 449-494. doi:10.1152/physrev.2001.81.1.449
- Sujatha S, Sowmya G, & Chaitanya M. (2016). Preparation, characterization and evaluation of finasteride ethosomes. *Inter J of Drug Deliv*, 8, 1-11.
- Tabbakhian, M., Tavakoli, N., Jaafari, M. R., & Daneshamouz, S. (2006). Enhancement of follicular delivery of finasteride by liposomes and niosomes 1. In vitro permeation and in vivo deposition studies using hamster flank and ear models. *Int J Pharm*, 323(1-2), 1-10. doi:10.1016/j.ijpharm.2006.05.041
- Trueb, R. M. (2002). Molecular mechanisms of androgenetic alopecia. *Exp Gerontol*, 37(8-9), 981-990.
- Uno H, Allegra F, Adachi K, & W., M. (1967). Studies of common baldness of the stumptailed macaque. I. Distribution of the hair follicle. *J Invest Dermatol.*, 49, 288-296.
- Williams, A. C., & Barry, B. W. (2004). Penetration enhancers. *Adv Drug Deliv Rev*, 56(5), 603-618. doi:10.1016/j.addr.2003.10.025
- Zhang, J., & Michniak-Kohn, B. (2011). Investigation of microemulsion microstructures and their relationship to transdermal permeation of model drugs: ketoprofen, lidocaine, and caffeine. *Int J Pharm*, 421(1), 34-44. doi:10.1016/j.ijpharm.2011.09.014







APPENDIX A

1. Cytotoxicity study of finasteride on dermal papilla cells

Table 5 Cytotoxicity of FN on DPCs and 2 different sources of HDPCs

Conc. Of FN (μM)	% Cell viability		
	DPCs	HDPCs1	HDPCs2
	Mean \pm SD	Mean \pm SD	Mean \pm SD
0	100.0 \pm 0.0	100.0 \pm 0.0	100.0 \pm 0.0
0.01	98.9 \pm 9.3	99.2 \pm 8.1	99.3 \pm 8.1
0.1	108.5 \pm 11.0	97.24 \pm 3.0	100.7 \pm 3.9
1	99.2 \pm 12.9	95.65 \pm 3.1	97.9 \pm 2.6
10	96.6 \pm 8.0	94.72 \pm 1.6	96.9 \pm 3.7
50	95.6 \pm 11.0	89.9 \pm 6.6	89.7 \pm 5.1
100	90.5 \pm 4.3	80.4 \pm 0.8*	86.15 \pm 5.6

* $P < 0.05$ versus non-treated control

2. Effect of finasteride on aggregation behavior of dermal papilla cells

Table 6 Aggregation size and aggregation number of DPCs

Conc. Of FN (μM)	Aggregation size	Aggregation number
	Mean \pm SD	Mean \pm SD
0	8323.38 \pm 2931.80	9.3 \pm 1.2
10	4629.42 \pm 3586.37	11.3 \pm 3.1
50	5087.43 \pm 3929.71	17.7 \pm 6.1*
100	5032.14 \pm 3338.53	20.3 \pm 3.8*



APPENDIX B

Standard curve for *in vitro* skin permeation study

Determination of FN in sample

Standard	:	Finasteride
Method	:	HPLC analysis
Analytical column	:	ReproSil-Pur Basic C18, 5 μ m, 250 x 4.6 mm
Mobile phase	:	Methanol:Water (70:30, v/v)
Flow rate	:	1.0 mL/min
UV Detector	:	wavelength 210 nm
Concentration (μ g/mL)	:	0.5, 1, 3, 5, 8, 10 μ g/mL

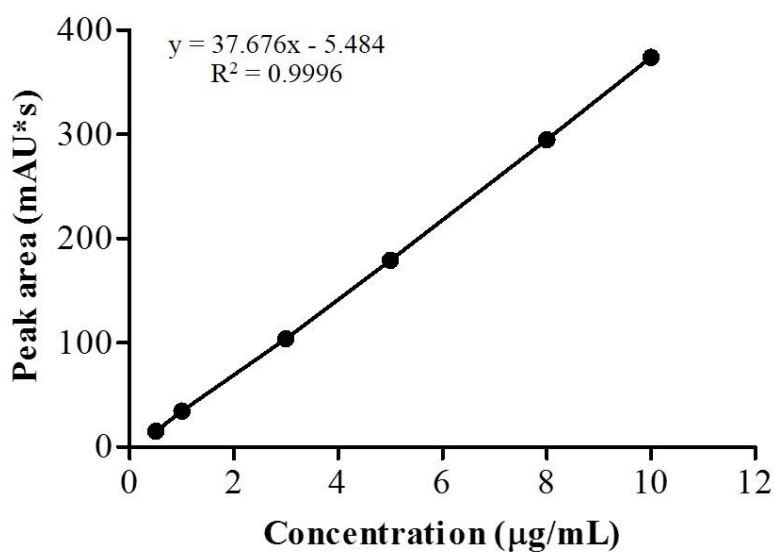


Figure 32 Standard curve for *in vitro* skin permeation study

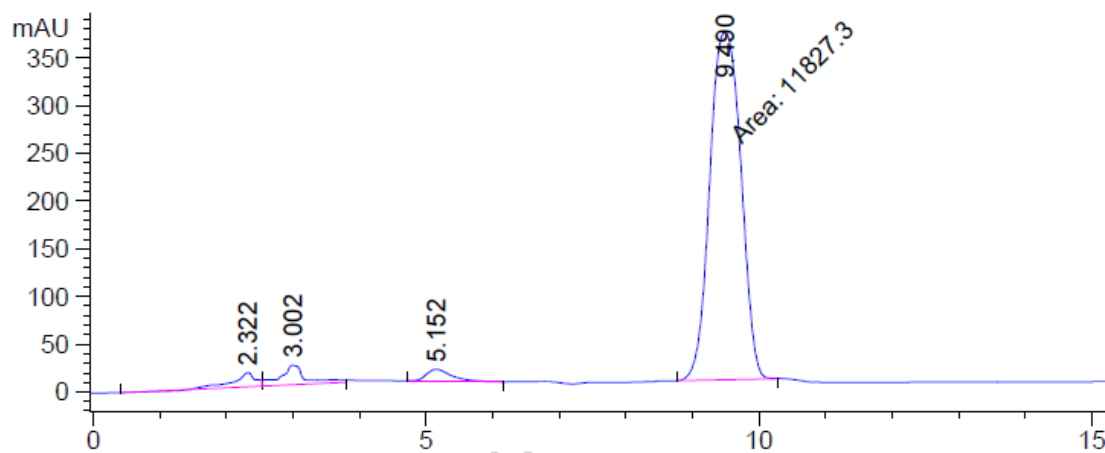


Figure 33 HPLC chromatogram of standard FN solution

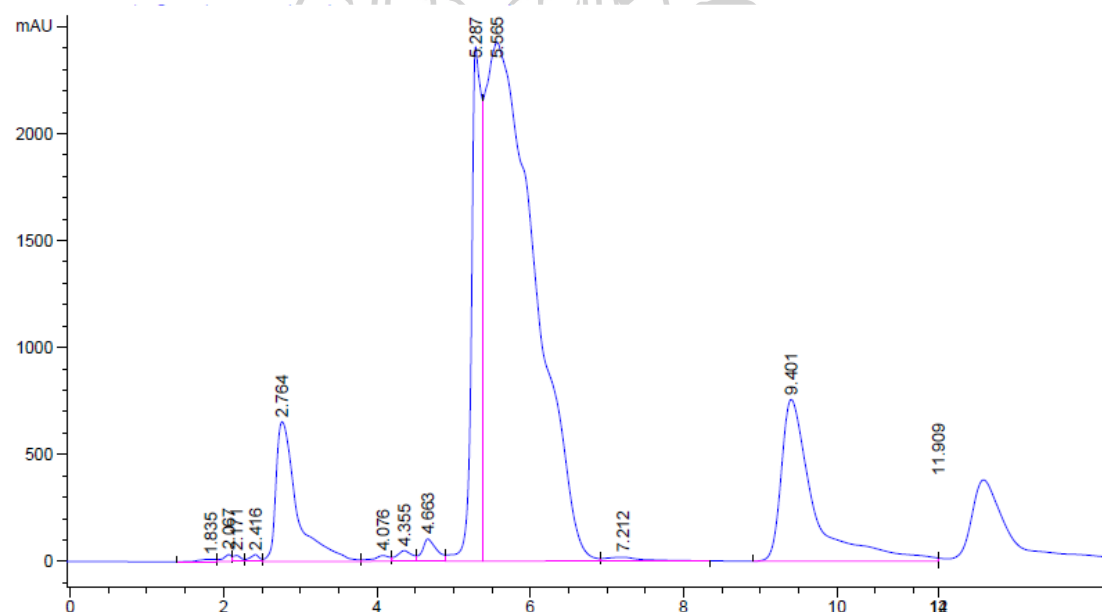


Figure 34 HPLC chromatogram of FN in sample



Physicochemical characteristics measurement of ME formulations

Table 7 Physicochemical characteristics of blank MEs and FN-loaded MEs (droplet size)

ME Formulation (Oil : Smix : Water)	Droplet size (nm)		
	Blank	0.1% FN*	0.3% FN*
	Mean±SD	Mean±SD	Mean±SD
ME1 (15 : 55 : 30) ^a	232.67±16.34	207.53±14.86	179.33±31.57
ME2 (5 : 65 : 30) ^b	238.50±14.76	267.48±13.28	212.58±18.76
ME3 (5 : 75 : 20) ^d	315.83±10.66	337.36±13.92	276.48±33.30
ME4 (15 : 75 : 10) ^c	361.89±16.96	324.80±25.26	355.57±67.29
ME5 (25 : 65 : 10) ^c	267.67±34.23	252.97±38.93	285.22±13.48
ME6 (25 : 55 : 20) ^a	267.67±34.23	214.60±14.88	176.91±34.70
ME7 (15 : 65 : 20) ^c	252.20±8.45	248.48±16.07	266.03±10.03

* Significantly different from the control (Blank) ($P<0.05$)

Table 8 Physicochemical characteristics of blank MEs and FN-loaded MEs (size distribution (PDI))

ME Formulation (Oil : Smix : Water)	PDI		
	Blank	0.1% FN*	0.3% FN
	Mean±SD	Mean±SD	Mean±SD
ME1 (15 : 55 : 30)	0.40±0.03	0.44±0.06	0.45±0.12
ME2 (5 : 65 : 30)	0.40±0.03	0.38±0.03	0.34±0.03
ME3 (5 : 75 : 20)	0.39±0.03	0.41±0.05	0.40±0.05
ME4 (15 : 75 : 10)	0.40±0.03	0.42±0.03	0.41±0.04
ME5 (25 : 65 : 10)	0.40±0.02	0.46±0.07	0.46±0.01
ME6 (25 : 55 : 20)	0.39±0.05	0.42±0.05	0.45±0.01
ME7 (15 : 65 : 20)	0.39±0.03	0.41±0.05	0.37±0.04

* Significantly different from the control (Blank) ($P<0.05$)

Table 9 Physicochemical characteristics of blank MEs and FN-loaded MEs (conductivity)

ME Formulation (Oil : Smix : Water)	Conductivity (mS/cm)		
	Blank	0.1% FN*	0.3% FN*
	Mean±SD	Mean±SD	Mean±SD
ME1 (15 : 55 : 30)	0.050±0.002	0.047±0.001	0.058±0.001
ME2 (5 : 65 : 30)	0.045±0.001	0.046±0.002	0.053±0.002
ME3 (5 : 75 : 20)	0.027±0.001	0.026±0.003	0.027±0.001
ME4 (15 : 75 : 10)	0.015±0.002	0.015±0.001	0.016±0.001
ME5 (25 : 65 : 10)	0.016±0.001	0.015±0.001	0.017±0.000
ME6 (25 : 55 : 20)	0.031±0.003	0.028±0.004	0.032±0.001
ME7 (15 : 65 : 20)	0.028±0.001	0.027±0.001	0.033±0.001

* Significantly different from the control (Blank) ($P < 0.05$)

Table 10 Physicochemical characteristics of blank MEs and FN-loaded MEs (pH)

ME Formulation (Oil : Smix : Water)	pH		
	Blank	0.1% FN*	0.3% FN*
	Mean±SD	Mean±SD	Mean±SD
ME1 (15 : 55 : 30) ^f	6.6±0.1	6.5±0.1	5.2±0.1
ME2 (5 : 65 : 30) ^b	7.6±0.1	7.4±0.1	6.6±0.1
ME3 (5 : 75 : 20) ^a	7.7±0.0	7.6±0.0	7.5±0.1
ME4 (15 : 75 : 10) ^c	7.3±0.0	7.3±0.0	6.4±0.0
ME5 (25 : 65 : 10) ^e	6.8±0.0	6.9±0.0	5.9±0.0
ME6 (25 : 55 : 20) ^g	6.5±0.0	6.5±0.0	5.3±0.1
ME7 (15 : 65 : 20) ^d	7.0±0.1	6.9±0.1	5.8±0.1

Table 11 Drug content of FN-loaded MEs presented by % entrapment efficiency

ME Formulation (Oil : Smix : Water)	Entrapment (%)
	Mean±SD
ME1 (15 : 55 : 30)	78.06±3.63
ME2 (5 : 65 : 30)	88.77±1.74
ME3 (5 : 75 : 20)	76.82±2.91
ME4 (15 : 75 : 10)	79.93±1.73
ME5 (25 : 65 : 10)	89.41±3.05
ME6 (25 : 55 : 20)	88.22±2.99
ME7 (15 : 65 : 20)	81.35±6.18

Table 12 Skin permeation flux of FN-loaded MEs

ME Formulation (Oil : Smix : Water)	Permeation flux ($\mu\text{g}/\text{cm}^2/\text{h}$)
	Mean±SD
ME1 (15 : 55 : 30)	2.32±0.19
ME2 (5 : 65 : 30)	1.07±0.31
ME3 (5 : 75 : 20)	1.95±1.00
ME4 (15 : 75 : 10)	0.65±0.02
ME5 (25 : 65 : 10)	0.44±0.03
ME6 (25 : 55 : 20)	1.49±0.14
ME7 (15 : 65 : 20)	1.04±0.14

VITA

NAME Napapat Rattanachitthawat

DATE OF BIRTH 8 January 1984

PLACE OF BIRTH Bangkok, Thailand

INSTITUTIONS ATTENDED Doctor of Philosophy, Ph.D. in pharmaceutical Technology
Silpakorn Univerisity, Thailand

HOME ADDRESS 189/42 moo 9, Tungsukla, Sriracha, Chonburi province, Thailand
20230

PUBLICATION Napapat Rattanachitthawat, Tatchakorn Pinkhien, Praneet Opanasopit, Tanasait Ngawhirunpat, Pithi Chanvorachote. (2019) "Finasteride enhances stem cell signals in human dermal papilla cells" In Vivo (in press)

